

1980

Project Completion  
Report No. 711523

## A STOCHASTIC MODEL OF SOIL EROSION

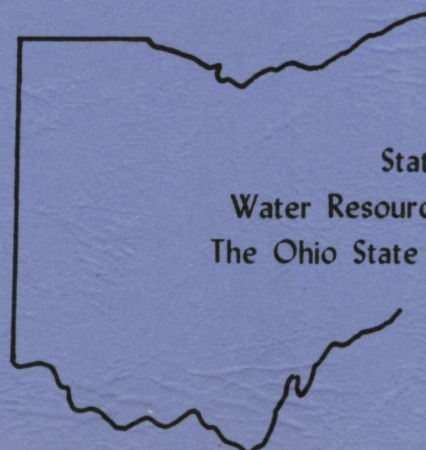
Tien H. Wu, Ph.D.  
Keith W. Bedford, Ph.D.  
and

Mostafa E. Mossaad  
Kenneth L. McCurdy  
Elfatih M. Ali

Department of Civil Engineering  
The Ohio State University

United States  
Department of the Interior

Contract No.  
A-056-OHIO



State of Ohio  
Water Resources Center  
The Ohio State University



A STOCHASTIC MODEL OF SOIL EROSION

Tien H. Wu, Ph.D.  
Keith W. Bedford, Ph.D.

and

Mostafa E. Mossaad  
Kenneth L. McCurdy  
Elfatih M. Ali

Department of Civil Engineering  
The Ohio State University

This Study was supported in part by the  
Office of Water Research and Technology,  
U.S. Department of the Interior  
Project A-056-OHIO





## TABLE OF CONTENTS

List of Figures	Page
	iv
List of Table	vii
CHAPTER	
1 INTRODUCTION	1
1.1 Problem Statement	1
1.2 Objectives and Scope	2
1.3 Acknowledgements	3
2 SURFACE ROUGHNESS MODEL	4
2.1 General Considerations	4
2.2 Method of Spectral Analysis	4
2.3 Generation of Surface with Regular Rill Pattern	9
2.4 The Method of Zero-Crossing Analysis	15
2.5 Generation of Surface with Random Rill Pattern	21
2.6 Concluding Remarks	22
3 EROSION MODEL	25
3.1 Rill Erosion Equation	26
3.2 Interrill Erosion Equation	34
3.3 Concluding Remarks	36
4 SIMULATION MODEL	38
4.1 Main Features of the Model	38
4.1.1 Routing of Water and Sediment	38

4.1.2 Erosion of the Surface	39
4.1.3 Temporal Change	41
4.2 Auxilliary Mechanisms	42
4.2.1 Ponding	42
4.2.2 Deposition Due to Ponding	44
4.2.3 Stability of Rill's Side Slopes	44
4.2.4 Low Humps	47
4.3 Structure of the Program	49
4.3.1 The Input Data	49
4.3.2 Analysis of Surface Roughness Data	51
4.3.3 Generation of the Random Surface	52
4.3.4 Computation of Overland Flow	55
4.3.5 Erosion Computation	56
4.4 Sensitivity Analysis	59
4.4.1 Geometric Limitations	59
4.4.2 Sensitivity to Time Interval	60
4.4.3 Sensitivity to Parameters in Erosion Equations	61
4.4.3.1 Coefficient $n$ in Mannings Equation(N)	61
4.4.3.2 The Constant $a_s$	65
4.4.3.3 The Exponent $p$	66
4.4.4 Sensitivity to Criterion of Side Slope Failure	66
4.4.5 Effect of Randomness in Elevation	67
4.4.6 Effect of Randomness in Rill Pattern	69
4.5 Concluding Remarks	73

5	MODEL PERFORMANCE	75
	5.1 Comparison with Field Measurements	75
	5.2 Influence of Physical Conditions	79
	5.2.1 Effect of Slope Gradient	79
	5.2.2 Effect of Slope Length	81
	5.2.3 Effect of Rainfall Intensity	81
	5.3 Evaluation of Eroding Surfaces	83
	5.4 Concluding Remarks	89
6	SUMMARY, CONCLUSIONS AND RECOMMENDATIONS	90
	6.1 Summary and Conclusions	90
	6.2 Recommendations for Further Research	91
	APPENDIX A Detachment of Rainfall	93
	APPENDIX B Comparison of Computed and measured rill erosion	104
	APPENDIX C References	106
	APPENDIX D Listing and Sample Output of The Computer Program	109

## LIST OF FIGURES

Figure	Title	Page
2.1	Natural Surface Roughness .....	5
2.2	Elevation Trace .....	6
2.3	Measurement Plot.....	6
2.4	Spectral Density Function of Surface Roughness .....	10
2.5	Simulation of Surface Roughness.....	13
2.6	Isotropy in Square Rill Pattern.....	14
2.7	Isotropy in Hexagonal Rill Pattern.....	14
2.8	Parameters used in Zero-Crossing Analysis.....	16
2.9	Sequences Computed in Zero-Crossing Analysis.....	18
2.10	Average Wave used in Constructing a Hexagonal Rill Pattern..	18
2.11	Uniform Rill Pattern.....	23
2.12	Random Rill Pattern .....	23
3.1	Surface Idealization.....	27
3.2	Rill Cross-Section.....	28
3.3	Rlow Over Interrill Area.....	28
3.4	Geometrical Basis for Interrill Erosion Computation.....	37
4.1	Typical Routing of Rill and Interrill Flow.....	40
4.2	Change in Rill Geometry due to Rill Erosion.....	40
4.3	Ponding Conditions.....	43
4.4	Deposition due to Ponding.....	43
4.5	Mechanism of Side-Slope Failure.....	46
4.6	Segment with Positive Side Slopes.....	46
4.7	Segment with a Negative Side Slope.....	46
4.8	Possible Cases associated with the low hump situation.....	48



4.9	Computational Scheme.....	50
4.10	Construction of the Hexagonal Mesh.....	54
4.11	Schematic Representation of Model Subroutines.....	58
4.12	Effect of Manning's Coeff. on erosion rate.....	64
4.13	Effect of Manning's Coeff. on R/I Erosion ratio.....	64
4.14	Effect of the factor SLIMIT on Erosion Rate.....	68
4.15	Effect of randomness in elevation on erosion rate.....	68
4.16	Test Samples from Uniform Rill Pattern.....	71
4.17	Test Samples from Random Rill Pattern.....	71
4.18	Effect of Rill Pattern Randomness on Flow; Test no. 1.....	72
4.19	Effect of Rill Pattern Randomness on Flow; Test no. 2.....	72
4.20	Irregularity in Generated surfaces.....	74
5.1	Soil Loss from the Clay Site.....	78
5.2	Soil Loss from the Sandy Clay Site.....	78
5.3	Effect of slope gradient on erosion rate.....	80
5.4	Effect of time on the slope gradient-Erosion rate relation...	80
5.5	Effect of slope length on erosion rate.....	82
5.6	Effect of slope length on R/I erosion ratio.....	82
5.7	Effect of Rainfall intensity on erosion rate;RNL=50mm/hr.....	84
5.8	Effect of Rainfall intensity on erosion rate;RNL=25mm/hr.....	84
5.9	Effect of Rainfall intensity on erosion rate;RNL=12.5mm/hr...	85
5.10	Relationship between Rainfall Intensity, Slope Gradient and Erosion Rate.....	85
5.11	Original Surface, $t=0$ .....	86
5.12	Eroded surface, $t= 200$ minutes.....	87
5.13	Eroded surface, $t= 400$ minutes.....	88

A.1	Apparatus for Raindrop test.....	94
A.2	Relation between shear strength and water content(a) Kaolinite (b) Corundite.....	96
A.3a.b.	Change in water content with Raindrops.....	97
A.3c.d.	Change in water content with Raindrops.....	98
A.4(a)	Weight of soil detached and number of Raindrops, Grundite ..	101
A.4(b)	Weight of soil detached and number of Raindrops, Kaolinite..	102

## LIST OF TABLES

Table		Page
2.1	Results of Zero-Crossing Analysis	19
2.2	Directions of Random Component	21
4.1	Parameters used in sensitivity Analysis	62
A.1	Makeup of Graded Tubes	95
A.2	Index Properties of Kaolinite and Grundite	100
B.1	Comparison between Measured and Computed Values of Rill Erosion	105





## 1. INTRODUCTION

### 1.1 Problem Statement

The removal of soil by moving water operates on the earth's surface from mass wasting on a geologic scale to small scale erosion on construction sites and slopes. The process presents important problems to engineering, agriculture and geology. While many erosion measurements have been made over the years, it is only recently that analytical expressions of the erosion process have been derived for rather simplified conditions. Because of the many factors that control erosion the study of its mechanics requires consideration of several disciplines. One way to study a complex process like erosion is to construct a mathematical model that contains as many of the controlling factors as can be handled by the computing process and then perform numerical tests that will assess the influence exerted by these factors. Then experiments can be done to study the individual factors. This report describes a first attempt at such a model and presents some of the results of simulations using this model.

The process of erosion begins when raindrops strike an inclined soil surface and detaches soil particles from larger aggregates. In the case of some cohesive soils the detached particles may themselves be composed of finer particles held together by physical-chemical forces. When the rainfall exceeds the infiltration rate, the overland flow begins and the detached soil particles are carried away. The overland flow tends to be concentrated in low areas, called rills, where erosion should also be most severe (e.g. ref. 24). Erosion during successive rainstorms deepens the rills and they become gullies. The quantity of soil eroded is clearly dependent on the topography of the eroded surface, which is composed of rills and inter-rill areas (24). Hence a realistic

erosion model should simulate the development of the eroded surface by computation of the erosion on different parts of the surface.

The random nature of the rill pattern and its contribution to the development of a drainage network was recognized by Leopold and Langbein ( 17 ), Horton ( 12 ), Scheidegger (32 ) and simple simulations of topographical change starting with an initial random surface have been presented by Schenck ( 33 ), Smart et al ( 36 ), and Seginer ( 34 ). On a given surface, simplified as a plane, equations of sediment transport may be used to compute the amount of erosion and various relations have been suggested by Meyer and Wischmeier (21), Foster and Meyer (6) (7), Li et al (18), and Komura (15). Smith (37) developed a numerical model that accounts for variations in slope, and rill geometry for unsteady state conditions. The equation may be solved to yield erosion in each time step. Thus, it is timely to combine the equations of erosion with the randomness of the surface topography in a model of the erosion on a sloped surface.

## 1.2 Objectives and Scope

The overall objective of this research is to develop a mathematical model of the progress of erosion on sloping ground. It is required that the model should be able to account for the irregular topography of the ground surface, the pattern of overland flow that is compatible with the topography, and the erosion and topographic change that results from this flow.

To attain the objective, three principal tasks were completed:

- (1) analysis of ground surface roughness and construction of the random surface model
- (2) study of sediment transport equations and construction

of the erosion model and (3) construction of the simulation model that computes the erosion and topographical changes. These models are described in Chapters 2, 3, and 4 respectively. In addition, tests were performed to evaluate the model's sensitivity to several important parameters. Limited numerical experiments were made to compare model performance with empirical results. This work is reported in Chap. 5.

The model presented here represents a first attempt and contains many simplifications out of necessity. Hence model predictions are only expected to provide order-of-magnitude estimates of the real process. Comparison of model performance with detailed experiments may be expected to identify shortcomings in the model and lead to refinements. In principle the model is not restricted to a particular scale. However, because of availability of data and the importance of erosion on construction sites and reclaimed land, we have used data from erosion plots for this work.

### 1.3 Acknowledgements

This research was supported by a grant from the Office of Water Research and Technology, Dept. of Interior. Most of the modeling work was done by M. E. Mossaad as his Ph.D. dissertation. The experiments on soil detachment described in Appendix A were performed by K. L. McCurdy.

The writers are grateful to professor V.T. Ricca and D.M. VanDoren Jr. for their contributions to this study.

## 2. SURFACE ROUGHNESS MODEL

### 2.1 General Considerations

The surface topography of a soil slope generally consists of a large number of humps of irregular shapes and sizes with depressions or rills, in between. When overland flow moves downslope, the water tends to concentrate in the meandering depressions, which constitute the flow paths as shown in Fig. 2.1.

A random surface model is required to generate a surface which has characteristics representative of the real surface. It is desirable that the statistical properties of the generated surface be as close as possible to those of the original surface. In addition, the numerical representation of the surface must be suitable for erosion computations. The trade off between those two conditions is the main consideration in the formulation of the random surface model.

### 2.2 Method of Spectral Analysis

Consider an elevation trace along any line on a slope surface, as shown in Fig. 2.2. The spacing between measurements, must be small enough to reveal the necessary details, namely, rills and humps. This profile can be considered as a continuous function,  $f(x)$ , with the distance,  $x$ , as the independent variable. Fourier analysis can then be used to express this function as a sum of an infinite number of sinusoidal terms.

According to the Fourier theorem, (Bath, 2), a periodic function  $x(t)$ , having a fundamental period,  $T$ , and satisfying the conditions known as Dirichlet's conditions, can be represented by an infinite Fourier series,

$$x(t) = \frac{A_0}{2} + \sum_{n=1}^{\infty} (a_n \cos n \omega_0 t + b_n \sin n \omega_0 t), \quad (2.1)$$



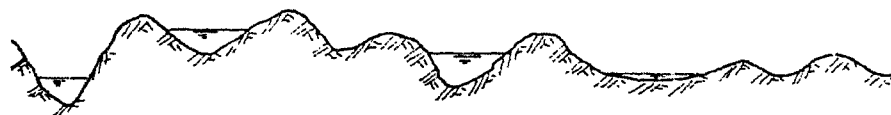
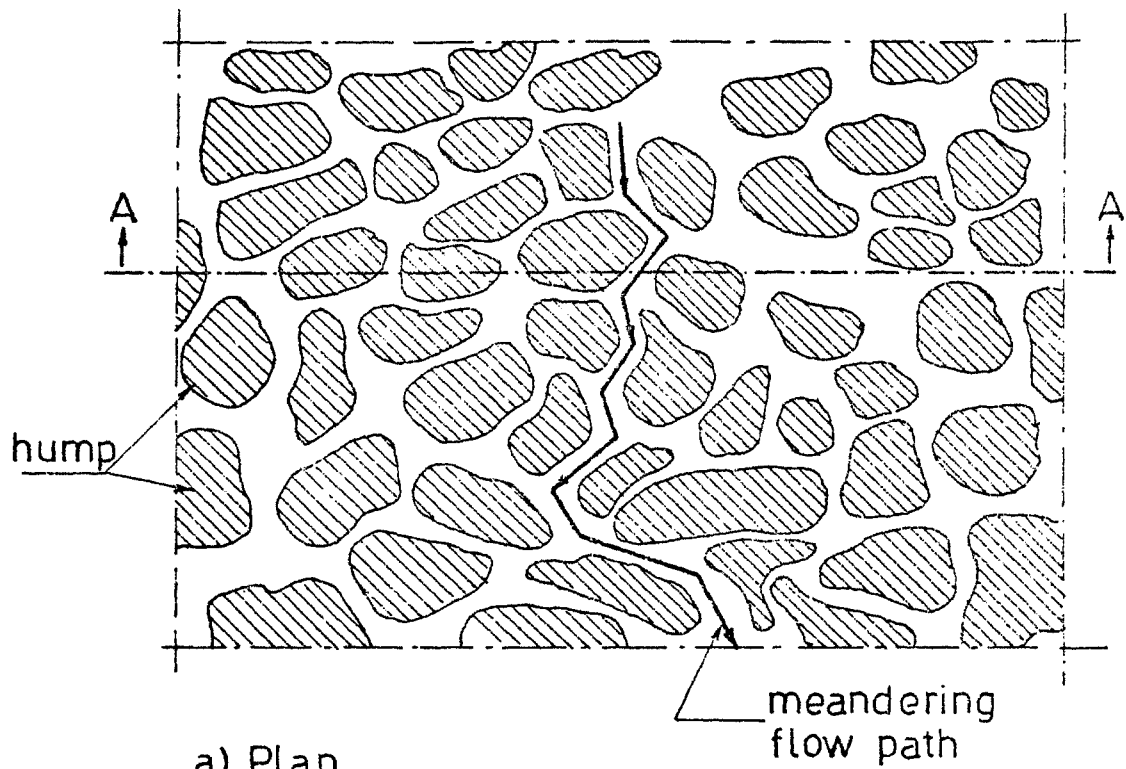


Figure 2.1 Natural Surface Roughness

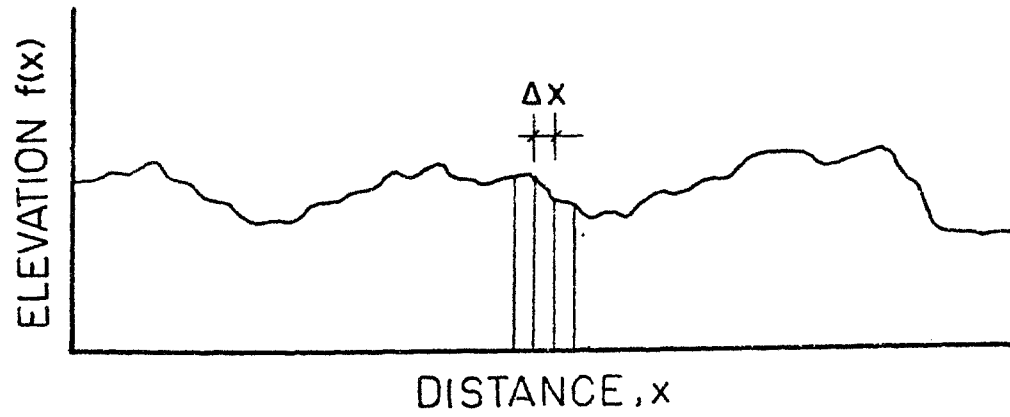


Figure 2.2 Elevation Trace

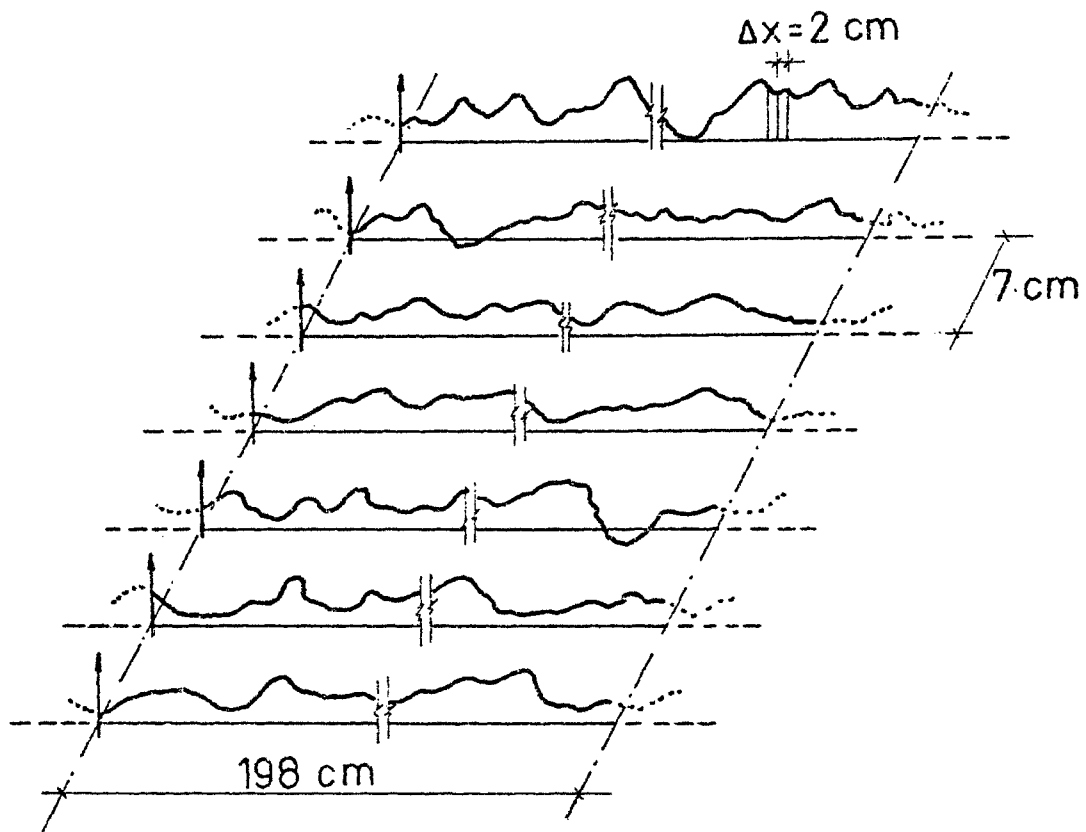


Figure 2.3 Measurement Plot

where  $w_0 = 2\pi/T$ , is the fundamental angular frequency,  $a_n$ , and  $b_n$  are Fourier coefficients.

Thus a data record must be expressed in the form of a finite number of sinusoidal waves. Each wave has its own contribution to the total variance of the record. This contribution depends on the value of the coefficients  $a_n$ , and  $b_n$  associated with this wave. An alternative terminology for the total variance is the total power.

: Field measurements of the surface roughness are usually carried out by measuring the elevation of a number of equidistant points along a certain line. A measurement plot is composed of several profiles or elevation traces.

The surface roughness as represented by the random variations of elevation with distance can be regarded as a stochastic process. Each one of the elevation traces can be taken as a realization of the same stochastic process, if the irregularity of the land surface is "homogeneous," a term introduced by Merva et al. (20). A surface is homogeneous if the nature of the irregularity does not change from location to location. This condition is usually fulfilled in cases where mechanical treatment of the surface is the same at all locations.

If each elevation trace represents a realization, then the group of traces in a measurement plot is considered an ensemble (See Figure 2.3). The properties of the stochastic process are better represented in an ensemble than in a single realization. It is therefore preferable to include the whole ensemble in the spectral analysis.

The classical method of analyzing an ensemble in time domain is to compute the autocorrelation function of each realization, then the overall autocorrelation function is calculated by averaging values of autocorrelation functions at each time lag (27). In spectral analysis, however,

the spectrum of a process contains the same information given by the autocorrelation function, but in frequency domain. Accordingly, the overall spectrum of a process can be computed by averaging Fourier coefficients of the same harmonic component for all realizations, then the average harmonic components are composed together to produce the spectrum.

According to Merva et al. (20), a surface is called isotropic if the statistical properties, estimated by measurements taken along two orthogonal traces, are identical. It is clear that such a condition cannot be met in plowed surfaces, or in surfaces which have experienced considerable erosion.

When field measurements are made along parallel traces, they represent elevation variation only in one direction. When the analysis of this data is used to generate a surface, the assumption of isotropy of the surface irregularities is then implied.

It is important to mention that the method of spectral analysis can be used to study the data in two-dimensional form directly. That is, the data of all points on a plot are treated as one data record (29). In fact, Shinozuka and Jan (35) described the procedure to use two-dimensional spectral analysis in generating a random surface. The generated surface in this case would probably be a better representative of the original one, but would impose greater difficulties on the operation of erosion mechanisms. Therefore, in the present simplified model, the random surface is generated using one-dimensional analysis only.

The present research utilizes a computer program for one-dimensional spectral analysis (14), as a subroutine in the model. For any data of an elevation trace, the program computes the coefficients,  $a$  and  $b$ , of every harmonic component. This provides enough information to compute the amplitude, phase, and the contribution of any component to the total variance of the original function.



The data used for spectral analysis consists of elevation measurements from plots of the dimensions shown in Figure 2.3. The data was a part of a study conducted by Van Doren [38] at Wooster, Ohio. Analysis was done for the plots which were plowed and then disked four times. Other plots were disked fewer times, and would probably exhibit less isotropy due to deeper tillage marks.

The results of spectral analysis are presented in the form of a curve showing the relationship between different harmonic components and the corresponding contributions to the total variance, or power. This curve is called the power spectrum.

A power spectrum of the plot used in this study is shown in Figure 2.4. The spectrum is divided into two types of roughness: the macro-roughness, which is the part composed of waves with lengths greater than 30 cm; and the micro-roughness, which is the part composed of waves with lengths less than or equal to 30 cm. The rill pattern, being formed of small-scale surface irregularities, is considered to be represented by the micro-roughness. Therefore, the wave with the highest peak, in the micro-roughness range of the spectral density function, is assumed to be the "basic" wave.

Figure 2.4 indicates that some of the waves in the macro-roughness range may have the greatest contribution to the variance of the surface. Those large waves are attributed to local topographic variations combined with the effect of tilling. Such waves have little effect on the formulation of the elementary rill pattern on the surface, and are ignored.

### 2.3 Generation of Surface with Regular Rill Pattern

In light of the assumptions and the observations discussed previously, it is now possible to lay out the procedure followed in this model for

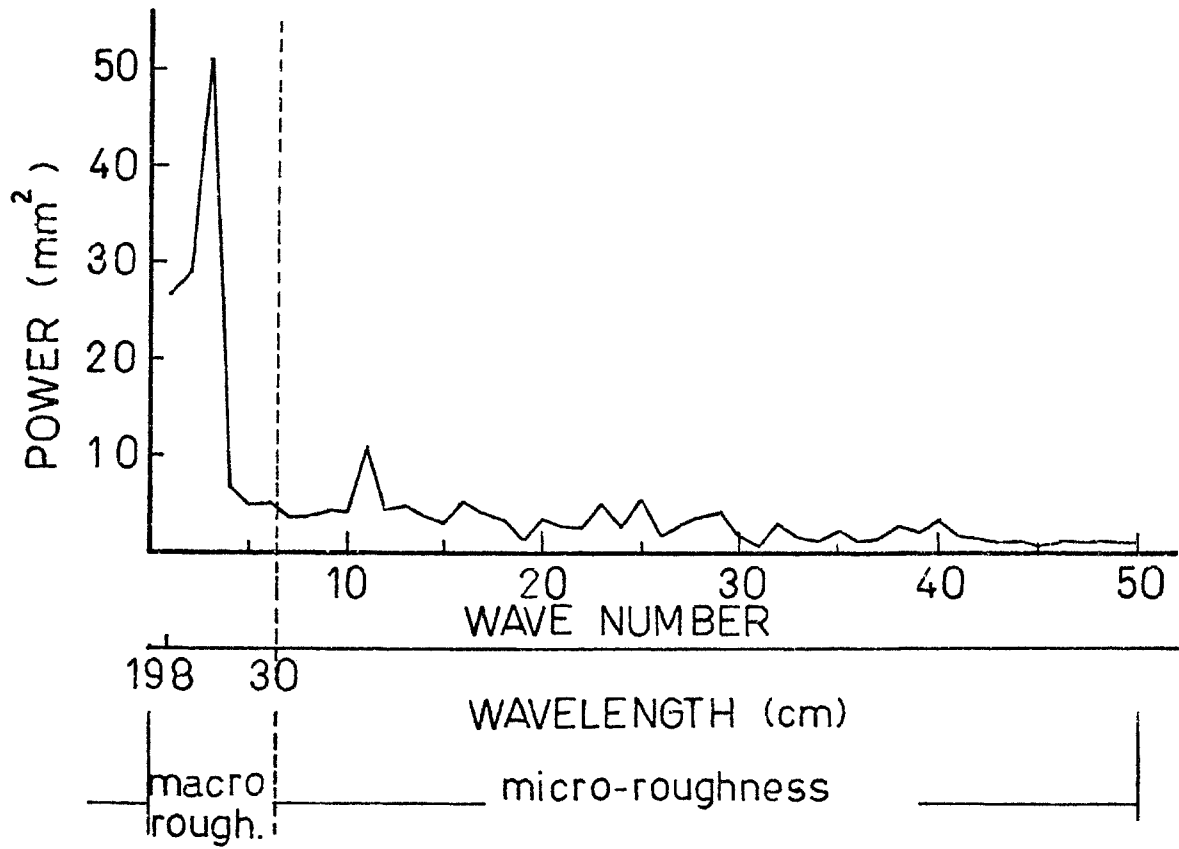


Figure 2.4 Spectral Density Function of Surface Roughness

generating a random surface on the basis of spectral analysis. The procedure is composed of two major steps. The first step is the spectral analysis of the roughness data. The second step is the numerical generation of the surface, based on the characteristics obtained from the first step.

(a) Analysis of the Data

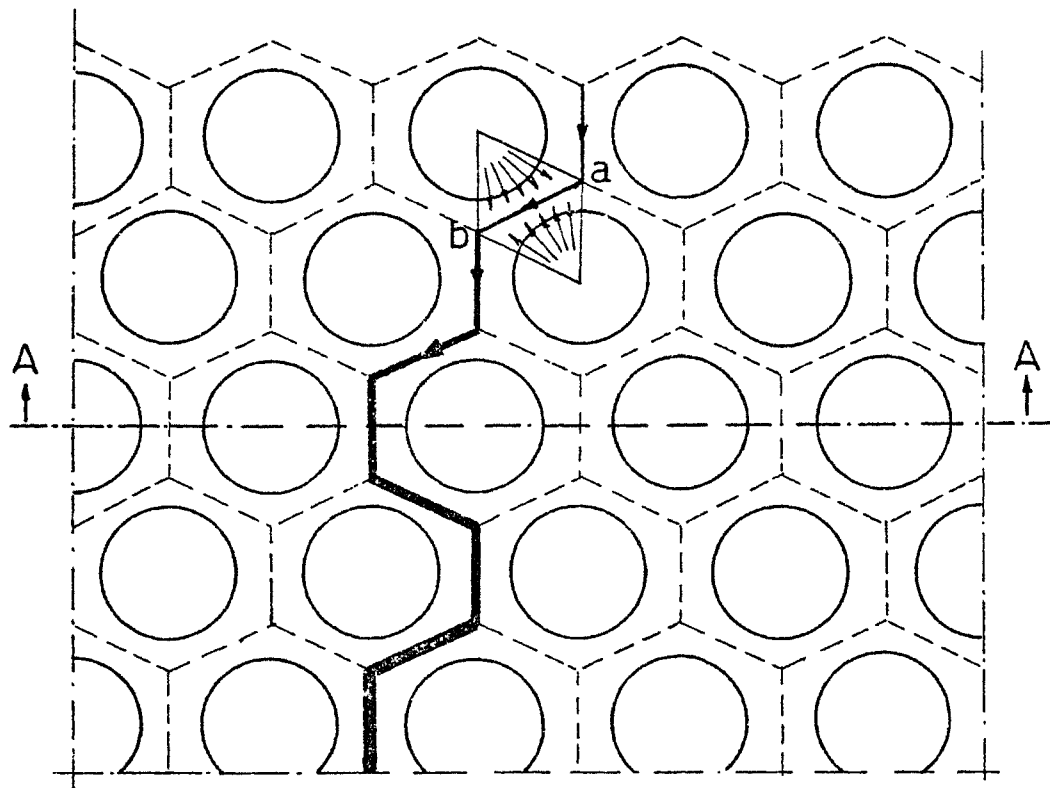
1. Perform spectral analysis on each one of the elevation traces obtained from the measurement plot.
2. Compute the average harmonic components by averaging the coefficients  $a$  and  $b$  from all elevation traces. The resulting composition of harmonic components is regarded as the spectrum of the measurement plot.
3. From within the range of micro-roughness, pick up the wave component with the highest contribution to variance. This is the basic wave.
4. Deduct the basic wave from each of the original elevation traces to obtain the residual data. The residual data is treated as a random component and is represented by a normal distribution.
5. Compute the mean and the standard deviation of the residual data from each trace. Then compute the average values which are the mean and the standard deviation for the whole plot.

The output of this step is the length and amplitude of the basic wave, the mean, and the standard deviation of the residual data.

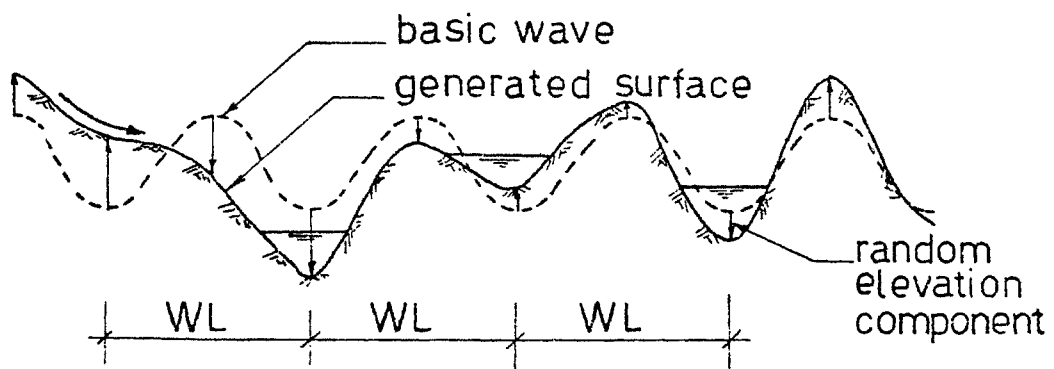
(b) Generation of the Surface

The random surface is generated by superposing a matrix of humps, which represent the basic wave, on a plane surface, which has a slope equal to the average slope of the actual surface. As shown in Figure 2.5, a hexagonal mesh is used to define the low zones around the humps. To obtain the elevations of the nodal points, and the hump centers, a random component drawn from the distribution of the residual data is added to the elevation of the basic wave.

The selection of a hexagonal mesh to simulate the elementary rill pattern is based on several considerations. In a rectangular grid, there is a possibility of three streams merging at a single point, since we have four branches connected together at each nodal point. This situation is seldom met in nature (34). With three members only meeting at each nodal point, the possibility of three streams merging at one point is much less. Accordingly, a hexagonal mesh provides a more realistic representation of a stream network. A hexagonal mesh is also a closer simulation of the actually curved rills. Moreover, a square mesh provides isotropy in two directions only, as shown in Figure 2.6, whereas a hexagonal mesh provides three directions of isotropy, as shown in Figure 2.7.



a) Plan



b) Section A-A

Figure 2.5 Simulation of Surface Roughness

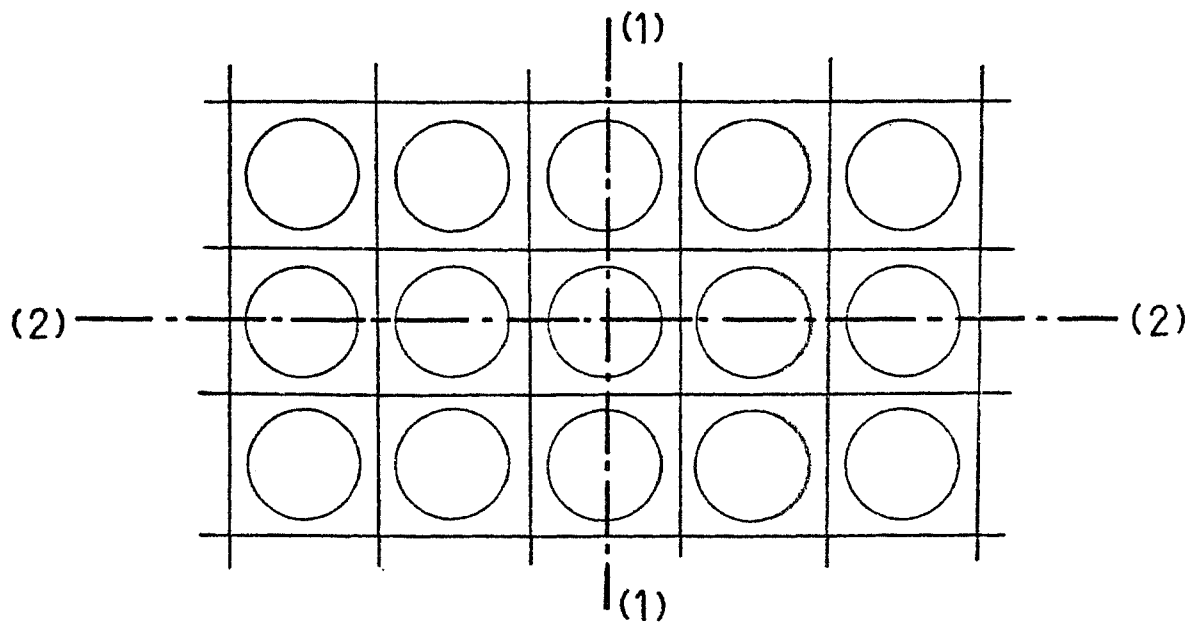


Figure 2.6 Isotropy in Square Rill Pattern

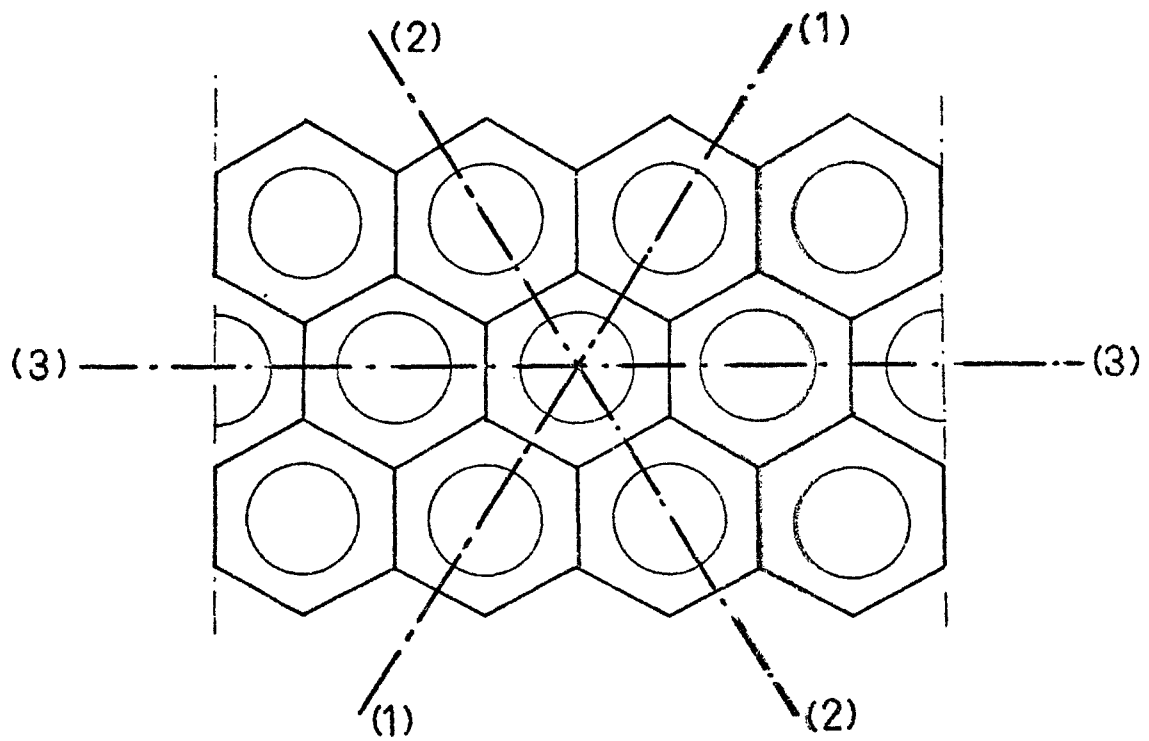


Figure 2.7 Isotropy in Hexagonal Rill Pattern

## 2.4 The Method of Zero-Crossing Analysis

A zero crossing is defined as the intersection of the continuous function,  $x(t)$ , with its mean line (Figure 2.8). Each point at which the function  $x(t)$  ceases to decline and starts to rise, or ceases to rise and starts to decline, is called a turning point. A turning point is a peak when it is a relative maximum and a trough when it is a relative minimum. The longitudinal distance along the mean line between successive zero crossings is the zero crossing distance. If there are more than one turning point in a zero crossing distance, the peak (or trough) with the largest departure from the mean line will be considered the only peak (or trough) in this distance.

The vertical distance between a peak and the mean line is the positive amplitude,  $(a_+)$ , and between a trough and mean line is the negative amplitude,  $(a_-)$ . Finally, the sum of the positive and negative amplitudes  $(a_+ + a_-)$  is the wave height and also the sum of two adjacent zero crossing distances is the wave length.

Zero-crossing analysis for long records are analyzed by means of a computer program. The first step is to identify the mean line. This can be done by the following procedure. The record is divided into  $q$  equal segments, such that each segment contains about 2 to 5 waves. For each part, the mean surface level is calculated and considered as a point at the center of the segment. Now there are  $q$  points, at the center of the  $q$  segments, and each point represents the the mean surface level within that part. The problem is to pass an appropriate curve through these  $q$  points such that it can be considered as the mean line of the record. A third degree polynomial is selected for this

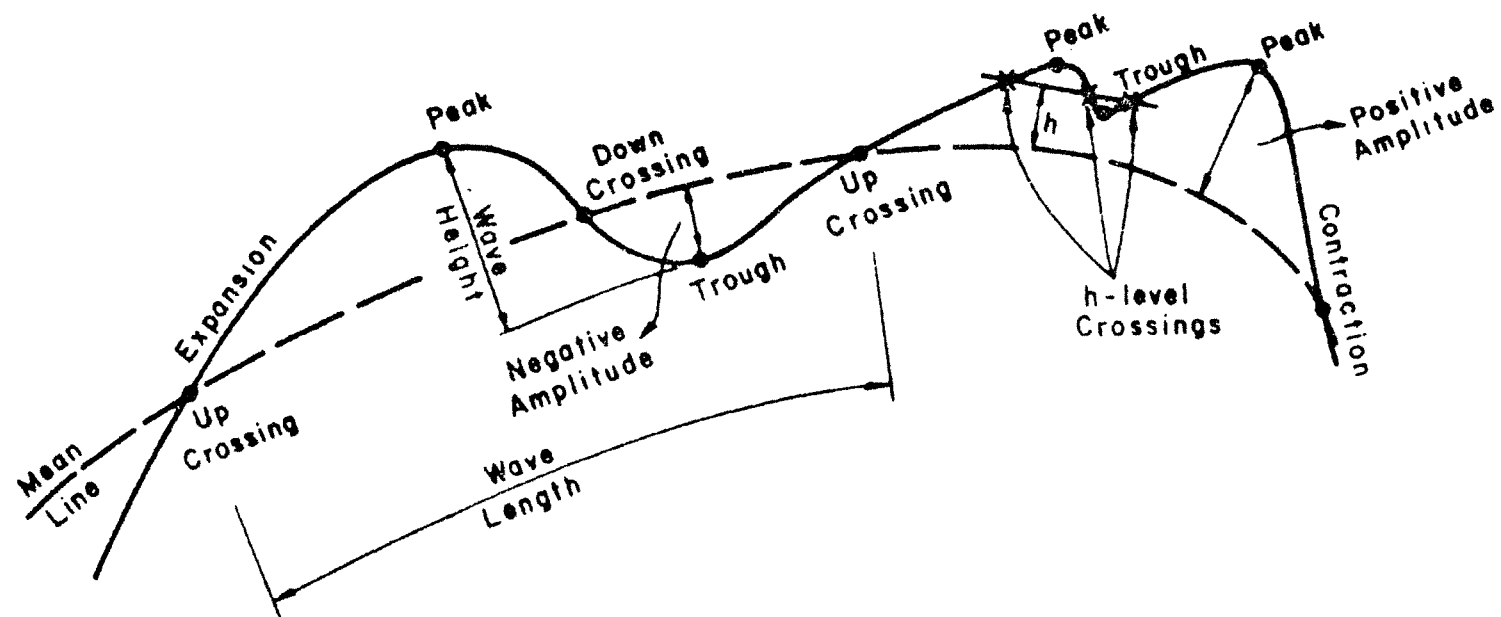


Figure 2.8 Parameters used in Zero-Crossing Analysis  
Source: Ref 19



purpose, so that not only the profile is unique and continuous, but also its first and second derivatives representing slope and curvature.

When the profile of the mean line is defined, the problem of determination of the crossings with the mean line can be reduced to the determination of the crossings of the mean-removed data with the horizontal axis. The sequence of wavelengths in any elevation trace, as shown in Figure 2.9, is represented by  $WL_1, WL_2, \dots$ . The computer program for zero-crossing analysis <sup>19</sup> provides the mean, the standard deviation, and the statistical distribution of the random variables representing wavelength,  $WL$ ; positive amplitude,  $A$ ; and negative amplitude,  $B$ .

The zero-crossing analysis was performed on the same roughness data from Wooster, Ohio. First, each one of the elevation traces was analyzed separately. Then, all of the traces were considered and analyzed as one record. The results are shown in Table 2.1. The average values for the wavelength and the waveheight are 17 cm and 29.5 mm, respectively.

The method of zero-crossing analysis can be more useful in studying the variation of the hump size. **The results** can be used to generate a random surface with a random rill pattern.

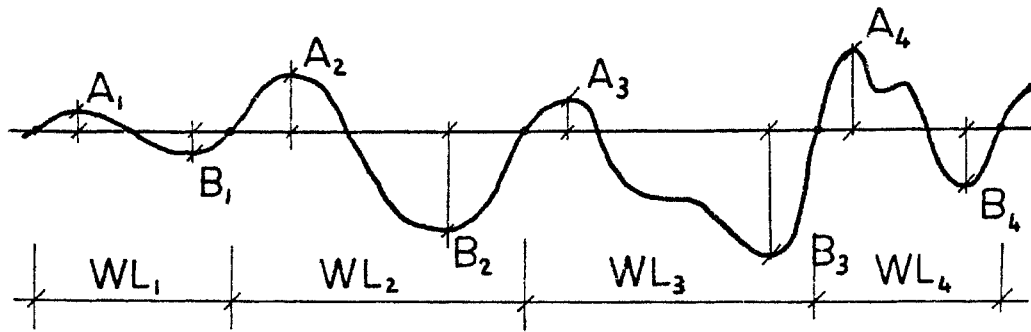


Figure 2.9 Sequences Computed in Zero-Crossing Analysis

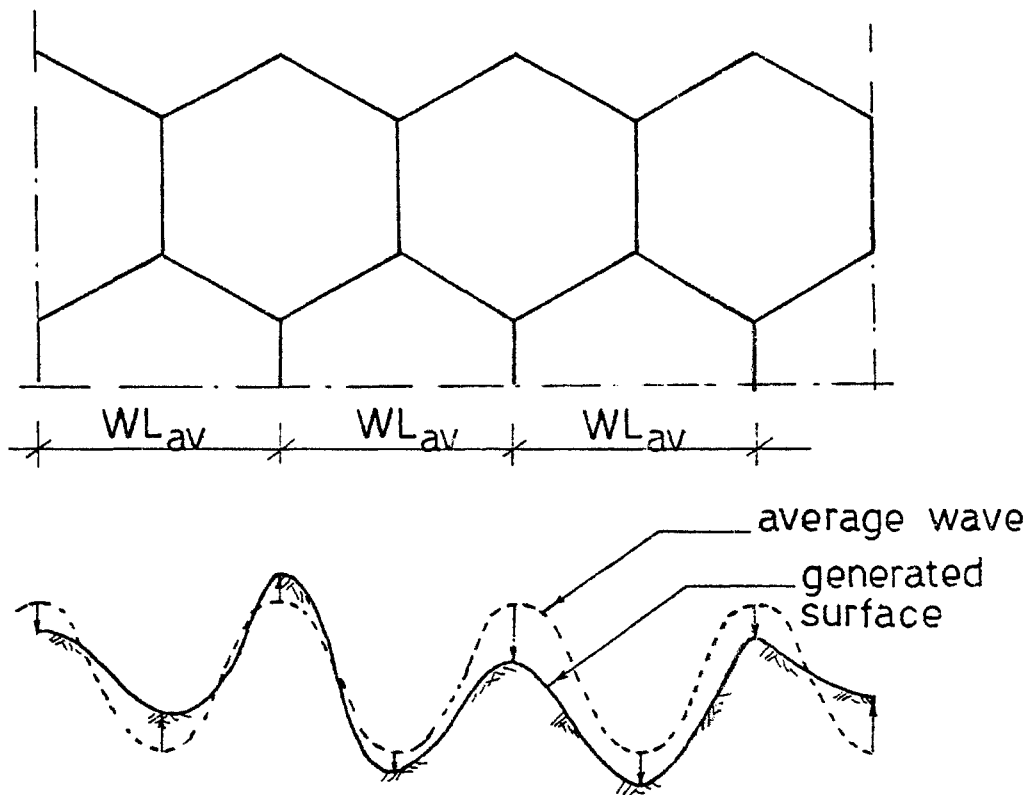


Figure 2.10 Average Wave used in Constructing a Hexagonal Rill Pattern

TABLE 2.1 RESULTS OF ZERO-CROSSING ANALYSIS

Elevation trace	MEAN VALUE			
	W L (cm)	+ Amp. (mm)	- Amp. (mm)	waveheight (mm)
Number				
1	11.04	9.60	12.99	22.59
2	13.54	14.50	15.14	29.64
3	12.89	12.16	17.96	30.12
4	12.23	12.34	12.86	25.20
5	11.28	13.19	14.92	28.11
6	27.72	14.68	22.45	37.13
7	19.53	14.19	18.56	32.75
Combined	13.96	13.52	15.23	28.75

Consider the elevation trace shown in Figure 2.9. The sequence of wavelengths can be expressed as follows:

$$\begin{aligned}
 WL_1 &= WL_{av} + X_1^1 + X_2^1 \\
 WL_2 &= WL_{av} + X_1^2 + X_2^2 \\
 &\vdots \\
 WL_n &= WL_{av} + X_1^n + X_2^n
 \end{aligned} \tag{3.2}$$

where  $X_1^i$  and  $X_2^i$  are two random components applied at the two ends of the distance,  $WL_{av}$ , in Figure 2.10.

It is reasonable to assume that  $X_1^i$  and  $X_2^i$  are two realizations of the same random variable,  $X$ . This variable is assumed to have a uniform distribution. The problem is then reduced to finding the parameters of this distribution. This can be simply done by computing, for each element,  $WL_i$ , of the wavelength sequence. The corresponding value of  $X_i$  is

$$X_i = \frac{1}{2} (WL_i - WL_{av}) \tag{3.3}$$

Then the mean and the standard deviation of  $X$  can be computed.

On the basis of the assumptions of homogeneity and isotropy, we can use the same random variable,  $X$ , in the two directions, across and along the slope surface.

## 2.5 Generation of Surface with Random Rill Pattern

The procedure to generate the surface with random rill pattern consists of the following steps:

1. Using  $WL_{av}$  as the width of the hexagon, generate a regular hexagonal mesh.
2. From the uniform distribution between the interval, (0,1), draw a random number for each nodal point. This number is used to determine the direction in which the random component of  $X$  will be applied. This is done according to the rule given in Table 2.2 below.

TABLE 2.2 DIRECTIONS OF RANDOM COMPONENT

Value of Random Number Drawn from U(0,1)	Direction of Random Component
$0.0 \leq r < 0.25$	upward
$0.25 \leq r < 0.50$	downward
$0.50 \leq r < 0.75$	left
$0.75 \leq r < 1.00$	right

3. From the uniform distribution of  $X$ , draw a random number for each nodal point. This number specifies the magnitude of the shift in the direction determined in Step (2).

4. Use the distribution of the residual data (Sec. 2.3) to generate a random component for the elevation of every nodal point.

Figures 2.11 and 2.12 show the rill patterns generated using hexagonal and random mesh, respectively.

## 2.6 Concluding Remarks

The use of the zero-crossing analysis to generate a random rill pattern may represent a better approximation of the surface. However, this irregularity imposes great difficulties in the coding of the flow-routing and erosion mechanisms. Therefore, the present erosion model uses the hexagonal mesh as a rill pattern. A limited number of calculations were made with a random rill pattern to assess the influence of rill pattern.

While the zero crossing analysis offers advantages, the present model uses the spectral analysis for analysis of the roughness data. The main reason for this is that spectral analysis allows us to recognize the relative importance of large-scale and small-scale surface irregularities. Therefore, we can define the part of the data which contributes most to the formation of the rill pattern. Moreover, the method of spectral analysis, although not fully utilized in this model, provides greater potential for improvement of surface roughness modeling.

The mechanism of selecting only one wave component of the spectrum as the basic wave created a problem in the simulation process. This

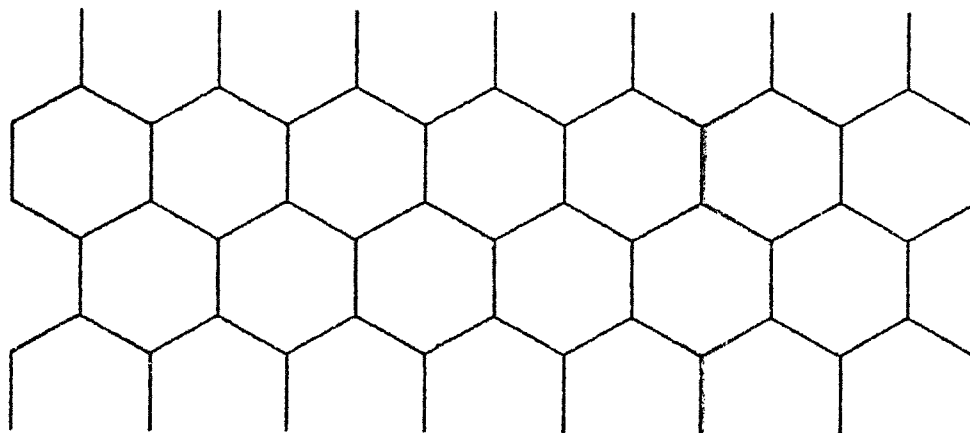


Figure 2.11 Uniform Rill Pattern

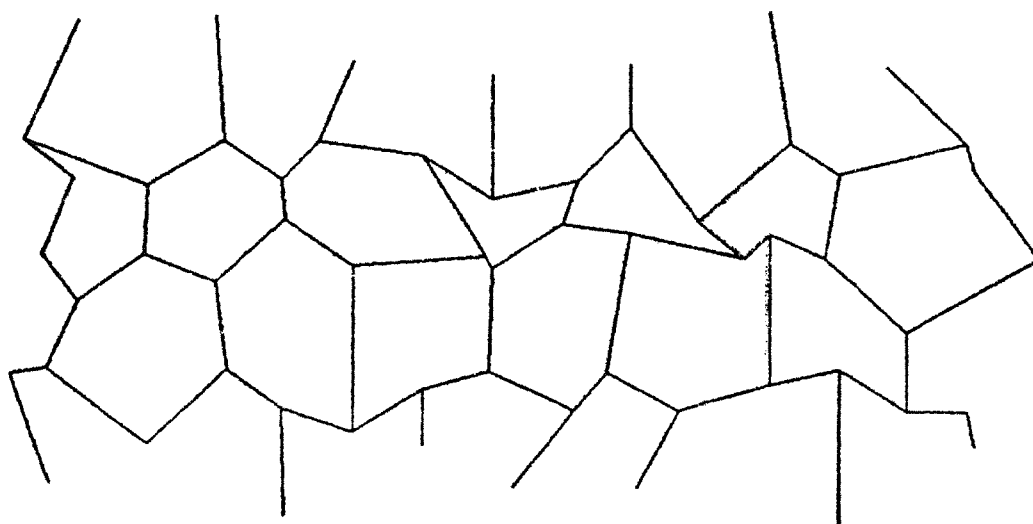


Figure 2.12 Random Rill Pattern

is because the amplitude of this wave alone is not large enough to represent the humps. We note that the average wavelength and wave height obtained by using the zero-crossing analysis are about 17 cm and 29.5 mm, respectively (see Table 2.1). This is, the average amplitude can be taken as about 15 mm. On the other hand, the length and amplitude of the basic wave as determined by spectral analysis of the same data are 18 cm and 3.7 mm, respectively. Thus the amplitude of the basic wave underestimates the height of the humps.

In the present program, the hump height is generated by a simplified solution. For a basic wave of length  $WL$ , the length of the hexagon's side is equal to  $WL / \sqrt{3}$ . If the surface is inclined with an angle of  $\theta$ , then each hump center is raised by the amount  $\frac{WL}{\sqrt{3}} \sin \theta$ . For a slope of  $20^\circ$ , which is the slope used in this analysis, the additional increment,  $\frac{WL}{\sqrt{3}} \sin \theta$ , is equal to 35 mm, about twice the average amplitude computed using zero-crossing analysis. This value is equal to 18.1 mm for a ten-degree-slope. When compared with the results of zero crossing analysis, we can see that the simplified approach represents a reasonable approximation. This procedure makes the elevation of the hump center, before we superpose the basic wave or the random component, is equal to the elevation of the highest nodal point around it. Then the basic wave and the random increments in elevation are added. Due to this randomness, some of the humps may be lower than some of the surrounding nodal points. Our model allows for some rill segments to be eliminated, depending upon the original roughness data.



### 3. EROSION MODEL

The subject of this chapter is the model for computation of erosion in rills and over interrill areas. Emphasis is placed on the development of computational procedures which are suitable for the surface model and are based on principles of hydraulics and sediment transport mechanics.

The present analysis considers only erosion of soil particles by the shearing action of flow in rills and over interrill areas. In other words, the direct detachment and transport process due to rainfall impact is not accounted for. The rainfall impact detaches soil particles from clods and causes the particles or aggregates of particles to be transported in a fashion similar to that of cohesionless soil particles (7).

Preliminary experiments were performed to measure the detachment of soil particles under the impact of raindrops. The results, presented in Appendix A, suggest that for a given soil and impact energy, a certain number of drops are required to break up a cohesive soil clod. After this the material would be transported as a cohesionless soil. Thus the erosion model presented here is general and can be adapted for cohesive soils by addition of a threshold rainfall, which is the amount required to break up the clods.

Consider the random surface composed of a matrix of humps surrounded by rills connecting the lower points. For the purpose of erosion computation, the geometrical configurations of the surface are simplified. The humps are assumed to be in the form of hexagonal

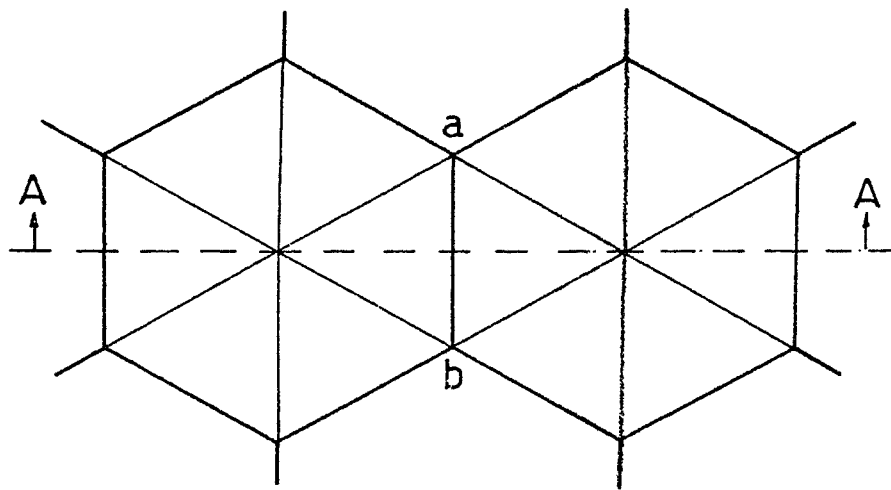
pyramids; the slope of each of the six sides is dependent upon the random outcome of surface generation. Rills are assumed to be formed of channels with triangular cross sections with the side slopes of the adjacent humps forming its boundaries, as shown in Figure 3.1. A channel between two nodal points is termed a "rill segment". In the remaining sections of this chapter, the equations of erosion of rills and of humps are derived.

### 3.1 Rill Erosion Equation

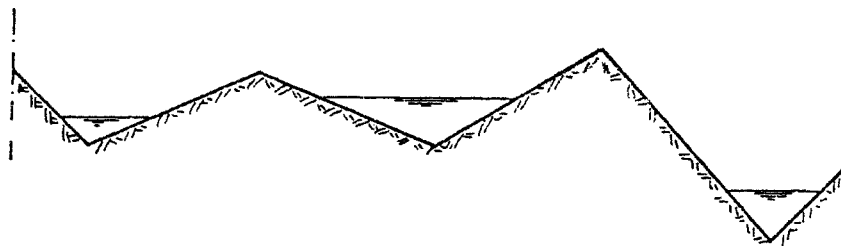
Consider a rill segment,  $ab$ , as shown in Figure 3.1(a). Let  $q_1$  be the rate of water flow received from upslope at point  $a$ , and  $q_2$  be the flow at  $b$ .  $q_2$  is greater than  $q_1$  by the amount of water drained from the two adjacent side slopes. The flow in the rill segment,  $ab$  is actually a spatially-varied flow with the rainfall acting as a lateral inflow. Researchers such as Yoon and Wenzel (41), Li et al (18), and Komura (15) have considered the overland flow as spatially-varied flow. However, since the present model deals with the erosion in short rill segments, equations of uniform flow are used.

Erosion due to rill flow is based on the concept of tractive force (10). Consider the triangular cross-section of a rill segment, as shown in Figure 3.2. The average value of the tractive force per unit wetted area, i.e., the unit tractive force,  $\tau_0$ , is given by:

$$\tau_0 = \gamma R S_f \quad (3.1)$$



a) Plan



b) Section A-A

Figure 3.1 Surface Idealization

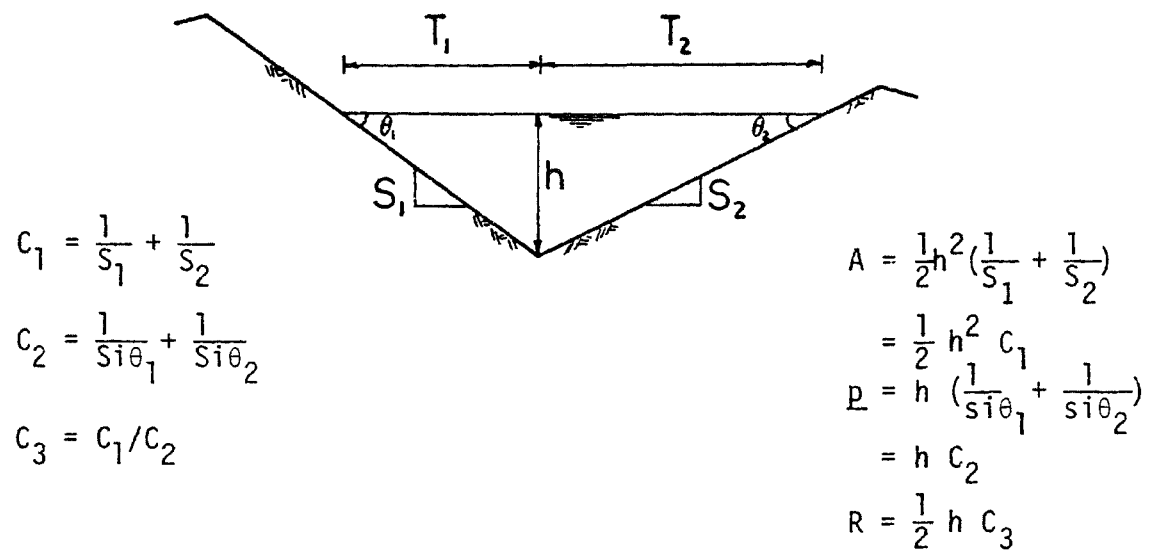


Figure 3.2 Rill Cross-section

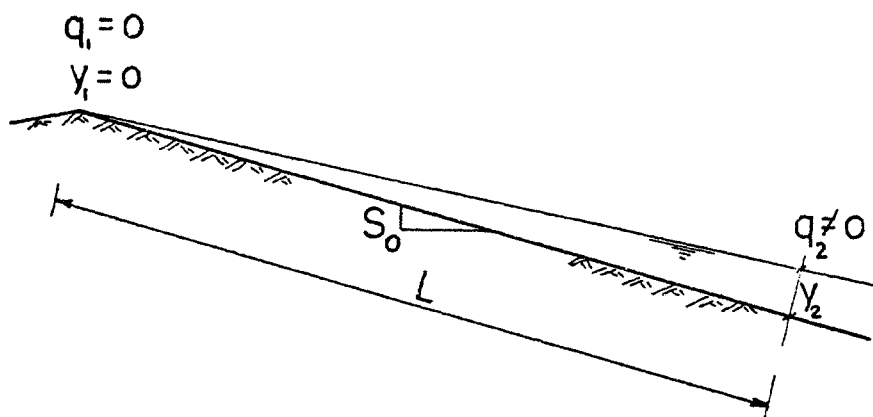


Figure 3.3 Flow Over Interrill Area

where

$\gamma$  = unit weight of water;

$R$  = hydraulic radius of the channel = Area/wetted perimeter;  
and,

$S_f$  = slope of the energy grade line.

Henderson (13) indicates that the slope of the energy line,  $S_f$ , can be approximated by the bed slope,  $S_0$ , for a mountain type channel. Using this approximation, Equation (3.1) becomes:

$$\tau_0 = \gamma R S_0 \quad (3.2)$$

According to Chow (4), the unit tractive force in channels, except for wide open channels, is not uniformly distributed along the wetted perimeter. Therefore, it is more appropriate to use the tractive force per unit length of the rill as expressed by the following equation:

$$F_0 = \tau_0 \times P = \gamma A S \quad (3.3)$$

where

$P$  = wetted perimeter; and

$A$  = cross-sectional area of the flow.

In terms of the geometrical features of the triangular cross-section, as given in Figure 3.2, we have:

$$F_0 = \frac{\gamma S_0}{2} h^2 \left( \frac{1}{S_1} + \frac{1}{S_2} \right) \quad (3.4)$$

Neglecting the variation of  $S_0$  along the segment ab, the value of  $F_0$  is then dependent upon  $h$  at any point. The values of  $h_1$  at a and  $h_2$  at b depend on the corresponding values,  $q_1$  and  $q_2$ . To obtain the flow depth,  $h$ , we start with the well-known Manning equation,

$$V = \frac{1}{n} R^{2/3} S_f^{1/2} \quad (3.5)$$

where

- $V$  = the mean velocity in meter/sec;
- $R$  = the hydraulic radius in meters;
- $S_f$  = the slope of the energy line; and,
- $n$  = the coefficient of roughness, specifically known as Manning's  $n$ .

Using the approximation  $S_f = S_0$ , and the relation  $q = V \cdot A$ , we get:

$$q = \frac{A}{n} R^{2/3} S_0^{1/2} \quad (3.6)$$

which can be expressed in terms of  $h$  as:

$$q = \left( \frac{1}{2} \frac{c_1 h^2}{n} \right) \left( \frac{1}{2} c_3 h \right)^{2/3} S_0^{1/2} \quad (3.7)$$

Therefore,

$$h = \frac{2^{5/3} n q}{c_1 c_3^{2/3} S_0^{1/2}} \quad (3.8)$$

where  $c_1$  and  $c_3$  are as defined in Figure 3.2.

The flow in rills has been so far treated as open channel flow. The flow characteristics are then used to compute the amount of soil eroded. This scheme implies that the effect of sediment already carried in the flow is not considered. That is, the concentration of sediment is assumed small enough so that the equation of motion for sediment-laden water can be approximated by the equation of motion for water only.

According to Li et al. (18), the continuity equation for sediment can be expressed as:

$$\frac{d q_s}{dx} = p_s \quad (3.9)$$

where

$q_s$  = the sediment discharge per unit width of channel, and

$p_s$  = the fine-sediment pick-up rate per unit area.

$q_s$  is a function of the flow characteristics and specifically, the flow tractive or shearing force. The bed load equation derived by Kalinske (10) is used to obtain  $q_s$ . It is expressed in the nondimensional form as:

$$\frac{q_s}{U_* D} = a_s \left[ \frac{U_*^2}{\left( \frac{\rho_s}{\rho_w} - 1 \right) g D} \right]^p \quad (3.10)$$

where

$q_s$  = the sediment discharge including suspended sediment in volume of material per unit time and unit width;

- $U_*$  = the friction velocity;  
 $D$  = the mean sediment size;  
 $\rho_s$  and  $\rho_w$  = densities of sediment and water, respectively;  
 $g$  = the gravity acceleration;  
 $a_s$  = a constant; and  
 $p$  = a dimensionless exponent.

The reasons for the use of Kalinske's equation are primarily empirical. Komura (15) used it in a mathematical model for slope erosion by overland flow and established the range of values for some parameters in the equation, when applied to overland flow. Calculations with Eq. (3.18) (Appendix B), gave results that are in reasonable agreement with measured rill erosion by Meyer (22). From theoretical considerations (40) there is no compelling reason to choose any of the existing sediment transport equations over any other.

Substituting for  $U_*$  by  $\tau_0 / \rho_w$ ,  $q_s$  can be expressed as:

$$q_s = \frac{\beta_1}{\rho_w^{(1+2p)/2}} \tau_0^{(1+2p)/2} \quad (3.11)$$

in which  $\tau_0$  = the unit tractive force and

$$\beta_1 = \frac{a_s}{\left(\frac{\rho_s}{\rho_w} - 1\right) g^p D^{p-1}} \quad (3.12)$$

Assuming that a similar relation exists between the "total" sediment discharge per unit length of the channel,  $Q_s$ , and the corresponding tractive force per unit length,  $F_0$ , Equation (3.11) can be rewritten in the form:



$$Q_s = \frac{\beta_1}{\rho_w^{(1+2p)/2}} F_0^{(1+2p)/2} \quad (3.13)$$

Similarly, the continuity equation for sediment, given by Equation (3.9), can be modified as:

$$\frac{dQ_s}{dx} = P_s \quad (3.14)$$

in which  $P_s$  is the fine-sediment pickup rate per unit length of the channel.

For a long slope, the average erosion rate per unit area is defined by Li et al. (18) as the average pickup rate along the slope and is expressed as:

$$E = \frac{1}{L} \int_L P_s dx \quad (3.15)$$

where  $L$  is the length of the slope in the  $x$ -direction. But for the short segments considered in our case,  $E$  is taken as directly equal to  $P_s$ . Accordingly, the erosion rate in volume per unit length of the channel,  $E_v$ , is given by:

$$E_v = \frac{dQ_s}{dx} \quad (3.16)$$

Taking the derivative of Equation (3.13), we obtain:

$$E_v = \left( \frac{1}{2} \frac{(1+2p) \beta_1}{\rho_w^{(1+2p)/2}} \frac{dF_0}{dx} \right) F_0^{(2p-1)/2} \quad (3.17)$$

in which  $F_0$  at any point is obtained from Equations (3.4) and (3.8), in terms of the water discharge.

Considering, again, the size of the channel, the term  $\frac{dF_0}{dx}$  can be rewritten in difference form. That is, for the rill segment of length  $\Delta L$ , the erosion rate of rills, in volume per unit time,  $E_r$ , can be expressed as:

$$E_r = \frac{1}{2} \frac{(1+2p) \beta_1}{\rho_w (1+2p)/2} \left( \frac{F_{02} - F_{01}}{\Delta L} \right) \left( \frac{F_{01} + F_{02}}{2} \right)^{\frac{2p-1}{2}} \times \Delta L$$

and the final computational form for  $E_r$  becomes:

$$E_r = \frac{1}{2} \frac{(1+2p) \beta_1}{\rho_w (1+2p)/2} (F_{02} - F_{01}) \left( \frac{F_{01} + F_{02}}{2} \right)^{\frac{2p-1}{2}} \quad (3.18)$$

where  $\beta_1$  is given by Equation (3.12) and  $F_{01}$  or  $F_{02}$  are computed from Equations (3.4) and (3.8).

### 3.2 Interrill Erosion Equation

A similar approach is used to express the erosion rate of interrill areas. The flow in this case is approximated by a sheet flow with  $q_1 = 0$  at the top and  $q_2$  at the bottom. Consider a surface with slope  $S_0$  and length  $L$ , as shown in Figure 3.3. Assume that the flow depth increases linearly downslope from  $y_1 = 0$  at the top to  $y_2$  at length  $L$ . The unit tractive force resulting from this flow at points a and b, respectively, is given by:

$$\tau_{0_1} = \gamma y_1 S_0 = 0 \quad (3.19)$$

and

$$\tau_{0_2} = \gamma y_2 S_0 \quad (3.20)$$

in which the wide-channel approximation,  $R \approx y$ , has been applied.

The flow depth is also determined using Manning's equation which gives, for this case:

$$q = \frac{1}{n} y^{2/3} S_0^{1/2} \quad (3.21)$$

The flow depth at any point is given in terms of the flow rate as,

$$y = \left( \frac{n q}{\sqrt{S_0}} \right)^{3/5} \quad (3.22)$$

Based on the continuity equation for sediment (Equation 3.9), in conjunction with Kalinske's bed load formula, an expression for erosion rate of interrill areas can be written as:

$$E_i = \frac{1}{2} \frac{\beta_1 (1+2p)}{\rho_w^{1+2p}} \frac{1}{L} \times \tau_{0_2}^{\frac{2p+1}{2}} \quad (3.23)$$

where

$E_i$  = erosion rate of interrill areas in volume per unit area per unit time;

$\beta_1$  = as given in Equation (3.12); and,

$\tau_{0_2}$  = the unit tractive force, or shear stresses, at distance L downslope, and is computed from Equations (3.22) and (3.20).

Although the water flows over the humps in a more or less radial fashion, the present analysis assumes a one-dimensional flow in the direction of the centerline of each one of the six sides of the hexagonal pyramid. Furthermore, the total amount of erosion from each triangular side is computed for the equivalent rectangle, as shown in Figure 3.4.

### 3.3 Concluding Remarks

It is important to notice that the derived erosion equations do not compare the transport capacity of the flow with its detachment capacity. The model, for simplicity, assumes that the slope surface will always provide the overland flow with an adequate sediment load. For cohesive soils this requires that rainfall impact detach sufficient soil particles to provide the sediment load. Where this requirement is not satisfied the model can be modified as described in Appendix A.

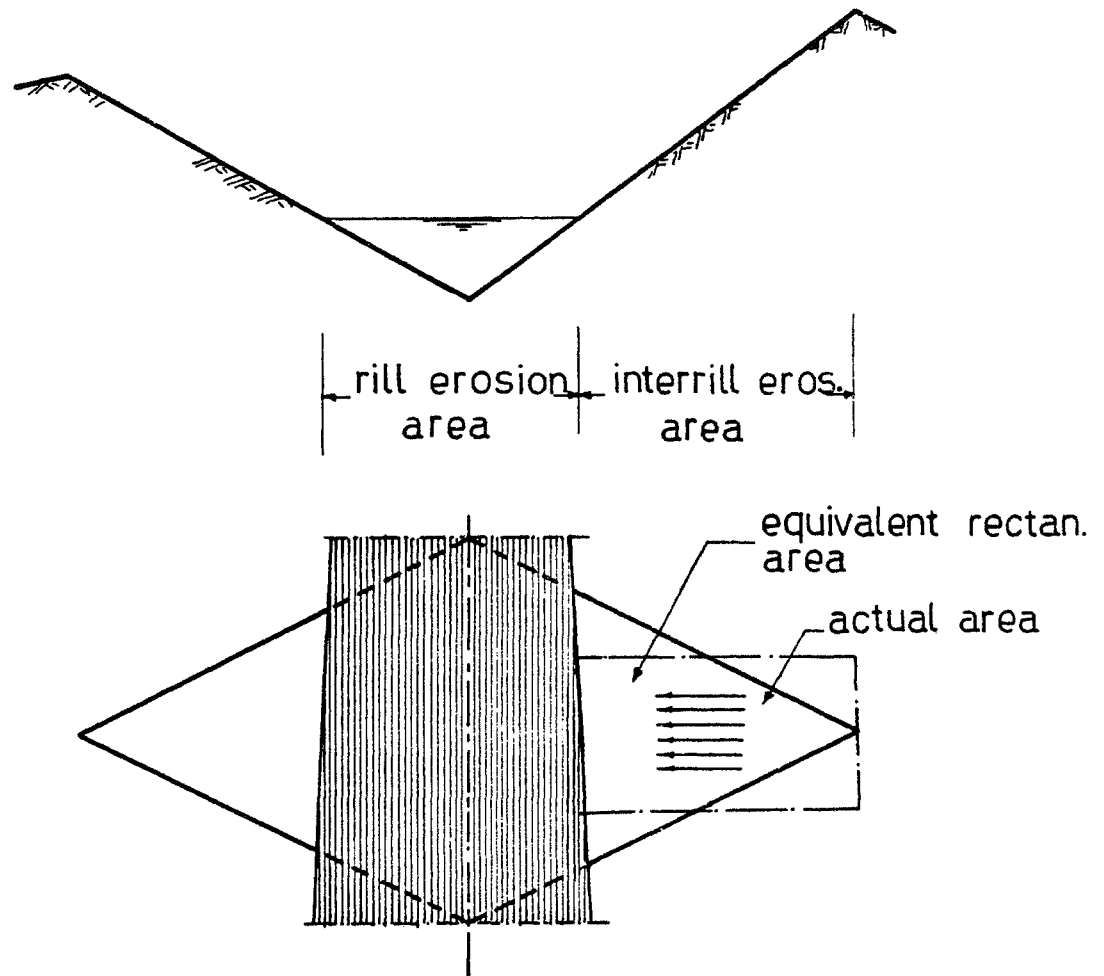


Figure 3.4 Geometrical Basis for Interrill Erosion Computation

## 4. SIMULATION MODEL

Based upon the theoretical and practical considerations discussed in Chapters 2 and 3, a computation scheme is constructed to simulate the process of slope erosion by rainfall. A random surface is first generated on the basis of the statistical properties of the original surface, as explained in Chapter 2. The overland flow is assumed to move downslope following the rill pattern created by a hexagonal mesh.

The computation schemes for simulating the main features of the model are described in Section 4.1. Those are the routing of the overland flow and the sediment load over the surface, the topographical changes due to erosion, and the changes in the process with successive time intervals. In addition, there are several auxiliary mechanisms which are very important; these are discussed in Sec. 4.2.

### 4.1 Main Features of Simulation Model

#### 4.1.1 Routing of Water and Sediment

Part of the rain falling on the test area is assumed to infiltrate through the surface layer. The rate of infiltration is known to decay with time. However, for simplicity, the model assumes a constant runoff coefficient, RNF, which is the fraction of rainfall that becomes runoff. This part is divided between the rills and the interrills, or the humps. However, the water falling on the

interrill areas, in excess of infiltration, is drained to the surrounding rill segments, as shown in Figure 4.1.

The flow in rills and its sediment load at any nodal point of the hexagonal mesh depends on its position in the mesh, as well as the random elevation. The hexagonal mesh allows for two types of nodal points, as represented by points a and b in Figure 4.1. Point a receives flow from two branches and discharges it in only one direction downslope. Whereas point b has only one inflow branch, then the flow routed downslope is divided between two branches.

The flow in rills moves forward only if the bed slope of the rill segment is positive. If the bed slope is either zero or negative, the flow routing of this rill is terminated at this point.

At points such as a in Figure 4.1, the flow merging from the two inflow branches is automatically directed to the third, the outflow branch. But for points such as b, the incoming water is divided between the outflow branches according to the ratio of the square root of the two bed slopes, i.e.,  $(S_{01}/S_{02})^{1/2}$ . This procedure complies with the slope exponent in Manning's formula as shown in Equation (3.5). As for the sediment load, we use the ratio of  $(S_{01}/S_{02})^{\frac{5}{16}(2p+1)}$  which is obtained from Equations (3.18) and (3.4) in which p is the exponent of Kalinske's bed load equation.

#### 4.1.2 Erosion of the Surface

Erosion of a rill segment affects its geometry in both cross-sectional and longitudinal directions. The amount of soil eroded by rill flow for one time interval is computed from Equation (3.18.)

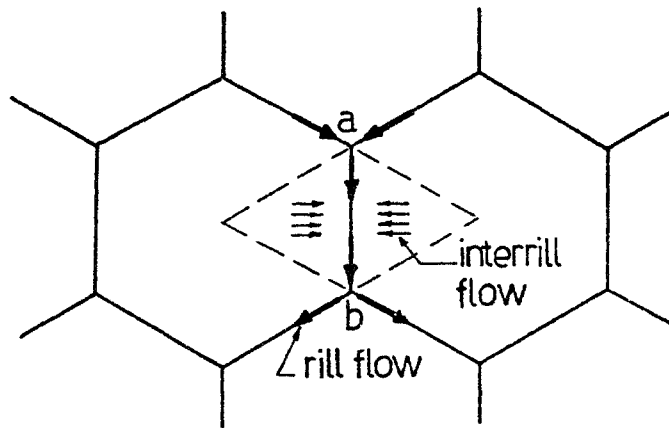


Figure 4.1 Typical Routing of Rill and Interrill Flow

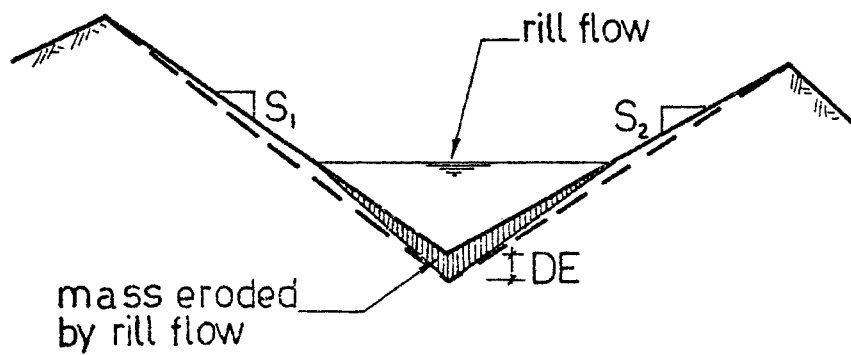


Figure 4.2 Change in Rill Geometry due to Rill Erosion



This amount is then removed from the rill cross-section as indicated by the shaded area in Figure 4.2. The bed level is then lowered by the distance, DE.

Interrill erosion is computed from Equation (3.23) for the area of the side slopes which lie above the water level. Interrill erosion is assumed to steepen the side slopes gradually. To account for this action in a simplistic manner, the new side slopes,  $S_1$  and  $S_2$ , to be considered for the next interval, are represented by the dashed lines on Figure 4.2. This is an approximation of the actual condition which results in different side slopes below and above the water. However, this approximation eliminates a computational difficulty.

In the longitudinal direction, the rill segment is assumed to be eroded uniformly. But since more than one rill segment always meet at each nodal point, the final decrease in the elevation of this nodal point is taken to be the average of the three values of DE computed for each branch.

#### 4.1.3 Temporal Change

The time-dependent nature of the erosion process is accounted for by computation of erosion for a number of time intervals. During each time interval, the elevations of all nodal points and humps remain constant. The changes in the surface geometry due to erosion are then computed at the end of the interval, and the new elevations of all points are used for the next time interval. The effect of the interval length on the model results is discussed later in Section 4.4.2

The water flow at any nodal point, during a time interval, is the sum of the rill flow arriving from upslope and the water drained

from the adjacent humps. The same mechanism applies for sediment load at any point. The total amount of sediment yield produced during any time interval is computed as the sum of sediment load at the nodal points at the bottom of the slope.

It has been mentioned earlier that runoff actually starts at different points on the surface after the rainfall rate has exceeded the infiltration rate. It is important to notice, however, that the computations begin at the time when the runoff that started at the top of the slope has reached the bottom. The amount of sediment eroded before that time is neglected.

## 4.2 Auxilliary Mechanisms

Beside the main computational schemes previously described, there is a number of auxilliary mechanisms which are very important for the simulation of the erosion process, and provide the model with more realistic features.

### 4.2.1 Ponding

Recalling the mechanism of flow routing discussed in Section 4.1.1, the flow in any rill segment moves forward only if the bed slope of the rill is positive. When the bed slope is either zero or negative, the model assumes that the water ponds and that the flow velocity becomes zero along this segment.

At the nodal points, where three segments are connected, the ponding mechanism is as follows. For a point such as a in Figure 4.3, ponding occurs when the branch ai has a slope less than or equal to zero. The inflow into segments ij and ik is then equal to zero. These

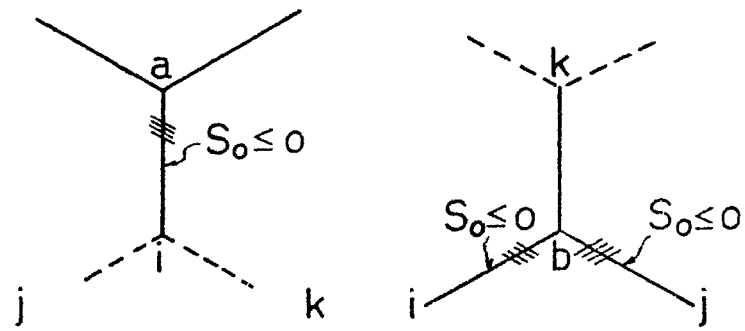


Figure 4.3 Ponding Conditions

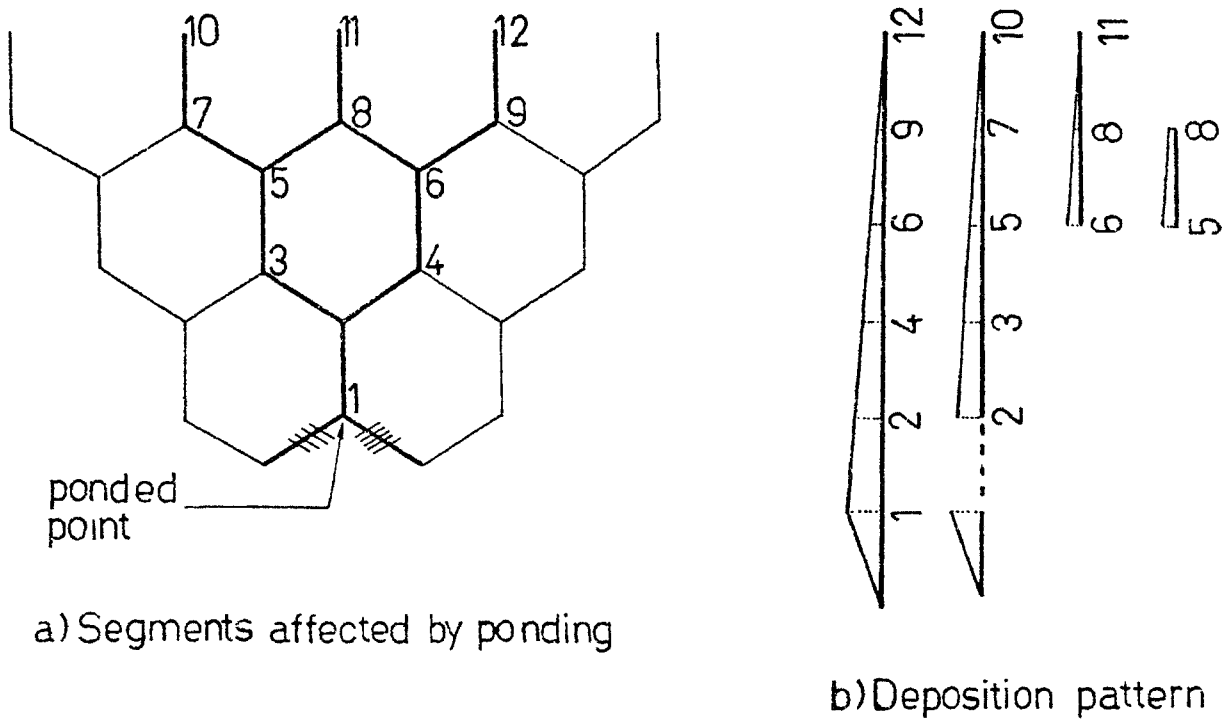


Figure 4.4 Deposition due to Ponding

rill segments then receive only water that is drained from adjacent humps. At a point such as b in Figure 4.3, complete ponding occurs only if both  $b_i$  and  $b_j$  have slopes less than or equal to zero. When only one of the two branches is ponded, then the flow is automatically routed through the other branch.

#### 4.2.2 Deposition Due to Ponding

Ponding occurs when the flow reaches zero velocity. The presence of ponding also influences the velocity of flow at points some distance upstream, and causes a reduction in the erosion rate at these points. This model uses a simplified mechanism to simulate the effect of ponding on deposition, and on reducing erosion at locations upslope.

Consider the case when ponding occurs at point 1 in Figure 4.4. This means that the bedslope of the lower branches is less than or equal to zero, and there is no other possibility for routing the flow. The flow in the segment 2.1 is assumed to approach a zero velocity at point 1. The total sediment load arriving at point 1 is then deposited on the bottom of several rill segments upstream and downstream of point 1. The pattern of depositing the sediment load is also shown in Figure 4.4. The final change in the elevation of any point is the net difference between this deposition and erosion as computed from Equations (3.18) and (3.23).

#### 4.2.3 Stability of Rills' Side Slopes

As described in Section 2.3, the process of rill development is a combination of erosion, slumping of undercut side slopes, and head

cuts. Since the progression of rill and interrill erosion steepens the side slopes, it is important to define a criterion with which we can check the stability of the side slopes at any time during the erosion process.

The stability criterion used in this model consists of a limiting gradient, SLIMIT, that a side slope can withstand. When the gradient exceeds SLIMIT, the slope fails and assumes a new, flatter gradient, SSTART. The side slopes are assumed to remain plane, before and after failure. The values of the two limits can be estimated from experience with the type of soil in question.

When a side slope fails, the top of the slope, which is the center of the hump, is lowered by a certain distance, as shown in Figure 4.5. Some of the sides of the hump may fail while others may be stable. Therefore, in computations, each side has its own elevation at its top. At the end of the test period, the final elevation of the hump center is computed as the average of the top elevation of the six sides.

The soil mass removed after each slope failure should be added to the sediment load of the rill segment in which failure occurred. Usually, the additional load cannot be carried by the transport capacity of the flow, and they require a more complicated account of deposition over the length of the rill. Therefore, these masses are presently ignored in the computation of the total sediment load. Due to this approximation, the model may be underestimating the total sediment yield.

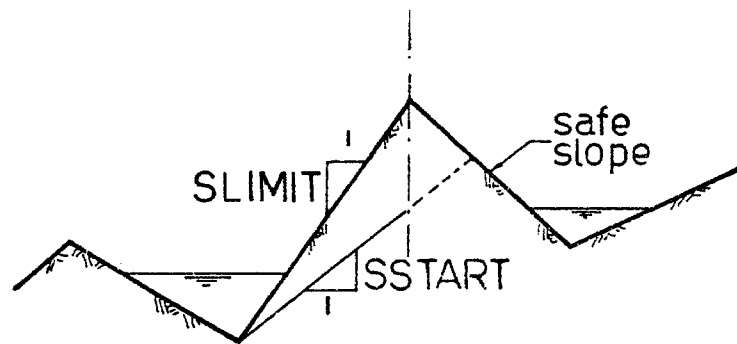
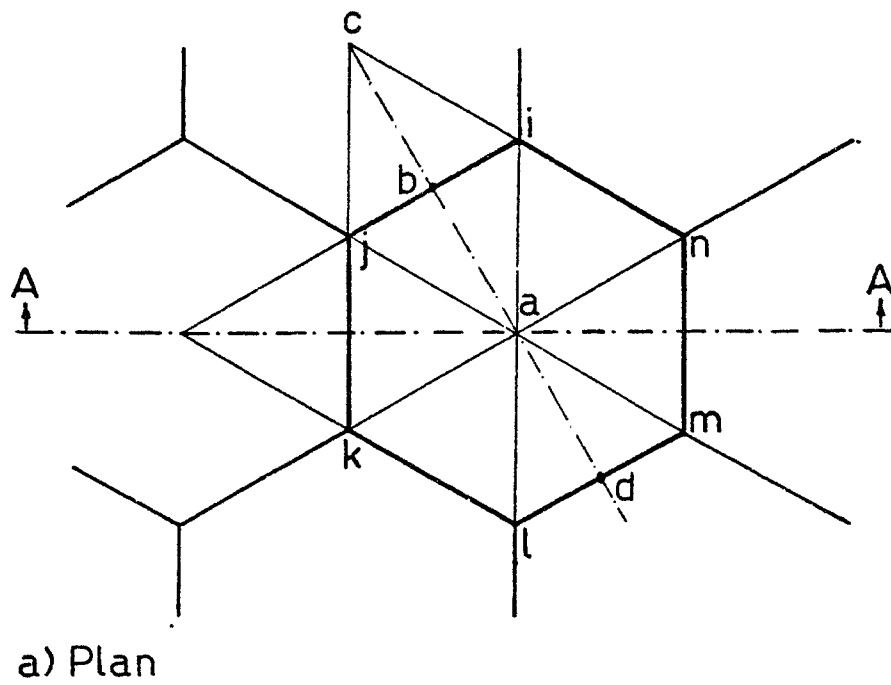


Figure 4.5 Mechanism of Side-Slope Failure

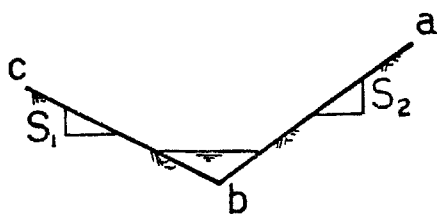


Figure 4.6 Segment with Positive Side Slopes

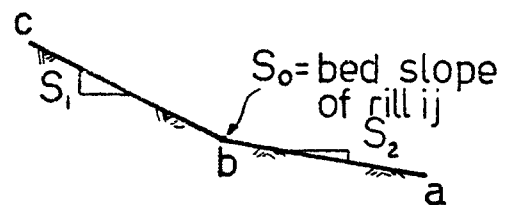


Figure 4.7 Segment with a negative side slope

#### 4.2.4 Low Humps

In this model, the elevation of a hump is usually greater than the elevations of all six nodal points of the surrounding hexagon. however, if, due to the random designation of elevations, one or more of the six points become higher than the hump center, then this hump is called a "low" hump. For example, in Figure 4.5, if point a is higher than both points i and j, then the cross-section of the rill segment ij would have the configurations shown in Figure 4.6. In this case, the two side slopes are positive. On the other hand, if point a happens to be lower than the average elevation of ij which is represented by point b, then the rill would have the cross-section shown in Figure 4.7. Such a condition prevents the development of a rill in the first place, and the flow routing is altered.

To illustrate the various possibilities that are associated with a low hump, consider the rill segment ij with the cross-section shown in Figure 4.7. The flow will move in either the direction of in or the direction ba, depending upon the slopes  $S_0$  and  $S_2$  in Figure 4.7. The flow is routed in the direction of maximum slope. On the other hand, the sign of  $S_p$  (Figure 4.8) determines whether the flow passing over the negative slope,  $S_2$ , would continue over slope  $S_p$  and join the rill flow in segment ml, or would just pond at a. Figure 4.8 illustrates the possible cases and the corresponding routing considered in each case.

<u>Sp</u>	<u>So</u>	<u>Computational mechanism</u>
(+)	$S_0 >  S_2 $	$(W_1 + h_1) + (W_2) \Rightarrow j$
(+)	$S_0 <  S_2 $	$(W_3 + h_3) \Rightarrow m1$
		$(W_1 + h_1) + (W_2) + (W_3 + h_3) \Rightarrow m1$

$W_1$ : water flowing on side slope  $C_6$   
 $h_1$ : hump erosion from side slope ab  
 $W_2$ : water flowing in rill ij  
 $h_3$ : hump erosion from side slope bc  
 $W_3$ : water flowing in side slope ba

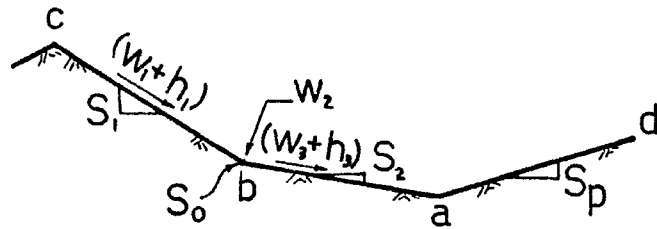

$$\begin{array}{ll} (-) & S_0 > |S_2| \quad (W_1 + h_1) + (W_2) \Rightarrow j \\ & (W_3 + h_3) \Rightarrow a; \text{ (ponding)} \\ (-) & S_0 < |S_2| \quad (W_1 + h_1) + (W_2) + (W_3 + h_3) \Rightarrow a; \text{ (ponding)} \end{array}$$

Figure 48 Possible Cases associated with the low hump situation



### 4.3 Structure of the Program

The computer program developed for the simulation model is composed of five main consecutive steps, as shown in Figure 5.9. This section presents the outlines of each computational step with the selected computer subroutines.

#### 4.3.1 The Input Data

The input data is divided into the three groups described below:

(a) Surface Roughness Data: This consists of the measured elevation traces of the original surface. The data variables of this group are:

YYP = a vector variable describing the elevation  
at all points on all elevation traces in  
sequence;

NPF = number of elevation traces;

NP = number of measurements on each trace;

DX = spacing between measurements;

TLEN = total length of the elevation trace.

(b) Physical Parameters: These are the variables describing the physical properties of the problem, used in erosion computations, namely:

UWT = unit weight of the soil, in  $\text{kg/m}^3$ ;

DMLM = representative diameter of soil particles,  
in mm;

RN = Manning's roughness coefficient;

Subroutines associated  
with different steps:

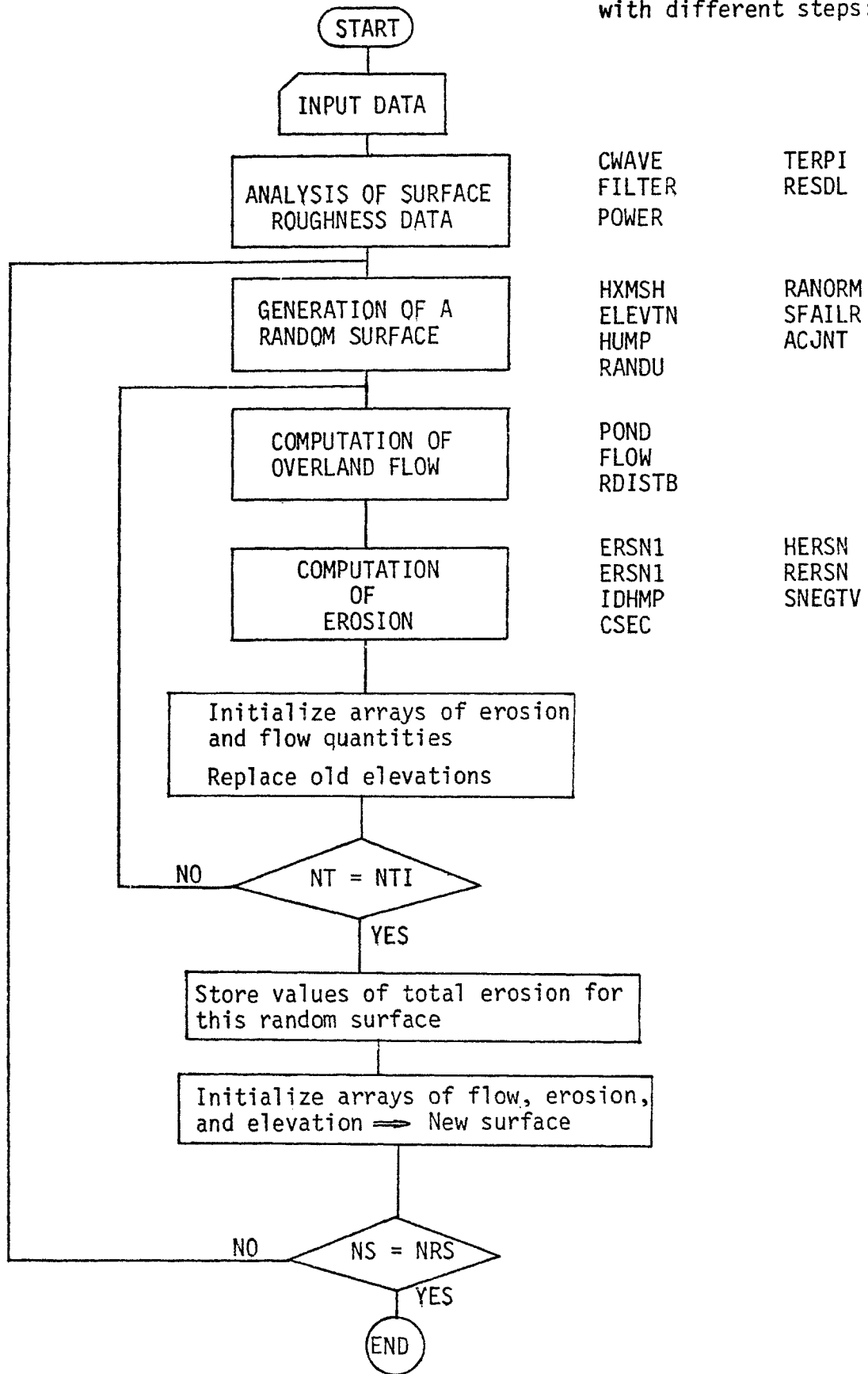


Figure 4.9 Computational Scheme

$G$  = gravity acceleration, in  $m/sec^2$ ;  
 $SG$  = soil specific weight;  
 $R0$  = water density,  $kg/m^3$ ;  
 $p$  = exponent of Kalinske's equation; see Equation (3.10);  
 $ASR$  = soil constant,  $a_s$ , in erosion equation; see Equations (3.18) and (3.12); and,  
 $ASH$  = soil constant,  $a_s$ , in interrill erosion equation; see Equations (3.23) and (4.12).

#### (c) Storm and Slope Data

$NX$  = number of nodal points in the cross-direction of the underlying rectangular mesh, see Section 4.3.3;  
 $NY$  = number of nodal points in the longitudinal direction of the underlying rectangular mesh;  
 $SLOPE$  = the average slope of the test area, in degrees;  
 $RNL$  = rainfall intensity in mm/hr;  
 $RNF$  = runoff coefficient, See Section 4.1.1;  
 $TI$  = length of time interval, in minutes;  
 $NTI$  = number of time intervals; and,  
 $NRS$  = number of random surfaces to be generated. A sample of size =  $NRS$  can then be used in any further statistical analysis.

#### 4.3.2 Analysis of Surface Roughness Data

The input to this step is the surface roughness data. The analysis is conducted in the following sequence:

1. For each of the elevation traces, remove the mean (Subroutine FILTER), then compute Fourier coefficients (Subroutine POWER). Fourier coefficients are computed using the method of Fast Fourier Transform, which is documented in the computer package called IMSL (15), and is called by Subroutine POWER,
2. Compute the average coefficients for each wave component (Subroutine CWAVE).
3. From the range of waves of length  $\leq 30$  cm, pick up the wave component with maximum contribution to total variance. Then compute the residuals from each trace (Subroutine CWAVE).
4. Compute the mean and the standard deviation of the residuals from each trace (Subroutine RESDL).
5. Compute the average mean and standard deviation for all traces (Subroutine CWAVE).

#### 4.3.3 Generation of the Random Surface

The input to this step is the amplitude, AMP, and the wavelength, WL, of the basic wave, plus the mean and the standard deviation of the residual data.

The computational procedure for generating a random surface is described as follows:

1. Compute the nodal coordinates of a rectangular mesh  $NX \times NY$  with the mesh size as indicated in Figure 4.10 (Subroutine HXMESH).
2. Assign codes to nodal points according to their location in the mesh. Points such as b are assigned code = 2, whereas points such as a are assigned code = 1. The remaining points of the rectangular mesh, such as c, are given code = 0. The hexagonal mesh is formed when points of code = 0 are eliminated, as shown by the solid lines in Figure 4.10.
3. Compute the elevations of the plane surface at nodal points using the value of SLOPE for the surface gradient (Subroutine ELEVTN).
4. Superimpose the basic wave on the plane surface according to the given values of amplitude.
5. Using Subroutines RANORM and RANDU, draw a random number for each nodal point and add it to the elevations obtained by Subroutine ELEVTN.

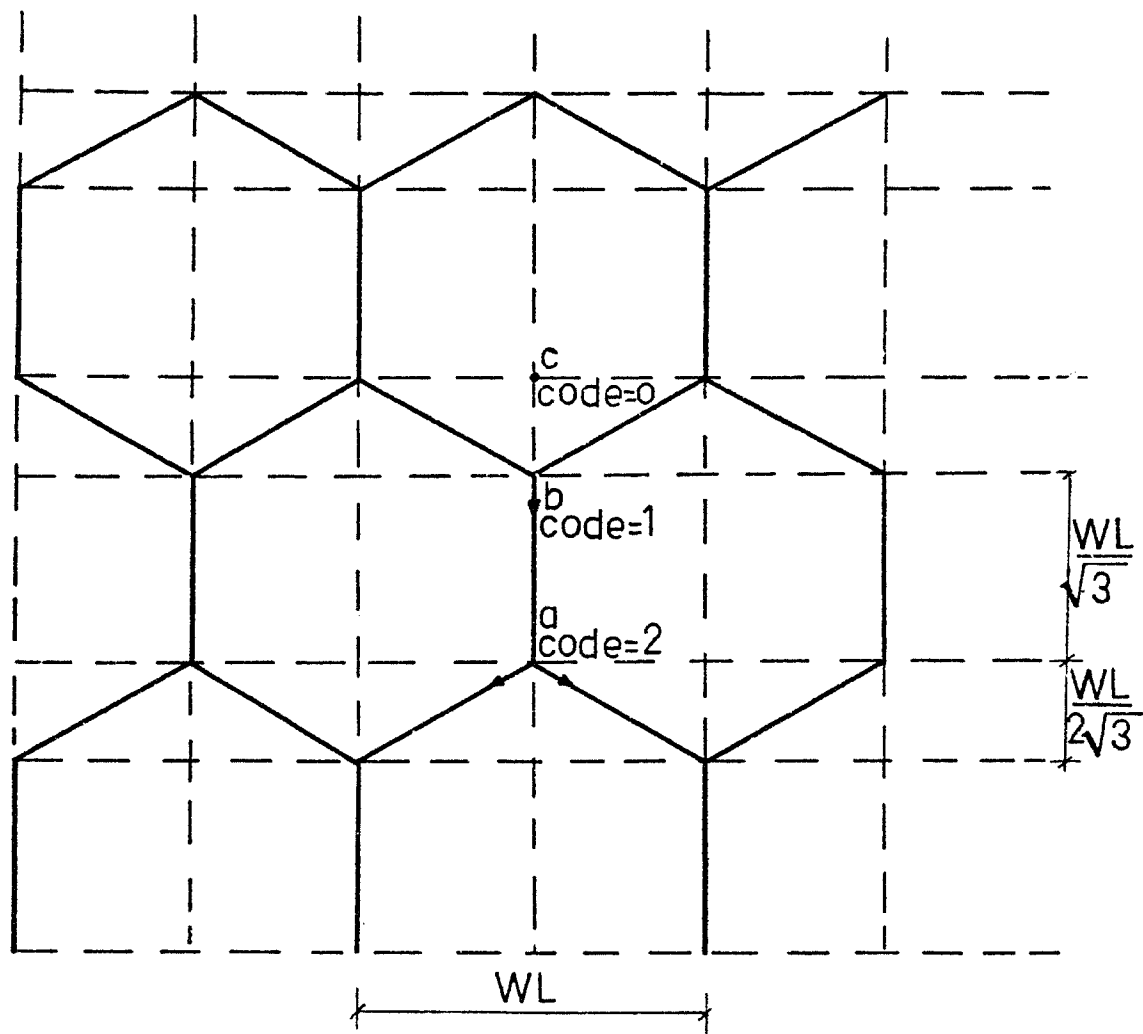


Figure 4.10 Construction of the Hexagonal Mesh

6. Draw another group of random numbers to randomize the elevations of the humps (Subroutine HUMP).
7. Check the stability of side slopes of all rill segments (Subroutine SFAILR). Criterion and mechanisms for this procedure are discussed in Section 4.2.3.

These steps generate the initial random surface, which is then subjected to overland flow and erosion.

#### 4.3.4 Computation of Overland Flow

Based on the considerations described in Sections 4.1 and 4.2, the routing of overland flow is carried out for each time interval as follows:

1. Survey all rill segments to check for ponding along any path, on the basis of the mechanisms explained in Section 4.2.1 (Subroutine POND).
2. Compute the flow at each nodal point (Subroutine FLOW).
3. When low humps exist, revise flow computations on the basis of the mechanism explained in Section 4.2.4 (Subroutine RDISTB).

#### 4.3.5 Erosion Computation

Given the elevation and the overland flow at every nodal point, the erosion in rill segments and over adjacent humps are computed. Rill segments whose upstream nodal point has code=1 are dealt with in Subroutine ERSN1. Rills whose upstream node has code = 2 are processed through Subroutine ERSN2. Computations for every rill segment are conducted in the following order:

1. For any rill segment, identify the surrounding humps which form its side slopes (Subroutine IDHMP).
2. Compute new values of bed slope and side slopes (Subroutine ERSN1, or ERSN1).
3. Determine flow depth and width in rill segment (Subroutine CSEC).
4. Compute erosion on side slopes of humps, or interrill erosion (Subroutine HERSN).
5. Compute rill erosion and the corresponding change in rill geometry on the basis of the mechanism explained in Section 4.1.2 (Subroutine RERSN).



6. Compute the total amount of soil eroded, and transported by the flow above a nodal point (Subroutine ERSN1 or ERSN2). If ponding exists along a rill path, the deposition mechanism described in Section 4.2.2 is applied.
7. Revise the distribution of sediment load at nodal points in order to account for the presence of low humps (Subroutine SNEGTV). The mechanism used in this step is explained in Section 4.2.4.
8. Calculate and store the total amount of sediment load received at nodal points at the bottom of the slope. This quantity represents the total sediment yield in a specific time interval.
9. Elevation of nodal points and humps are revised to account for erosion during the preceding time interval. Arrays of flow and erosion are initialized, in preparation for the new values of the next time interval.

The computation steps explained in Sections 4.3.4 and 4.3.5 are repeated for successive time intervals until the end of the test period. Figure 4.11 shows a schematic representation of the relation between different subroutines.

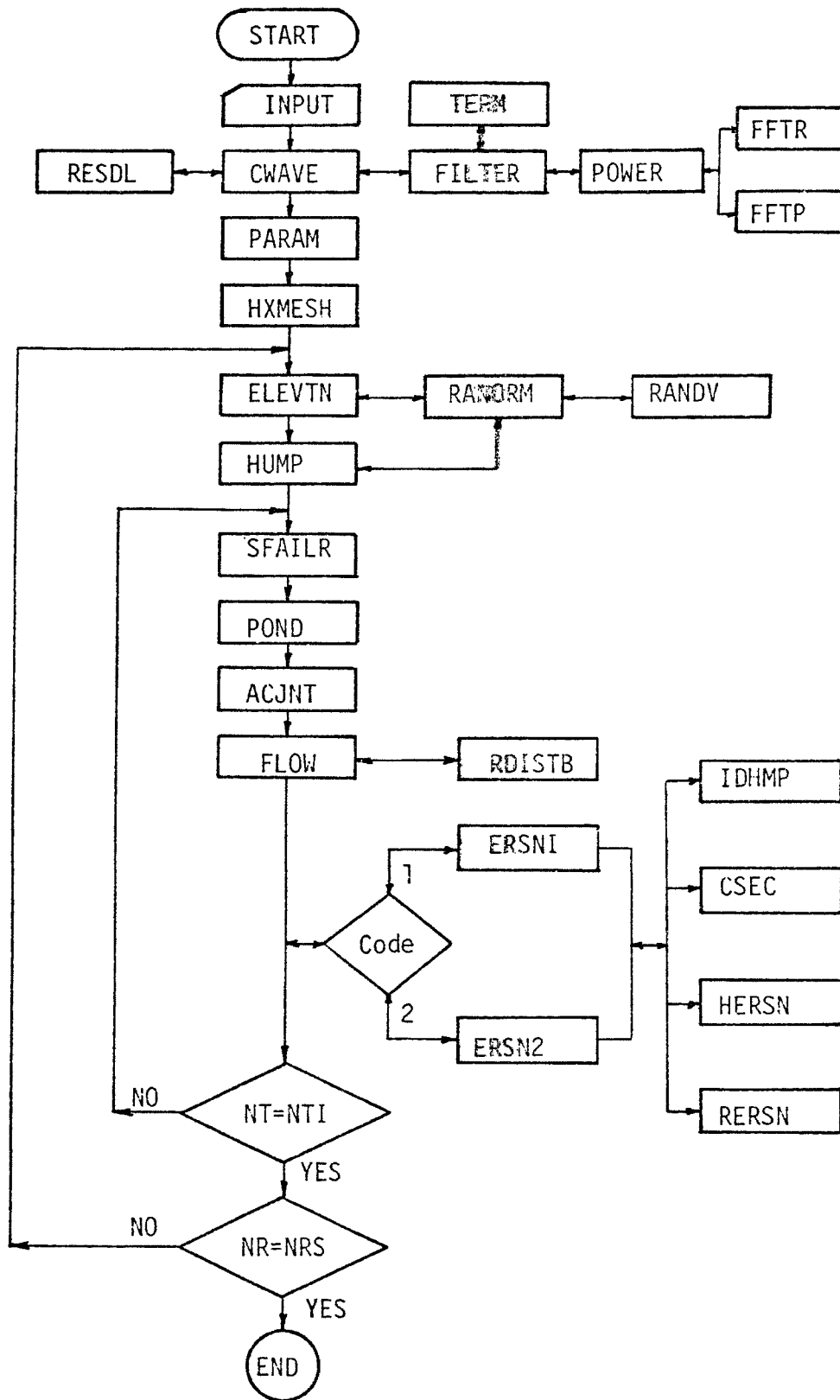


Figure 4.11 Schematic Representation of Model Subroutines

#### 4.4 Sensitivity Analysis

This section considers the sensitivity of the model to the different parameters and factors incorporated into the model. The computational procedure of the computer program is long and thus requires a preliminary study to determine reasonable limits of time and space to which the model can be applied. Accordingly, the first part of the sensitivity analysis investigates the effect of the length of time interval and the dimensions of the test area on model performance.

The second part of this analysis examines the sensitivity of the model to the important parameters in erosion equations. Those are  $n$ ,  $a_s$ , and  $p$ , which appear in Equations (3.8) and (3.12).

The last part of this chapter investigates the sensitivity of the model to randomness in the rill pattern.

In most of the cases studied, the criterion for judging the performance of the model is the shape of the curve relating the soil Erosion Rate, in  $N/m^2/hr$ , to time (ER vs. T). When relevant, we also use the relation between Rill-Interrill Erosion Ratio and time (R/I vs. T).

##### 4.4.1 Geometric Limitations

The width of the hexagonal mesh element is determined by the spectral analysis of the surface roughness and is taken to be the length of the basic wave. For a given mesh size, we study the effect of the size of the test area on model performance. Tests were conducted using a rectangular area covered by a 20 x 50 mesh (i.e.,  $NX = 20$

and  $NY = 50$ , as defined in Section 4.3.1) and a  $50 \times 20$  mesh. The results show large fluctuations in the ER vs. T curve for the  $20 \times 50$  mesh.

A closer study of the numerical scheme indicated that this phenomenon is related to ponding. If the width of the test area is small, then ponding at any rill segment, especially the ones near the bottom of the slope, causes a significant drop in the ER vs. T curve. Then, in subsequent intervals, when deposition elevates a point and removes the ponding situation, the amount of sediment reaching the bottom rises.

The ER vs. T curve for a  $50 \times 20$  mesh for exactly the same conditions has much smaller fluctuations. To keep the fluctuations small, subsequent runs are conducted using a  $65 \times 30$  mesh.

#### 4.4.2 Sensitivity to Time Interval

The study of the effect of the length of time interval is important in dynamic simulation models. Results of calculations with time intervals ranging from 2.0 to 360 minutes indicate a significant change in the shape of the ER vs. T curve with increasing time interval. The erosion rate at any time is larger for shorter intervals. This is attributed to the change in side slopes after slope failure and the effect of updating the elevations after each time interval.

To avoid excessive computation costs, a time interval of 10 minutes is used in the rest of the study. The computed erosion rate is about .80 of that for the smallest time interval of 2 minutes.

#### 4.4.3 Sensitivity to Parameters in Erosion Equations

The erosion model approximates the flow in rills and over interrill areas by a uniform flow, as expressed by the Manning equation (Equation 3.5). Therefore, it is important to investigate the effect of Manning's coefficient on the results of the model. Other important parameters in the erosion models are the exponent,  $p$ , and the constant,  $a_s$ , in Kalinske's bed load equation (Equation 3.10). However,  $a_s$  for rill erosion may be considerably different from  $a_s$  for interrill erosion. Therefore, ASR is used to denote  $a_s$  in the rill erosion equation, (Equation 3.18) and ASH is used in interrill erosion equation (Equation 3.23).

Table 4.1 indicates the values adopted for different parameters in the sensitivity analysis.

##### 4.4.3.1 Coefficient $n$ in Manning's Equation

The value of  $n$  is strongly dependent on the roughness of the surface over which water flows. Values of  $n$ , for a variety of cases, are reported by Chow (4). However, because of the small scale at which the erosion problem is analyzed, it is very difficult to choose the appropriate values of  $n$ . To test the model, values of 0.02, 0.03, 0.04 and 0.05 were used for  $n$ . As shown in Table 4.1, when other parameters were tested,  $n$  was taken to be 0.04.

TABLE 4.1 PARAMETERS USED IN SENSITIVITY ANALYSIS

Parameters Fixed During the Analysis	Parameters Varied During the Analysis*
NX x NY = 65 x 30	N = 0.02, 0.03, (0.04), 0.05
RNL = 64 mm/hr	ASR = 200, 300, (400), 500
RNF = 0.5	ASH = 10, (20), 30, 40
TTIME = 6 hours	P = (1.5), 1.75, 2, 2.5
TI = 10 min.	SLIMIT = 1.1, 1.2, 1.3, (1.4)
D = 0.01 mm	
SLOPE = $20^{\circ} \approx 37\%$	
SSTART = 1,1	

\* Values in parentheses are used when testing other parameters.

The ER vs. T curves for different values of  $n$  are shown in Figure 4.12. In general, the erosion rate increases with the increase of  $n$ . The fluctuation of the ER vs. T curve increases with  $n$ . This can be attributed to the effect of the ponding mechanism, since with higher erosion rate, associated with increasing  $n$ , the flow carries more sediment and ponding becomes more important.

The effect of Manning's coefficient on the rill-interrill erosion characteristics is shown in Figure 4.13. This effect varies with time during the test period. At late times, when erosion is sufficiently accelerated, higher values of  $n$  result in higher rill-interrill erosion ratio. The reason for this is explained below.

The erosion mechanism as described in Section 4.1.2 directly relates the erosion of the bed of a rill with the erosion from its sides. That is, if a rill bed is lowered by a certain distance, the slopes of the sides are increased by a corresponding amount. But the increase in the slope of the bed is less than that of the sides because erosion lowers both ends of the rill segment, although by different amounts. Therefore, the rill erosion actually increases the interrill erosion of adjacent humps more than the rill erosion in the segment itself. Since rills comprise only a small fraction of the surface, the progress of erosion results in a continuous reduction in the rill-interrill erosion ratio.

After a time interrill erosion causes the side slopes to reach failure limit (SLIMIT). Subsequent interrill erosion will be significantly reduced, causing the rill-interrill erosion ratio to increase

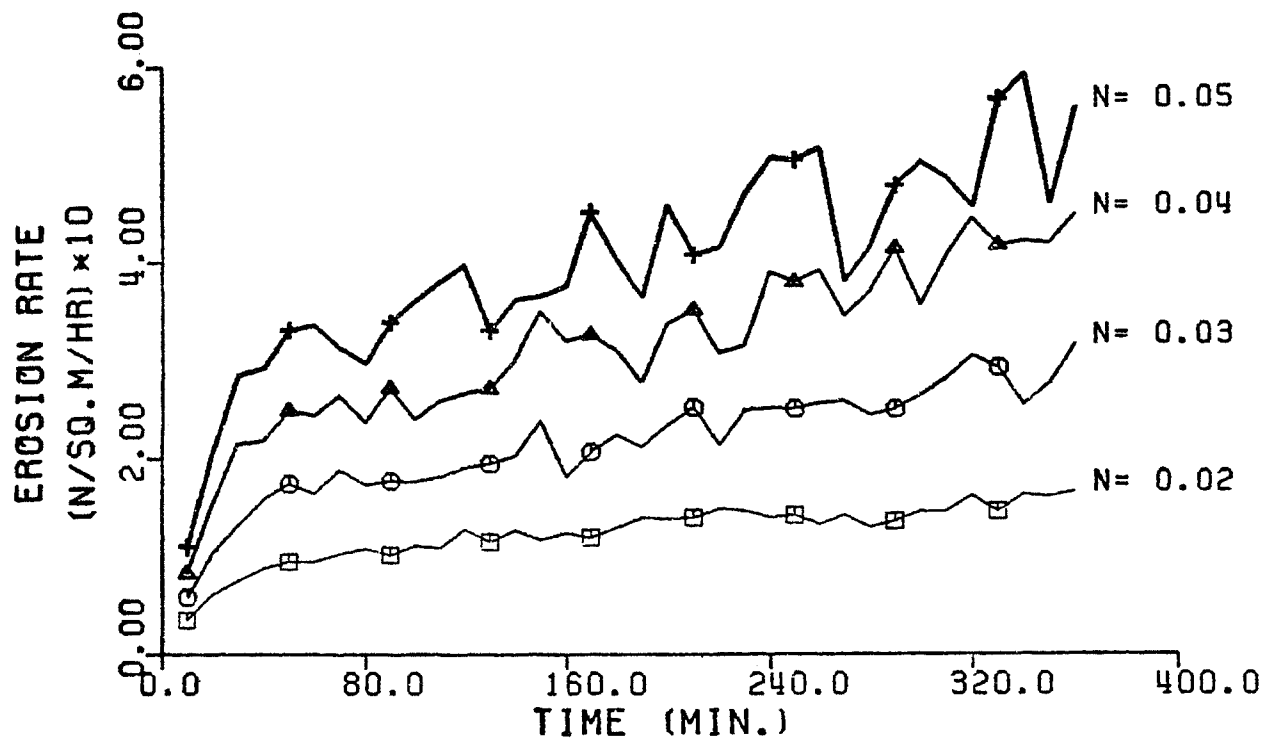


Figure 4.12 Effect of Manning's Coeff. on erosion rate

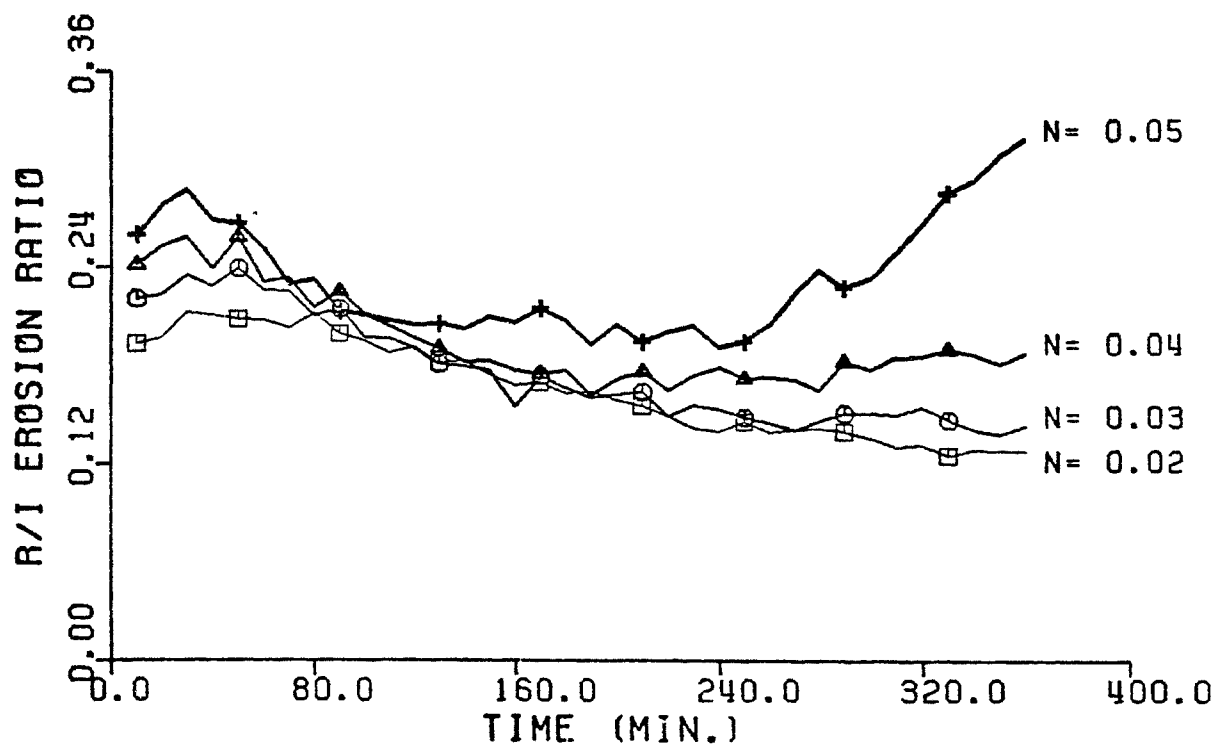


Figure 4.13 Effect of Manning's Coeff. on R/T Erosion ratio



for the rill segment in question. Thus, we can see that the overall R/I ratio will decrease with time until side slope failure begins to affect a large enough number of humps in every time interval. At this point, interrill erosion ceases to increase, while the rill erosion continues to increase, and the trend of the R/I vs. T curve is reversed. The time at which the R/I ratio begins to increase depends on parameters which control erosion. In this test, higher values of  $n$  result in greater erosion rates, and shorten the time to reach this point. We can see from Figure 4.13 that the R/I ratio begins to increase at 240 minutes where  $n = 0.05$ . When the test period is extended for the case of  $n = 0.04$ , the R/I ratio begins to increase after about 380 minutes.

In summary, we find that, within the tested range, i.e., 0.02 to 0.05, the model is sensitive to Manning's coefficient. Its value affects both the total erosion rate, and the rill-interrill erosion ratio.

#### 4.4.3.2 The Constant $a_s$

According to Komura (15'), the value of  $a_s$  when rills and gullies exist (denoted by ASR), is about 300. For interrill erosion,  $a_s$  (denoted by ASH) takes on a value of about 30.

The sensitivity to ASR was tested for values equal to 200, 300, 400 and 500. When other parameters were tested, ASR was taken to be 400. It was found that the model is not sensitive to the value of ASR.

The second test used ASH values of 10, 20, 30 and 40. When other

parameters were tested, ASH was given a value of 20. The erosion rate generally increases with the increase of ASH. The maximum erosion rate for ASH = 40 is about three times that for ASH = 10.

#### 4.4.3.3 The Exponent $p$

The parameter  $p$  is an empirical exponent in the Kalinski equation (3.10). For open channels, Kalinske and Brown (see ref. 31) suggest a value of 2 for  $p$ .

To investigate the effect of  $p$  on the model, erosion was computed for  $p$  values of 1.5, 1.75, 2.0, and 2.5. It was found that smaller values of  $p$  result in higher rates of erosion. The erosion rate is sensitive to  $p$  and increases about 10 times when  $p$  is reduced from 2.5 to 1.5. The R/I ratio is less sensitive but generally, smaller values of  $p$  produce higher rill-interrill erosion ratio. For example, at the end of the test, R/I ratio for  $p = 1.5$  is twice as much as that for  $p = 2.5$ ,

#### 4.4.4. Sensitivity to Criterion of Side Slope Failure

The mechanism of side slope failure, although simple, is very important in erosion simulation over longer time periods. The two controlling factors are the upper and lower limits of the slopes, SLIMIT and SSTART, respectively.

The purpose of this test is to study the behavior of this model under different values of the quantity (SLIMIT - SSTART). To do so, SSTART was assigned a fixed value of 1.1, whereas SLIMIT varied from 1.1 to 1.4. The influence of this factor on the erosion rate is

shown in Figure 4.14. The sensitivity of the model to the quantity (SLIMIT - SSTART) is generally low, but it increases somewhat as the erosion progresses.

#### 4.4.5 Effect of Randomness in Elevation

This part of the analysis is aimed at studying the sensitivity of the model to the randomness in elevations of nodal points on humps. Therefore, a comparison is made between the model results when randomness is included and when it is omitted in the slope surface.

The case when randomness is included can be represented by the results in Figure 4.14, described in the previous section. The test is repeated under the same conditions, except with the random component set equal to zero. The latter scheme results in a surface with identical humps. Furthermore, all rill segments emerging out of a nodal point of code - 1 will have a bed slope equal to the average slope.

Figure 4.15 shows the relationship between the erosion rate and time for the uniform surface. In comparison with the results in Figure 4.15, we can see that the uniform surface produces higher rates of erosion at all times. The erosion rate increases nearly uniformly with time, with little or no fluctuation, depending on the value of SLIMIT. It seems obvious that the non-random case presents a surface with less "obstacles", and with no possibility of ponding along rill paths. Thus, water flows downslope in identical channels, resulting in uniform erosion of the surface. It is therefore possible

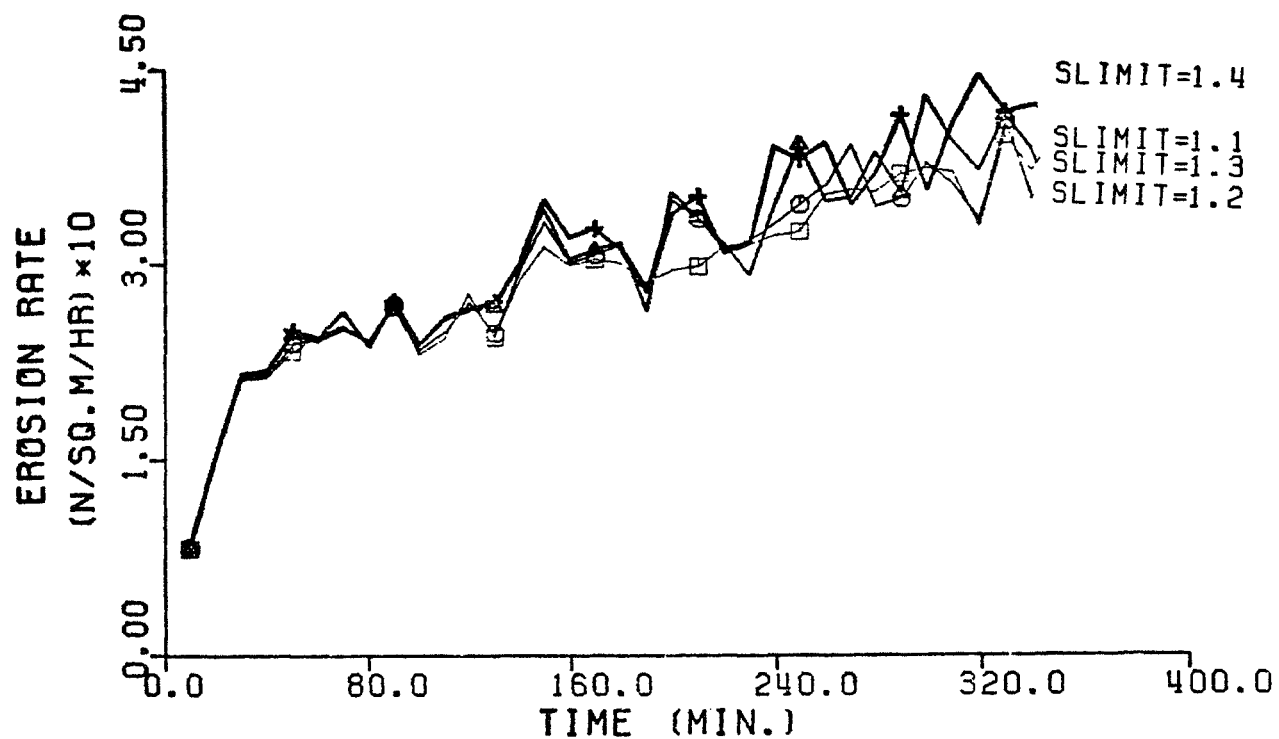


Figure 4.14 Effect of the factor SLIMIT on Erosion Rate

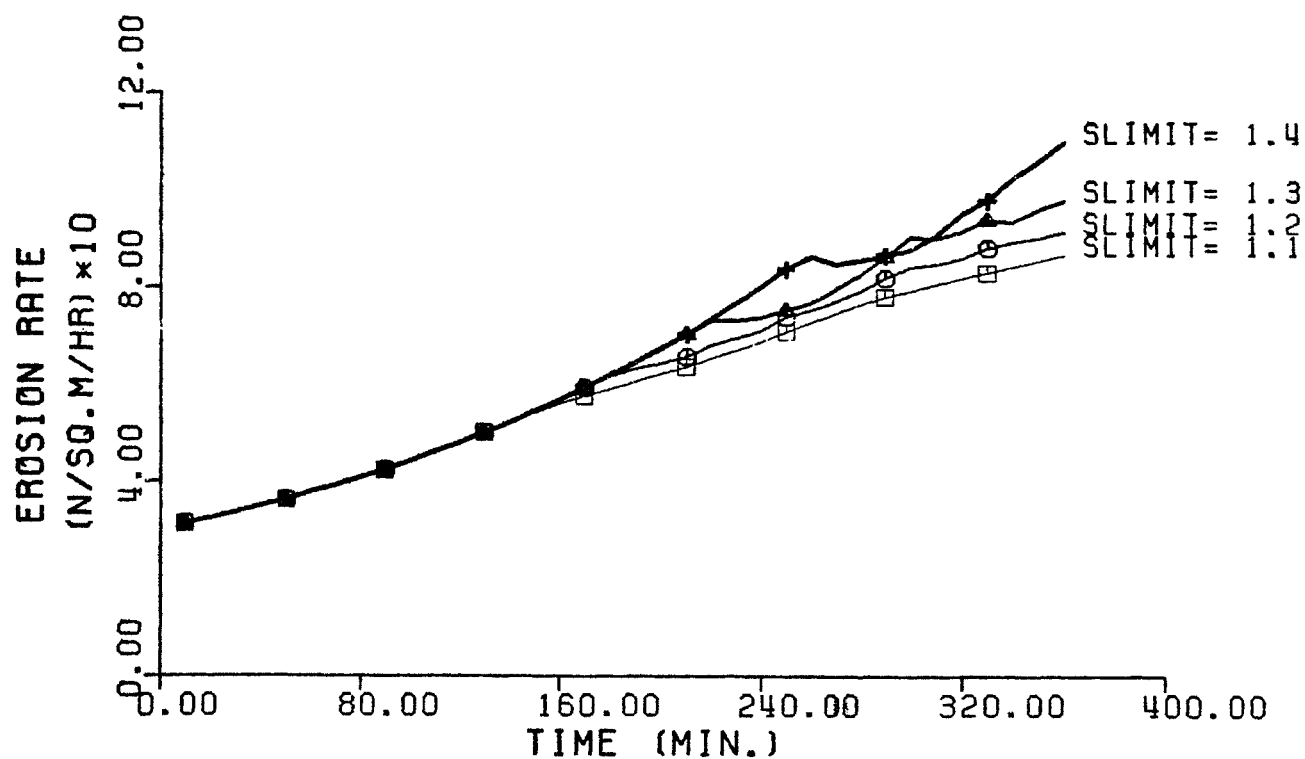


Figure 4.15 Effect of randomness in elevation on erosion rate

to conclude that the randomness in elevations of the surface points has a considerable effect on the results of the model.

Further examination of the shape of the erosion rate curve provides better understanding of the way the mechanism of side slope failure operates. Figure 4.15 represents the results of four identical surfaces, but with different limits for the side slope failure. In the case of  $SLIMIT = 1.1$ , the erosion rate increases uniformly with time for a period of about 160 minutes. At this point, the side slopes of all rill segments reached the limit ( $SLIMIT$ ), and the rate of interrill erosion remains the same with time. The total erosion rate, however, continues to increase, with a lower rate, due to the increase in rill erosion.

#### 4.4.6 Effect of Randomness in Rill Pattern

As described in Section 2.2, the surface of a new soil slope consists of many humps and depressions. The actual path of overland flow is quite irregular, at least in the early stages of erosion, before well-defined master rills are formed (Horton, 12).

The hexagonal rill pattern is an important simplification. Hence, an attempt was made in this section to compare the performance of the model with that of a model using a random rill pattern.

The random rill pattern is generated according to the procedure described in Section 2.4.2, using the results of zero-crossing analysis. The amount of soil eroded at any point is directly dependent on the flow characteristics at this point. Therefore, instead of comparing amounts of soil eroded, we can use the flow as a basis for comparison.

Consequently, the problem is reduced to a comparison between water quantities flowing in different rill segments. Such comparison is far from being complete, yet it serves as an indication of the potential effect of the rill pattern.

The random surface used in the comparison covers an area of  $NX = 15$  and  $NY = 8$ , with an average slope of 20 degrees. For the random rill pattern, the surface was generated according to the procedure described in Section 2.5. . For simplicity, we assume a unit amount of water to be drained into each rill segment from adjacent humps. At nodal points, the flow is also divided between different segments according to the rules described in section 4.1.1.

Because the rill flow increases downslope, we must compare the flow in rill segments at the same position on the slope. Two samples in each surface are selected to make the comparison. The first sample consists of the rill segments of the 4th "row" from the top. The second sample consists of rill segments in the 6th "row". The location of samples are shown in Figures 4.16 and 4.17. Each sample contains 14 segments.

Figures 4.18 and 4.19 show the distributions of the flow obtained in each case. The results indicate that the null hypothesis,  $H_0$ , that the two samples belong to the same distribution, is rejected in the test on the 4th row. The same hypothesis, however, is accepted in the other test. The significance level in both tests is 0.05. It can be seen from Figures 4.18 and 4.19 that the distribution of rill flow using uniform rill pattern has larger variation. It is not possible, however, to draw more specific conclusions about the overall

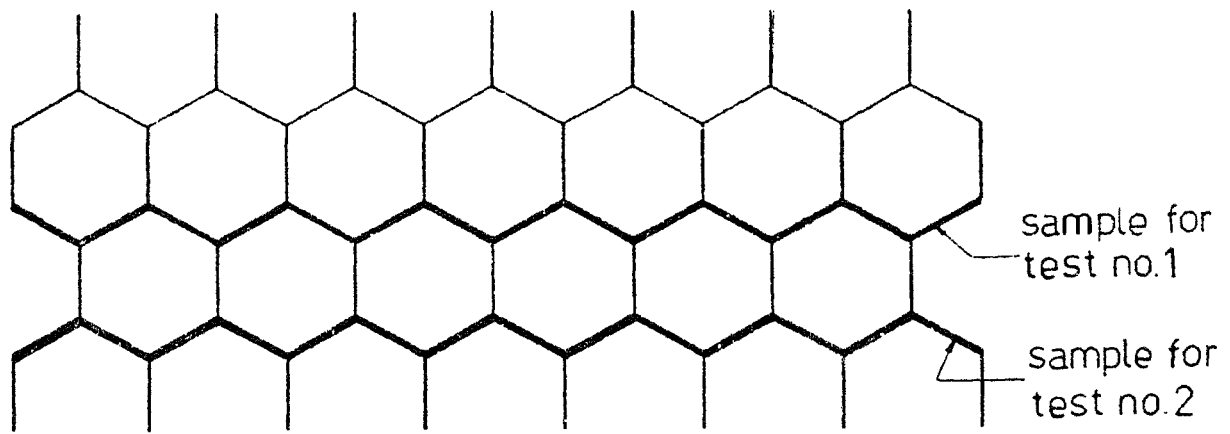


Figure 4.16 Test Samples from Uniform Rill Pattern

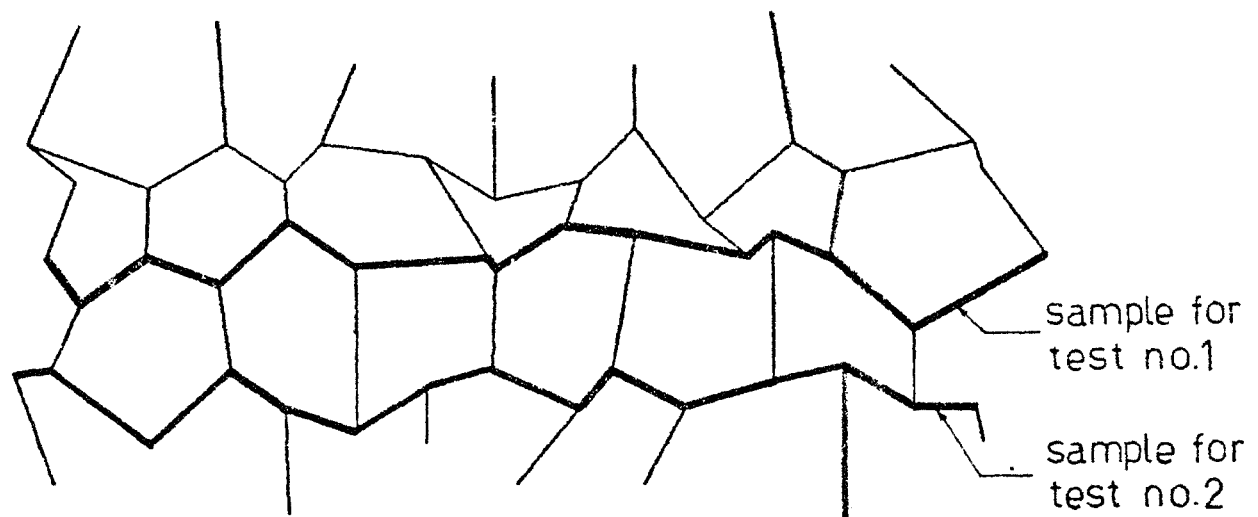


Figure 4.17 Test Samples from Random Rill Pattern

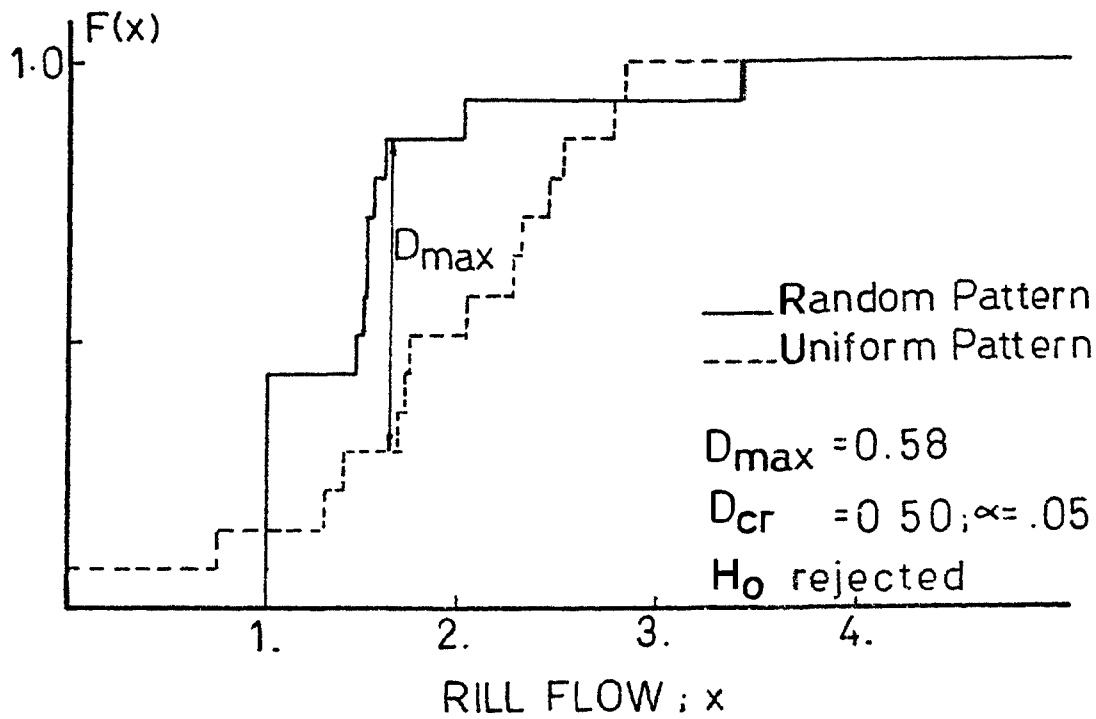


Figure 4.18 Effect of Rill Pattern Randomness on Flow; Test no. 1

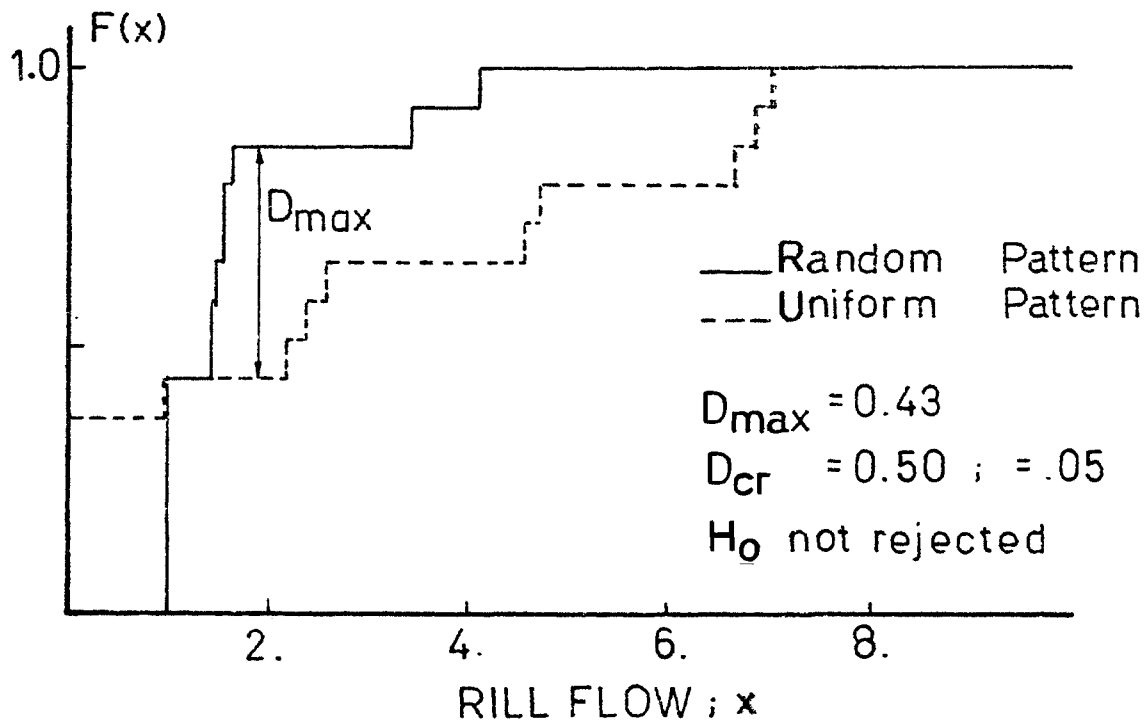


Figure 4.19 Effect of Rill Pattern Randomness on Flow; Test no. 2



effect of randomness in rill patterns on the model performance.

#### 4.5 Concluding Remarks

The simulation model described in this chapter represents a simplification of the real process. The sensitivity tests have shown that the erosion rate is very sensitive to Manning's coefficient  $n$  and the parameter  $p$  in Kalinske's equation. Thus refinement of the erosion model would rely heavily on improvements in basic understanding of overland flow and sediment transport.

The most important characteristic of the model is the attempt to account for the randomness of rill flow caused by random surface roughness. The auxiliary mechanisms of ponding and low humps add to the randomness. Beginning with the mesh shown in Figure 4.20(a) without any random component on the surface elevations, the cross section would be A.A. When the random component of elevation is imposed, profiles such as those in Figure 4.20(c) and (d) may be obtained. In the first, the random components alter the heights of points on the profile, yet the original rill pattern is basically the same, with minor differences only in the size of the rills. On the other hand, if some points such as 3 and 7 have relatively large negative random components, low humps are created and this results in a different rill pattern, as shown in Figure 4.20(d). Thus the uniform hexagonal mesh serves only as a reference frame for computations and does not impose a fixed rill pattern. The fact that the flow for the hexagonal rill pattern has a larger variance than that for the random rill pattern suggests that the hexagonal pattern does not impose serious restrictions on the flow pattern.

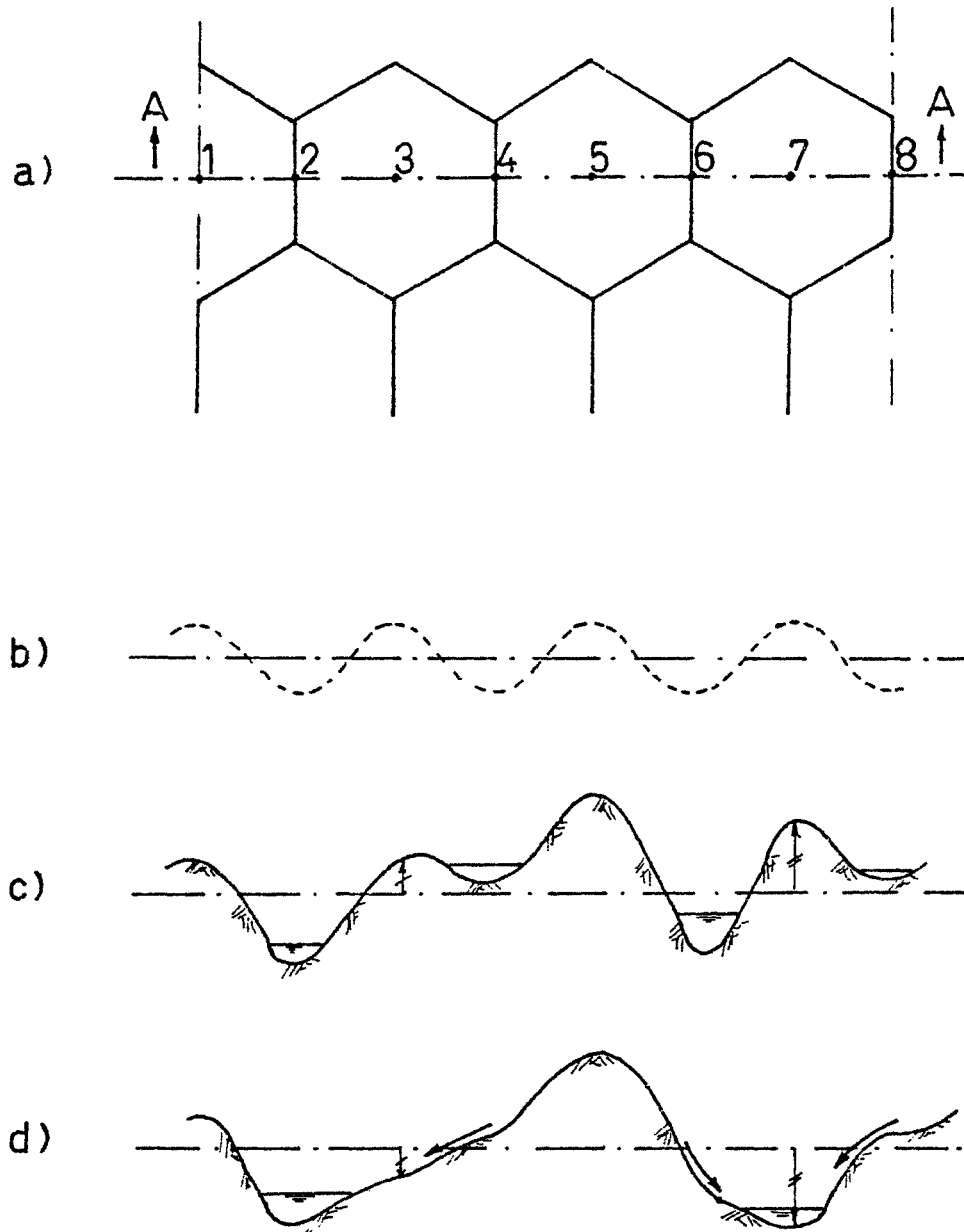


Figure 4.20 Irregularity in Generated Surfaces

## 5. MODEL PERFORMANCE

The simulation model was tested by comparison of the model performance with results of field experiments. However, the data obtained in most field studies are not adequate to allow detailed comparison between model and observed performance. Hence only order-of-magnitude comparisons could be made. One such case is described in Section 5.1.

An evaluation of the general characteristics of the model can be made by studying the influence of physical conditions on predicted erosion. The most important physical conditions are slope gradient, slope length, and rainfall intensity. There is plenty of empirical evidence on how these conditions influence erosion. Hence a general comparison can be made to see if the model performance is qualitatively in agreement with empirical knowledge. This is described in Section 5.2.

### 5.1 Comparison with Field Measurements

Erosion measurements from highway embankments were used to compare with model performance. Barnett et al. (1) conducted field experiments at four different locations using rainfall simulators. At each location, seven plots with different treatments were prepared; one of these was left with a bare surface. Each site was graded to  $2\frac{1}{2}:1$  slope, seeded, rototilled, and then firmed with a cultipacker. At two of the four locations, the soil was classified as clay. The soil at the other two locations was classified as sandy clay loam.

The test storm was applied at an intensity of 6.25 cm per hour in two increments of 20 minutes each. The first increment, 3.13 cm in 30 minutes, corresponds to a one-year frequency storm; the entire test represents a 10-year frequency storm for the geographical region of Georgia.

Among the many parameters and measurements that are needed as input data to the model, some are common for slope erosion problems. These include ASR, ASH and  $p$ , and the constants describing the properties of water. On the other hand, the representative size of soil particles, the Manning's coefficient, and the surface roughness measurements are unique characteristics that must be determined for each site. Since much of the input data are not available for the test plots, it was necessary to assume reasonable values and use these for the calculations.

It is not surprising that no information about the surface roughness was reported in the paper by Barnett et al. With due reservations, the roughness data obtained from Wooster, Ohio, which has been analyzed in Chapter 2, was used here to represent a well-cultivated surface.

Since the field study was not concerned with comparing flow and erosion with any theoretical model, no estimate of Manning's coefficient,  $n$ , was presented. Use was made of the results of the investigation by Ree et al. (30) on the value of  $n$  in overland flow. Values as high as 0.3 were reported in their study for poor-cover conditions. For the bare surface in question, computations are made for a range of  $n$  from 0.025 to 0.2.

According to Foster and Meyer (8), clay particles are detached by rainfall as aggregates. These aggregates move along the bottom of the rills as cohesionless particles. The previous consideration is the basis for the choice of the values of the soil particle representative diameter,  $D$ , in the two types of soils. For the plot classified as clay, the reported gradation is 39% sand, 27% silt, and 34% clay. The clay particles in the USDA classification have a diameter of less than 0.002 mm. Therefore, to represent the clay aggregates and to allow for the non-aggregated sand and silt, the value of  $D = 0.01$  mm was selected as the median diameter. For the second plot, with the gradation of 57% sand, 17% silt and 26% clay, a value of 0.05 mm was chosen for  $D$ .

Using a time interval of 2 minutes, the total soil loss at the middle, and at the end of a 60-minute storm period was computed. The computed soil losses for the two sites are shown in Figures 5.1 and 5.2. The results indicate that in order to achieve soil losses comparable to the measure values, the Manning's coefficient  $n$  should be around 0.085 for the clay site and over 0.2 for the sandy clay site. For a bare slope, those  $n$  values seem too high when compared with the estimates by Ree et al. (30). However, the values of  $n$  for overland flow in general, and for bare slopes in particular, are not yet well established. Hence, the discrepancy is not considered conclusive.

It is also possible that the model underestimates the soil loss, because of the approximation used in the side slope failure mechanism, (Section 4.4.2) or because of incorrect values of  $ASH$  (Section 4.4.3.2) or  $P$  (Section 4.4.3.3). Thus, it is difficult to determine

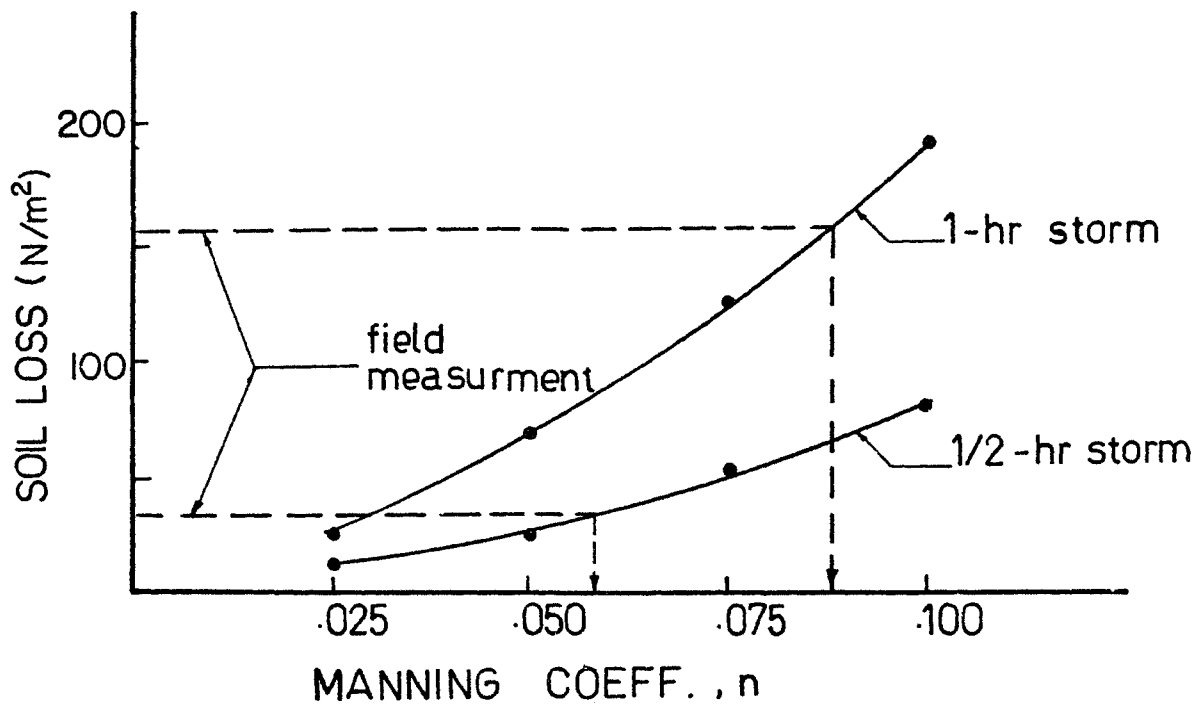


Figure 5.1 Soil Loss from the Clay Site \*

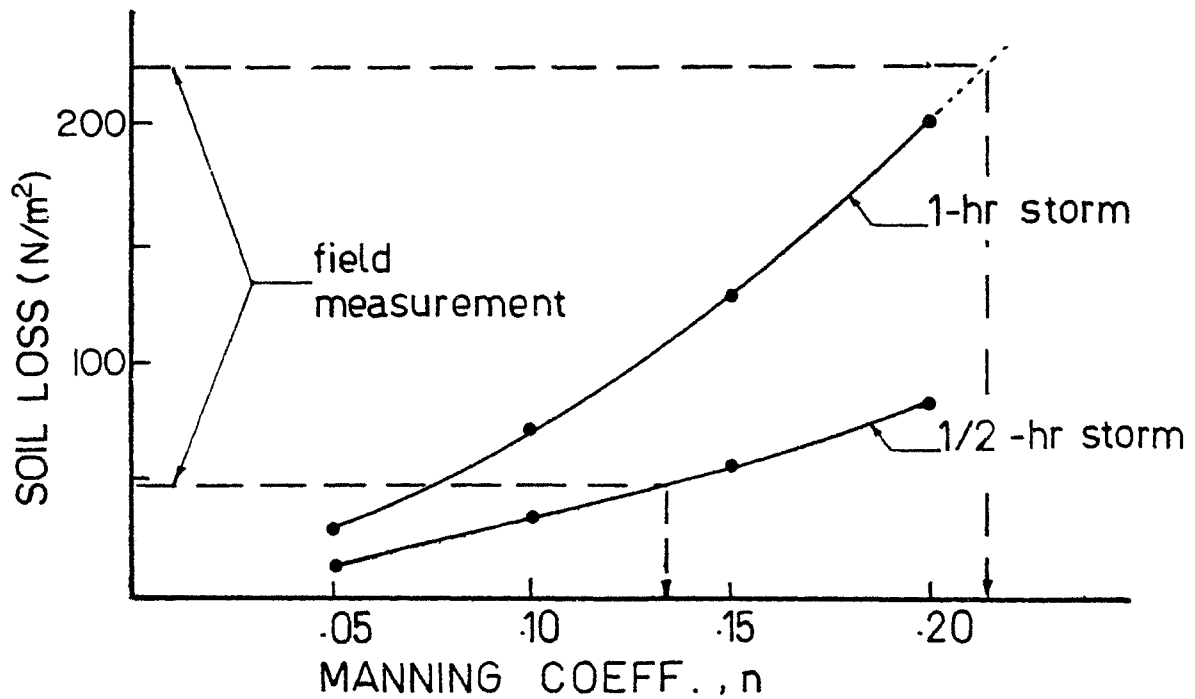


Figure 5.2 Soil Loss from the Sandy Clay Site \*

\* Model parameter ASR, ASH,P,SLIMIT are equal to values in ( ) in table 4.1

the specific source of discrepancy between the field measurements and the model results, because of the factors discussed in the introduction to this chapter. Therefore, it seems inevitable that a proper verification of the present model requires specific surface preparation and measurements.

## 5.2 Influence of Physical Conditions

### 5.2.1 Effect of Slope Gradient

The slope gradient of a soil surface is one of the most important factors which control erosion. Investigators, since the earliest erosion studies, have always attempted to determine the relation between the slope gradient and the erosion. Experimental as well as theoretical studies agree that soil erosion increases with slope gradient. A unique relation, however, has not been established (see ref., 18).

To study the effect of slope gradient on the model predictions, the erosion rate was computed for four plots with slopes of 5, 10, 15 and 20 degrees. Figure 5.3 shows the change of erosion rate with time for the four cases. The results indicate that steeper slopes result in larger erosion rates. The relation between slope gradient and erosion rate is time-dependent, as shown in Figure 5.4. This behavior may provide a possible explanation for the differences in the results of experimental studies on the effect of slope gradient on the erosion rate.

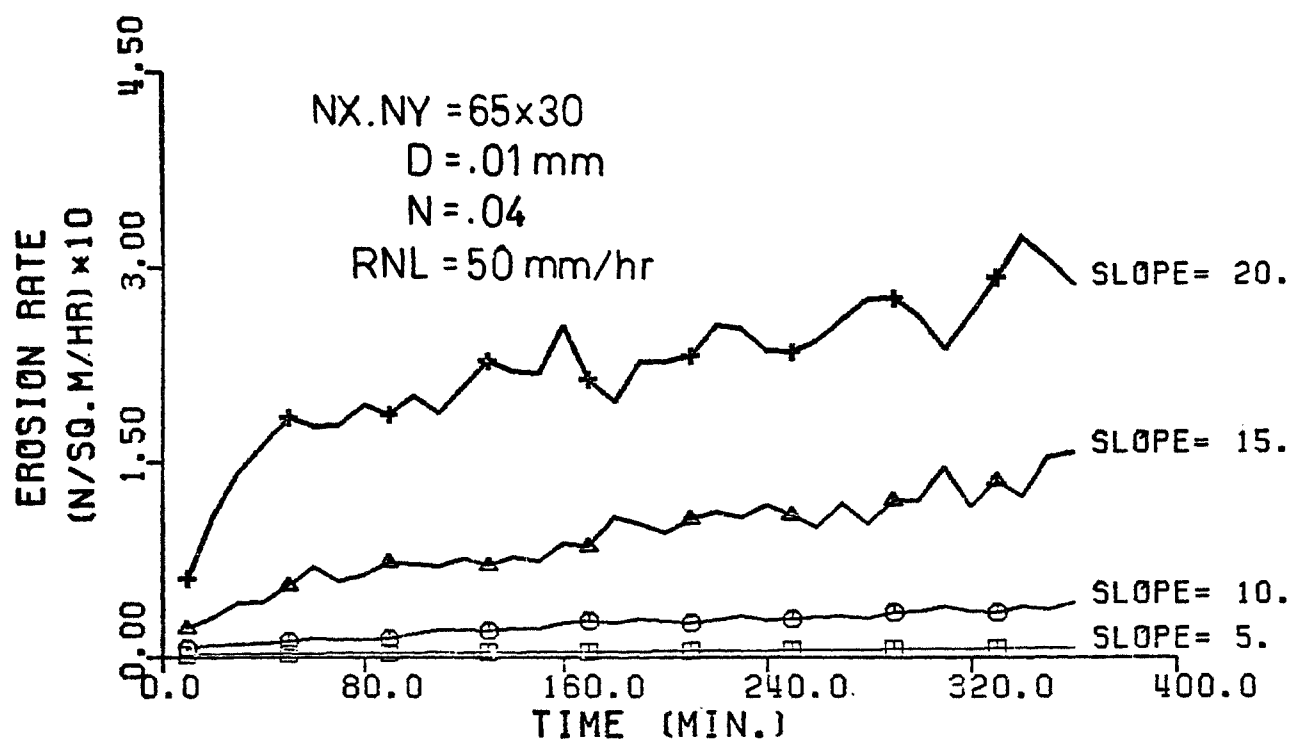


Figure 5.3 Effect of slope gradient on erosion rate

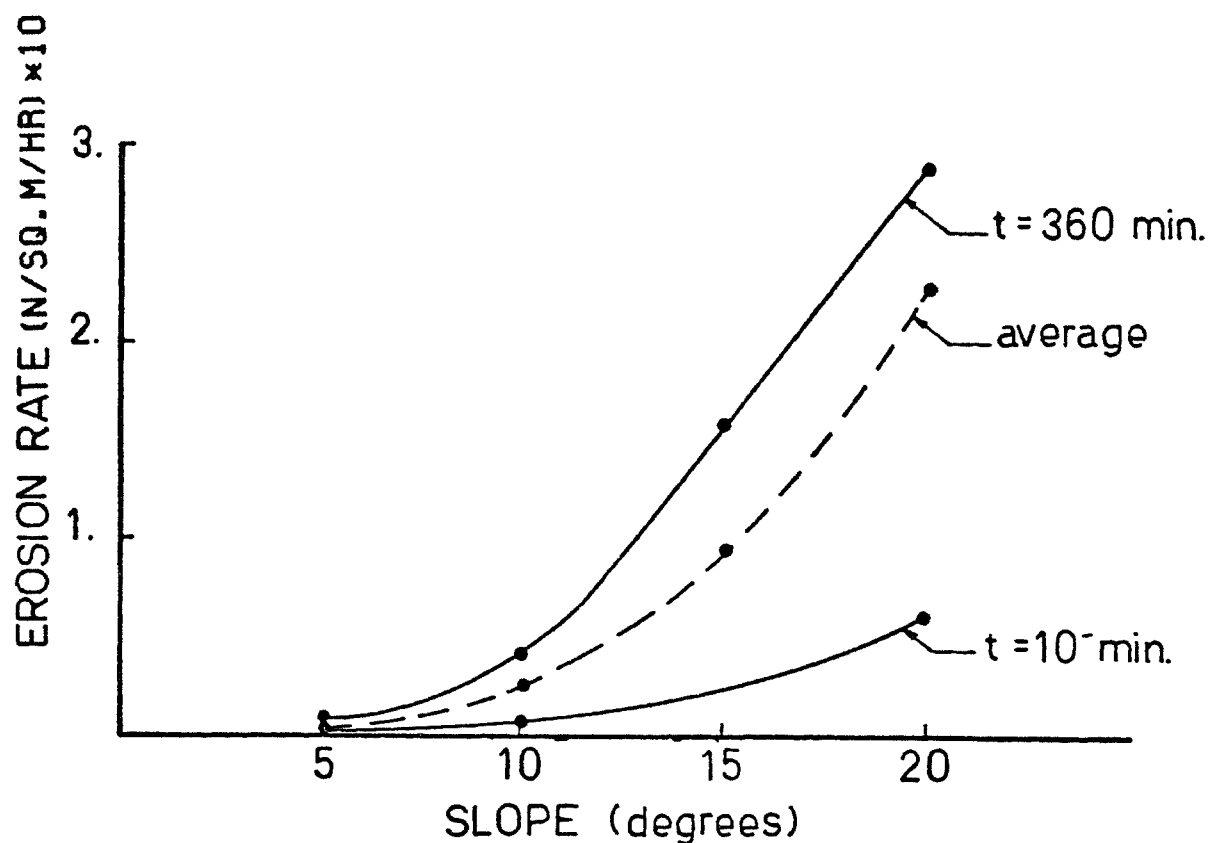


Figure 5.4 Effect of time on the slope gradient - Erosion rate relation



### 5.2.2 Effect of Slope Length

Since the overland flow tends to increase downslope, longer slopes result in longer and deeper rills and increased erosion. Therefore, the slope length can be expected to have a significant influence on the rill-interrill erosion features.

The relation between the erosion rate and time was computed for three plots of lengths 0.73, 2.29 and 3.85 meters. These values correspond to values of  $NY$  of 10, 30 and 50, respectively, as shown in Figure 5.5. The computed results are shown in Figure 5.5, and indicate that the erosion rate decreases with the increase of slope length. This behavior is not in agreement with empirical observations (see Reference 19). Determination of the reasons for this discrepancy requires additional investigation.

The effect of the slope length on the rill-interrill erosion is very important, since transport and detachment capacities of rills increase with distance downslope. Figure 5.6 shows the relation between rill-interrill erosion ratio with time for the same plots. It is clear that the contribution of rills increases with slope length. This means that rill erosion increases with distance down slope. Such behavior has been observed in many experimental studies ( 22,23,24 ).

### 5.2.3 Effect of Rainfall Intensity

Rainfall characteristics, such as intensity, angle of incidence, spatial, and temporal distribution, have variable impact on the erosion process. The present model takes into account only the rainfall intensity.

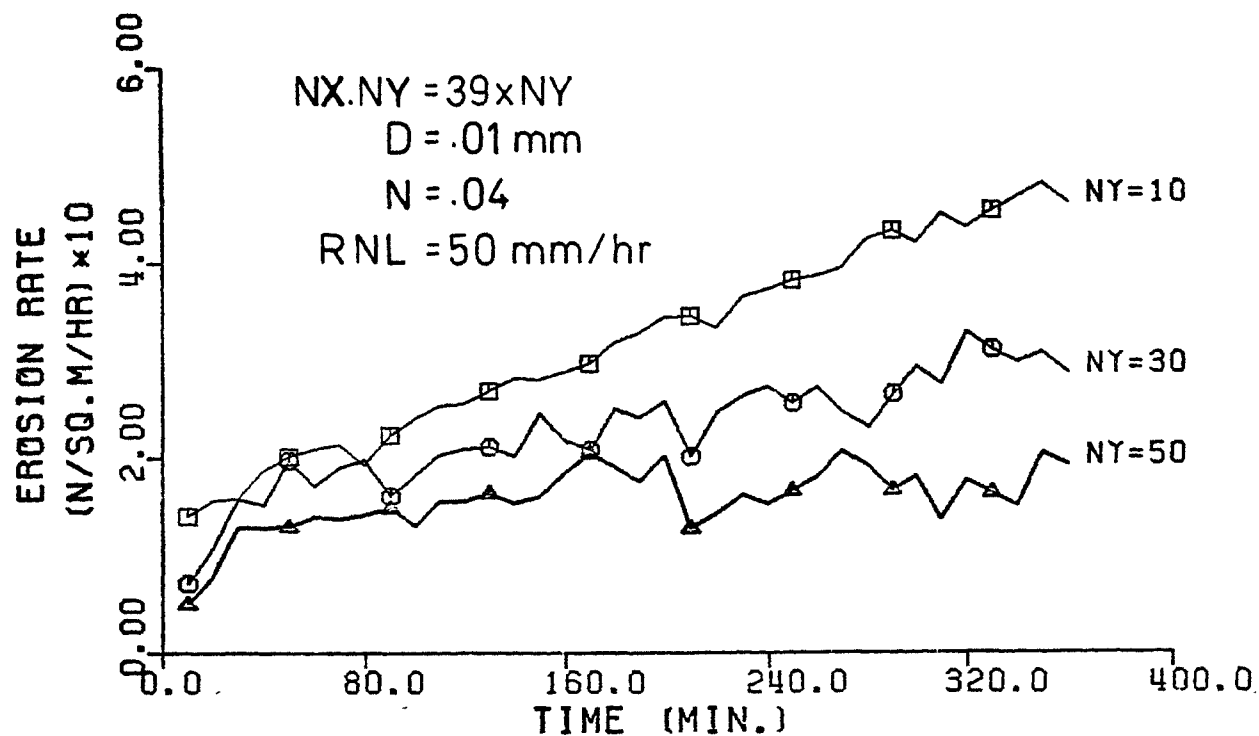


Figure 5.5 Effect of slope length on erosion rate

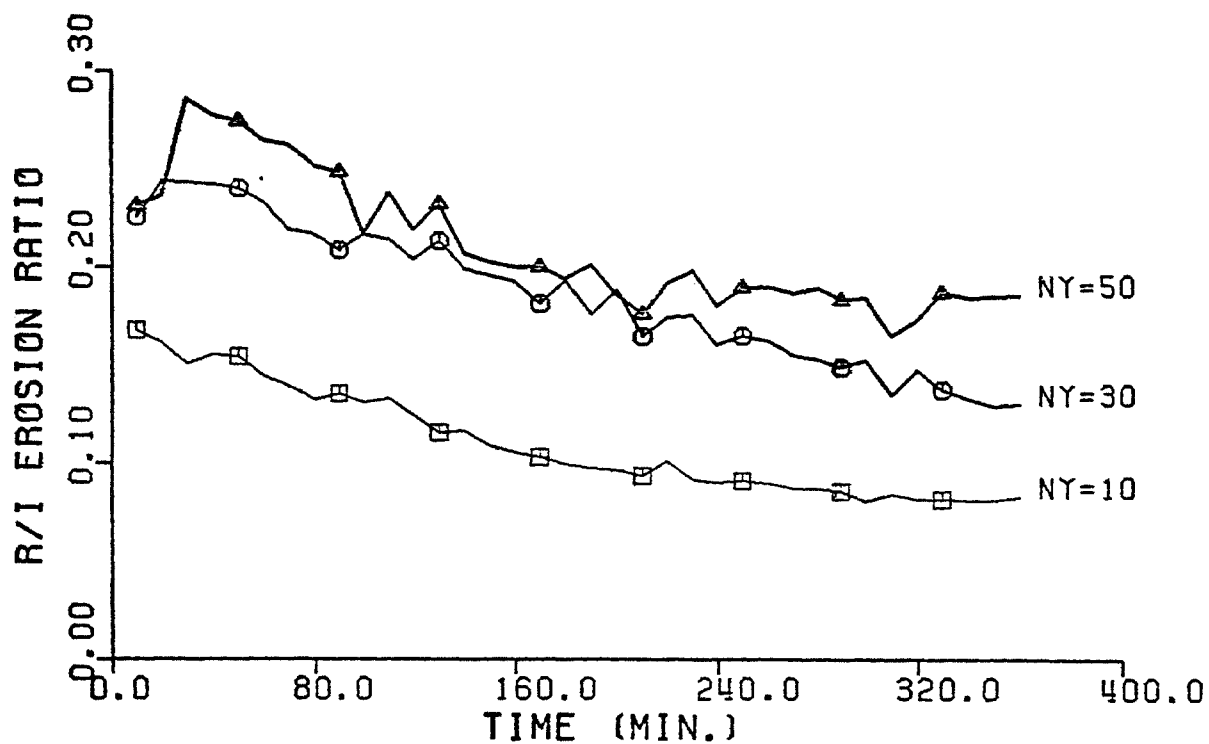


Figure 5.6 Effect of slope length on R/I erosion ratio

Three storms with rainfall intensities of 50, 25 and 12.5 mm/hour were considered, with rain periods of 3, 6 and 12 hours, respectively. This means that at the end of each test, all plots would have received the same amount of rainfall, which is 150 mm. Each of the three storms was applied to three plots with slopes of 5, 10 and 20 degrees, respectively. Results of the three storms are shown in Figures 5.7, 5.8 and 5.9.

As expected, storms of larger intensity result in higher erosion rates at all times. The relation between rainfall intensity and erosion rate seems to be dependent on the average slope gradient of the plot, as shown from Figure 5.10.

### 5.3 Evaluation of Eroding Surfaces

The purpose of this section is to illustrate the temporal and spatial changes in the surface geometry under erosion, as simulated by this model.

The original surface generated by the model is shown in Figure 5.11. Subsequent changes in the surface geometry caused by erosion are shown in Figures 5.12 and 5.13 at times 200, and 400 minutes, respectively. For the constant rainfall intensity of 50 mm/hr, the total amount of rain at the end of the test is 333 mm. The figures illustrate the growth of rill size with time and the effect of the random surface elevations on development of nonuniform rill pattern. The results are in qualitative agreement with observed rilling on slopes.

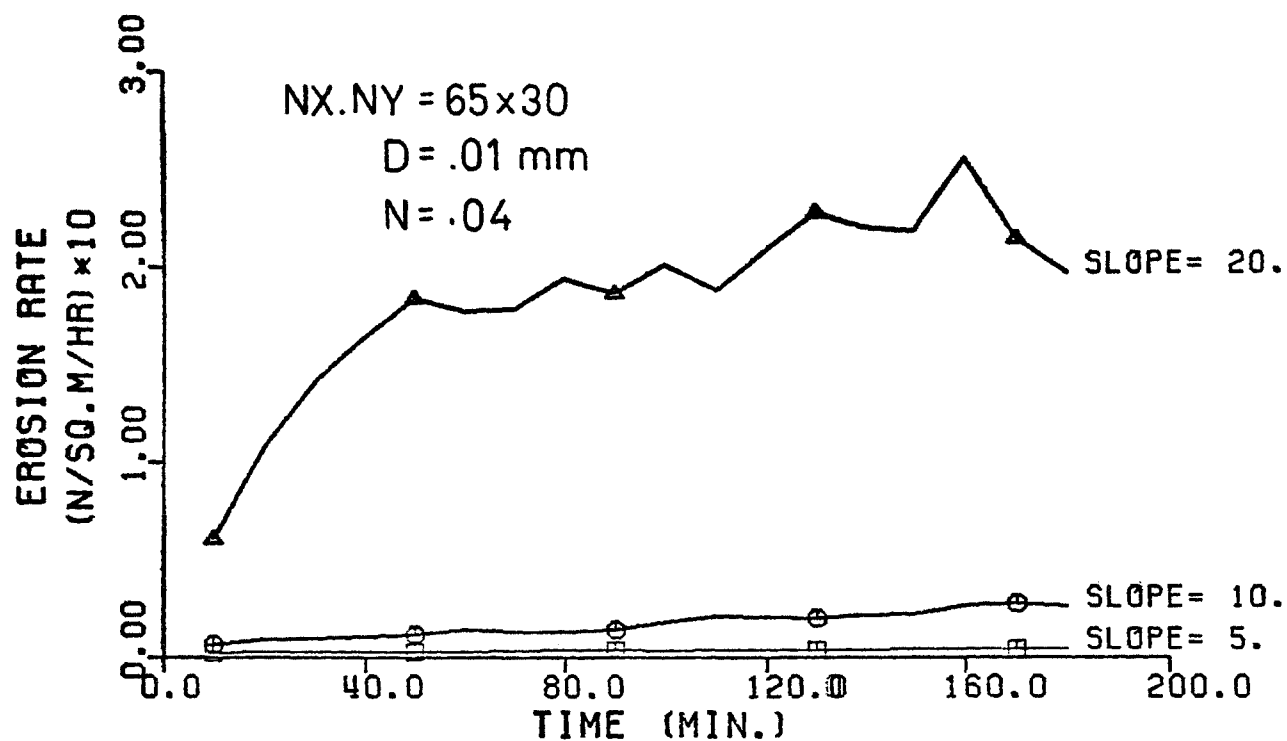


Figure 5.7 Effect of Rainfall intensity on erosion rate;  
RNL = 50 mm/hr

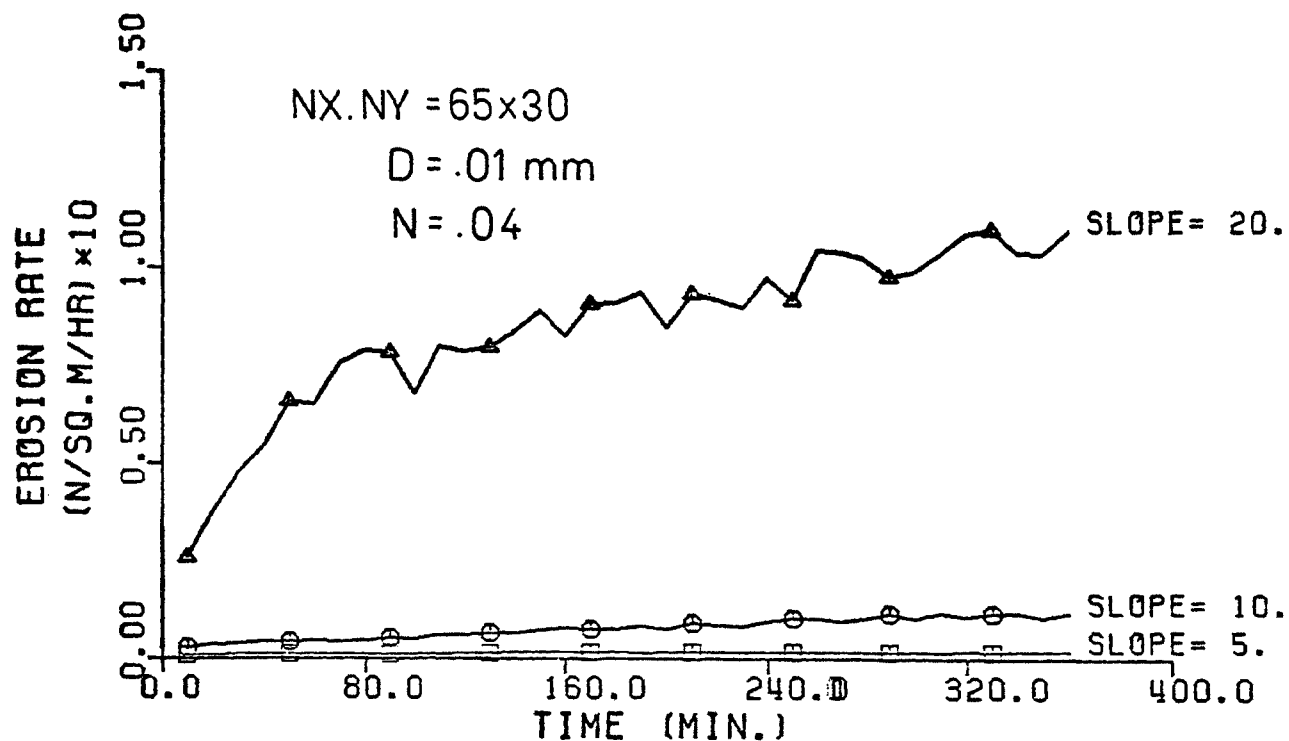


Figure 5.8. Effect of Rainfall intensity on erosion rate;  
RNL = 25 mm/hr

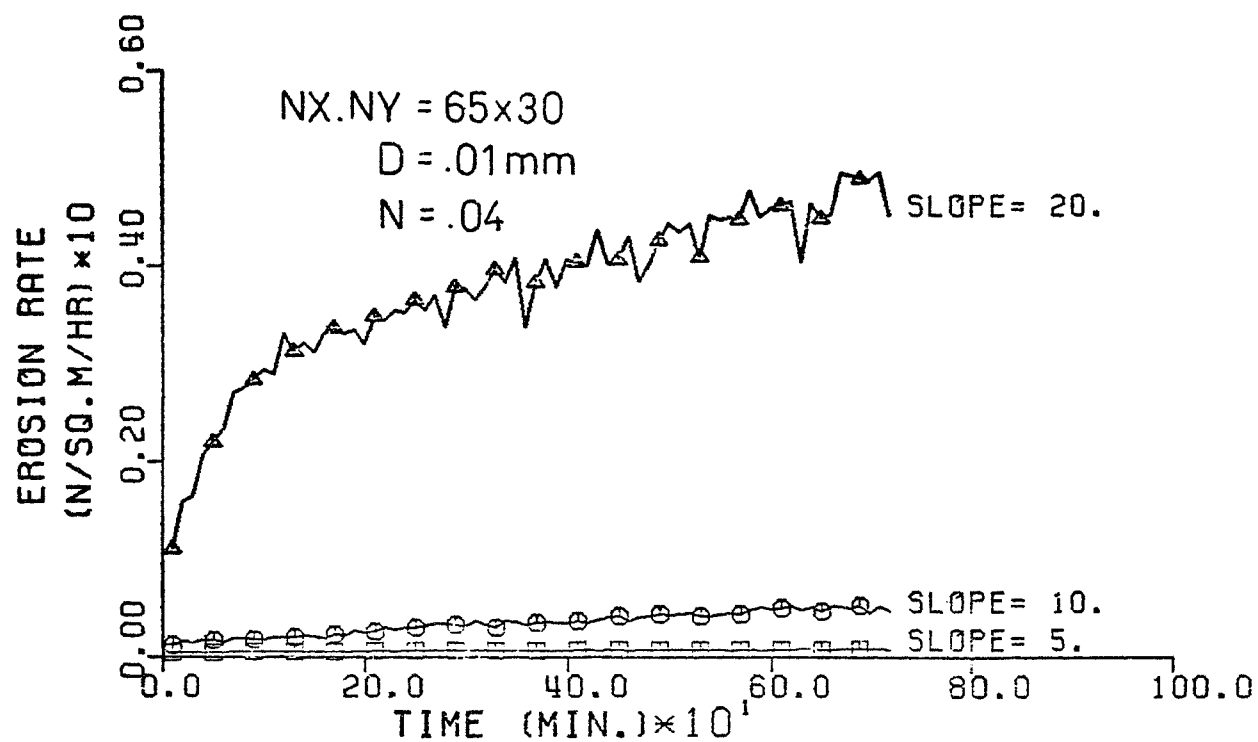


Figure 5.9 Effect of Rainfall intensity on erosion rate;  
 RNL = 12.5 mm/hr

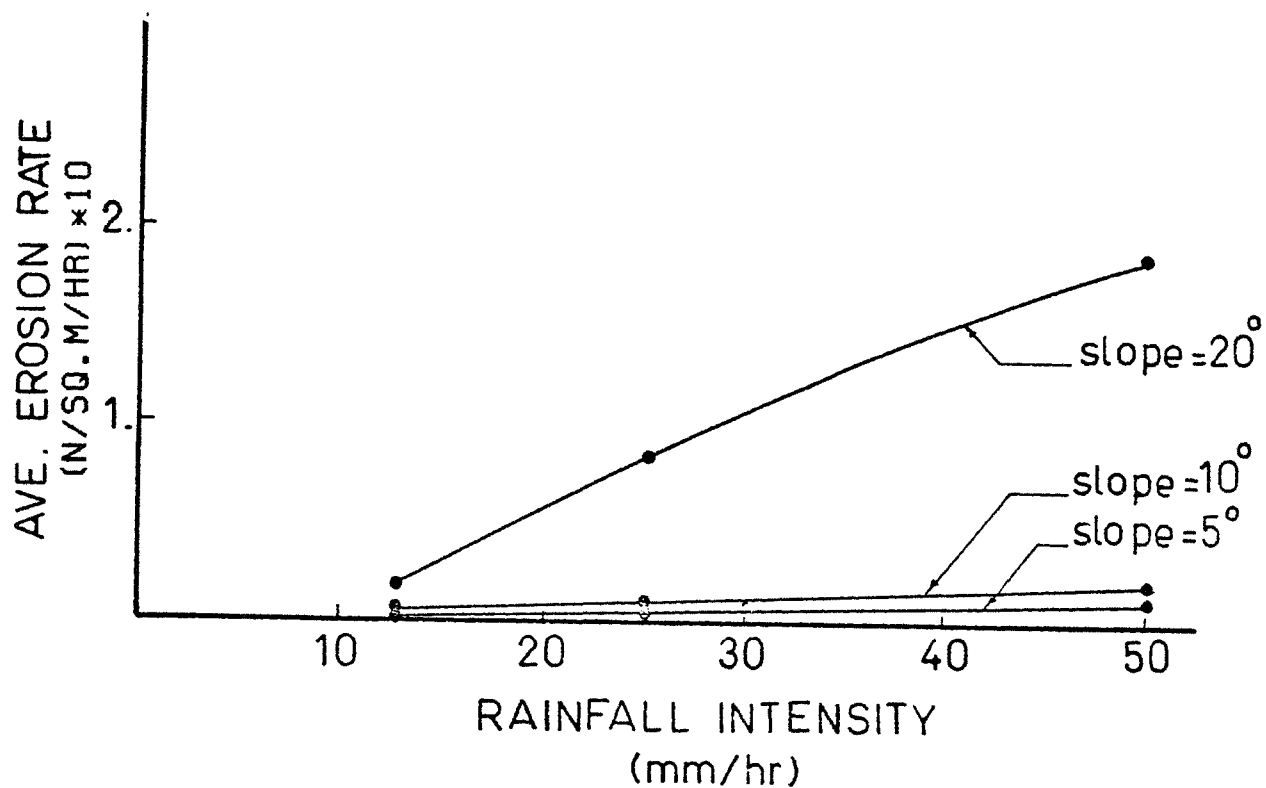


Figure 5.10 Relationship between Rainfall Intensity, Slope  
 Gradient and Erosion Rate

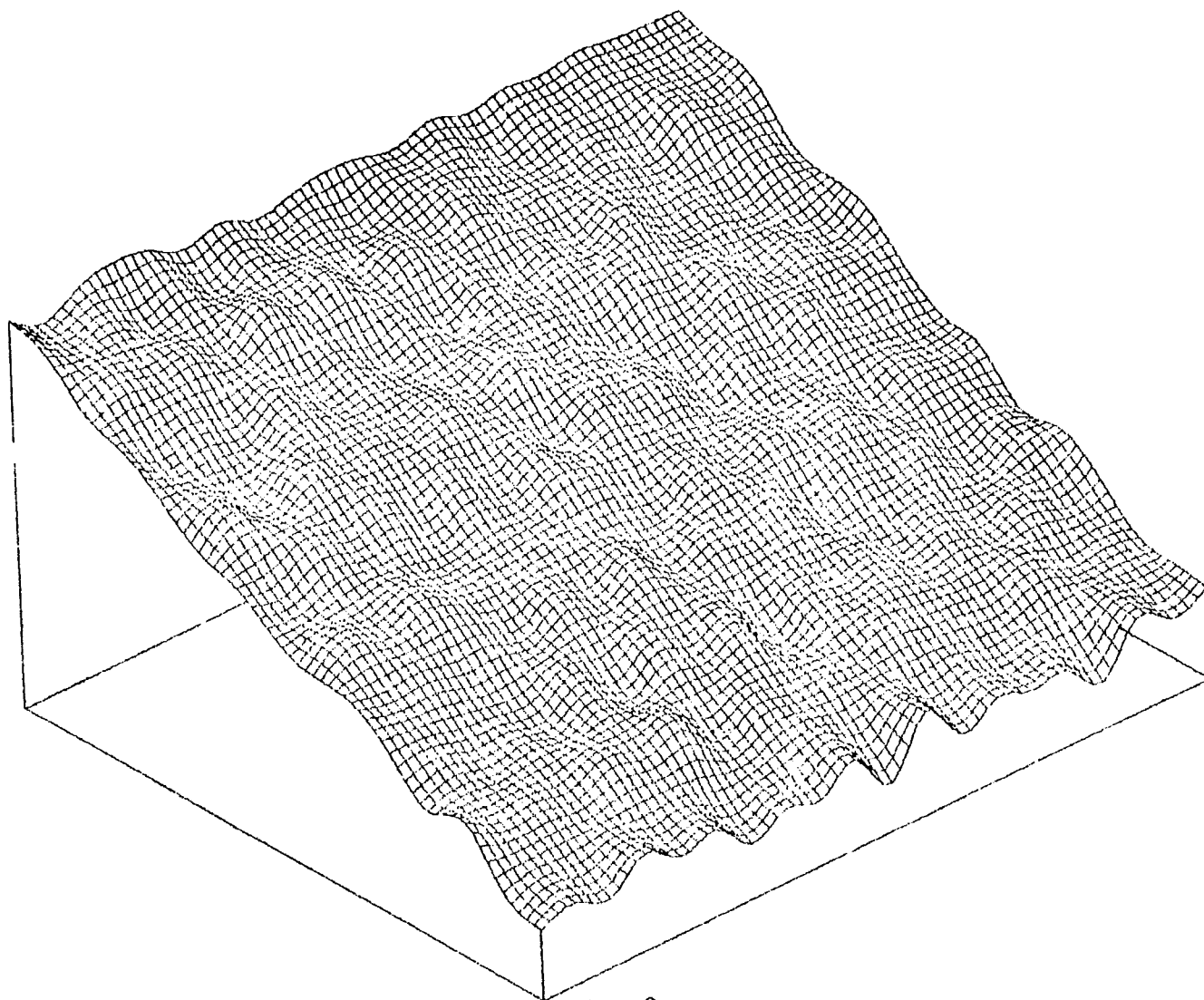


Figure 5.11 Original Surface,  $t = 0$

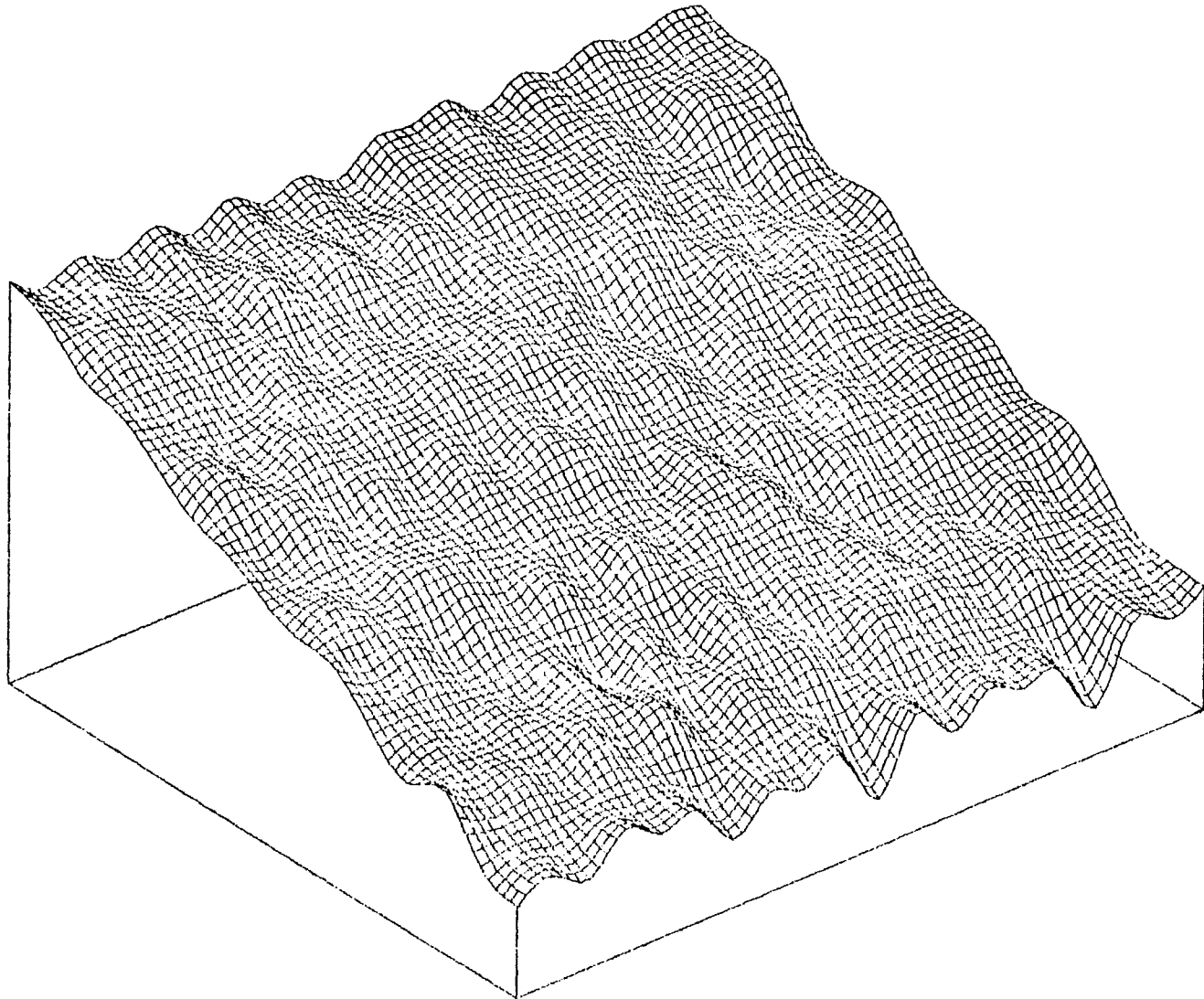


Figure 5.12 Eroded Surface;  $t = 200$  minutes

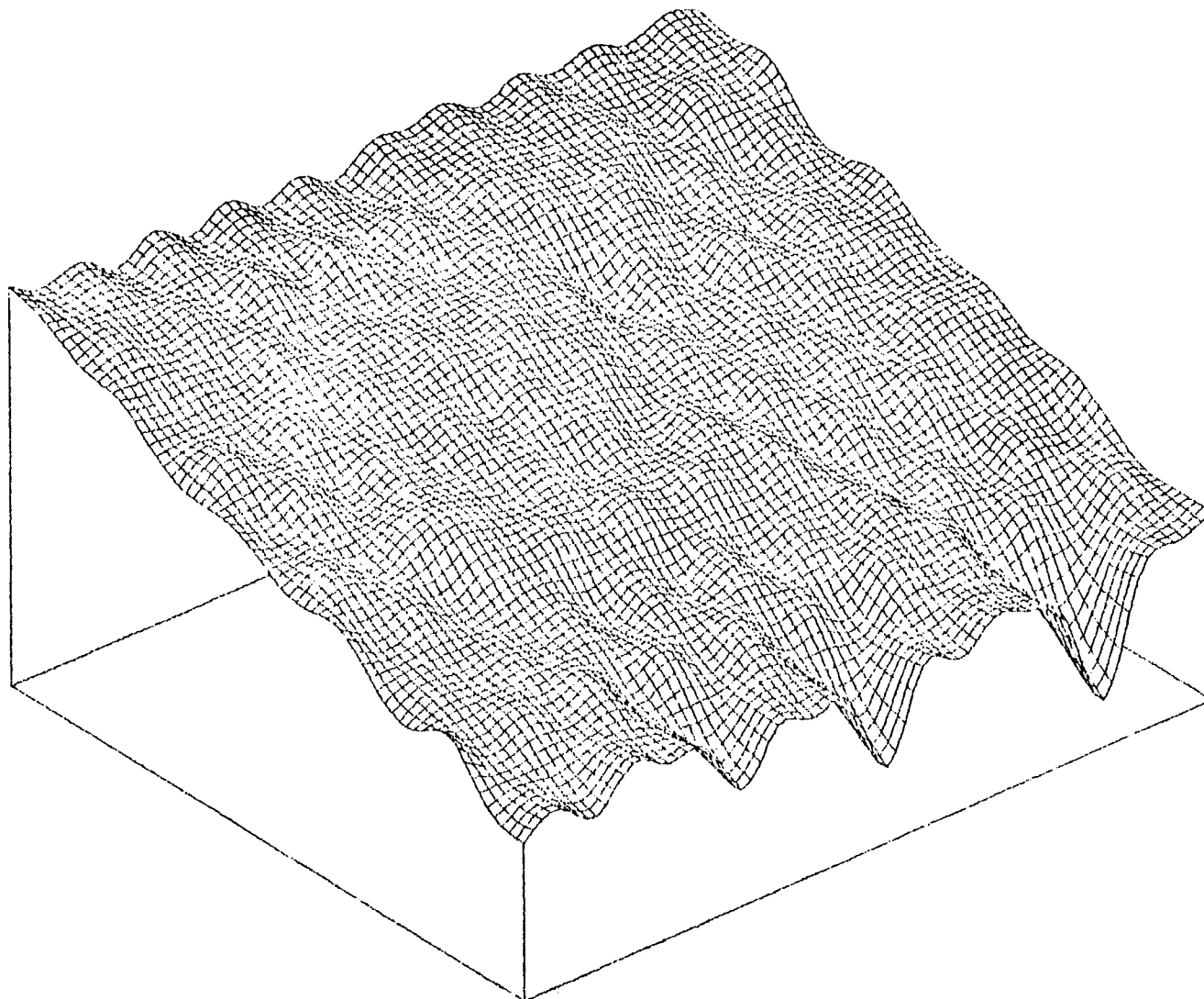


Figure 5.13 Eroded Surface,  $t = 400$  minutes



### 5.3 Concluding Remarks

The limited number of tests that have been carried out indicate that the model calculates erosion rates that are of the right order of magnitude. The model performance is also in general agreement with available experience on the influence of the important physical conditions of slope gradient, slope length and rainfall intensity. It is realized that the tests are very approximate in nature and do not provide a verification of the model. An adequate test of the model would require a specially designed field experiment in which all of the model inputs and outputs will be measured. Then one will be in a better position to identify shortcomings in the model.

## 6. SUMMARY, CONCLUSIONS AND RECOMMENDATIONS

### 6.1 Summary and Conclusions

The review of literature on soil erosion reveals the need to consider the effect of the random rill patterns which develop as a result of the surface roughness characteristics. A model has been developed to account for this effect in the simulation of the erosion process. The model computes the erosion and flow pattern and also the rill-interrill characteristics as they change with space and time.

The measured roughness of a surface is analyzed and used to generate random surfaces for the simulation process. Computations are carried out over a number of time intervals; the steady state condition is assumed for each interval. Changes in the surface geometry, due to erosion during an interval are used to revise the surface for the subsequent interval. The model includes simplified mechanisms to simulate ponding, deposition, and failure of side slopes of rills.

A sensitivity analysis of the model was made to examine the effect of important parameters and mechanisms. The length of time intervals is important because of the cumulative effect of the surface-updating procedure. Therefore, shorter time intervals give better estimates of erosion rate. Manning's coefficient has a strong influence on the erosion rate; the erosion rate increases with the increasing values of Manning's coefficient,  $n$ . The transport capacities of flow in rills and over interrill areas also depends on the constants ASR and ASH. The value of ASR does not have

significant effect on the total erosion rate. However, an increase in ASR produces higher rill-interrill erosion ratio. The model is more sensitive to the value of ASH. An increase in ASH increases the erosion rate and, at the same time, decreases rill-interrill erosion ratio. The model is sensitive to the exponent  $p$  in Kalinske's bed load equation. A lower value of  $p$  results in a higher erosion rate and a higher rill-interrill erosion ratio.

The randomness in the surface elevation has a significant effect on reducing the erosion rate. Surfaces with greater random variations experience smaller erosion rates. Randomness in the rill pattern appears to have a smaller effect; the distribution of rill flow for the uniform rill pattern has more variations than that for the random rill pattern. However, the results are not considered conclusive because of the small sample size used in the analysis.

The model predictions were compared with some data from field experiments. The results are of the right order of magnitude, but it is not possible to make detailed comparisons because many parameters and data, including the original surface roughness, are not available.

The effects of the slope gradient, length of the slope, and rainfall intensity on the erosion rate were also studied. The results are in general agreement with experience.

## 6.2 Recommendations for Further Research

Because this is a first step in stochastic simulation of the erosion process, numerous problems both in formulation and in documentation have been encountered. Consequently, many simplifications

were made. The structure of the simulation model, however, has sufficient flexibility to allow refinements of the different sub-models and mechanisms.

Proper verification of the model requires field experiments in which the model inputs and outputs are accurately determined. This will allow a more detailed evaluation of the model. Presently, there is great uncertainty about the appropriate values for Manning's coefficient, the constant  $a_s$ , and the exponent  $p$  for overland flow.

Possible improvements of the model include separation of the detachment and the transport capacity of the rill flow, and consideration of energy continuity at nodal points. The study of the random rill patterns should be pursued further.

It is important to note that the stochastic model considers only the random characteristics of the surface roughness. Other factors such as rainfall distribution, soil properties, and infiltration, are also random in nature, and contribute to the randomness of the overall behavior. Recently, Freeze (9) presented a simulation model that accounts for some of those factors in overland flow. A similar technique can be used to account for these factors in the erosion model.

## APPENDIX A. DETACHMENT BY RAINFALL

### A.1 INTRODUCTION

Field experiments, Mutchler and Young (26) Young and Weirsmas (42), have shown that raindrop impact is a major factor in soil detachment and empirical relations between the amount of soil detached and rainfall energy and intensity have been proposed (3,8). Detailed studies of the energy and forces of raindrop impact were made by Mutchler (25), Palmer (28), and Laws (16). A recent study by Cruse and Larson (5) indicated that the amount of soil detached by a raindrop of given size and velocity is dependent on the shear strength of the soil. The limited experimental work described in this appendix is a preliminary investigation to study the factors that control detachment by raindrop. The techniques and methods developed by Palmer (28) and Laws (16) for producing raindrops were used in this investigation. The objective is to find an approximate and simple relation that can be used in the erosion model.

### A.2 EXPERIMENTAL PROGRAM

The experimental program consists of measurement of the soil detached by raindrops from specially prepared soil samples. Two sizes of raindrops, 5.0mm and 3.7mm, falling through a distance of 2.4m. were used. A schematic diagram of the equipment used for raindrop tests is shown in Fig. A.1. At the top is the reservoir for the water supply. Raindrops are formed by passing the water through the graded tube. The dimensions of the graded tube are chosen for the required drop diameter according to the results of Palmer. Table A.1 gives the tube sizes used to form drops

- 1. Reservoir
- 2. Graded Tube
- 3. Lucite Shield
- 4. Container
- 5. Soil Sample
- 6. Brass Pedestal

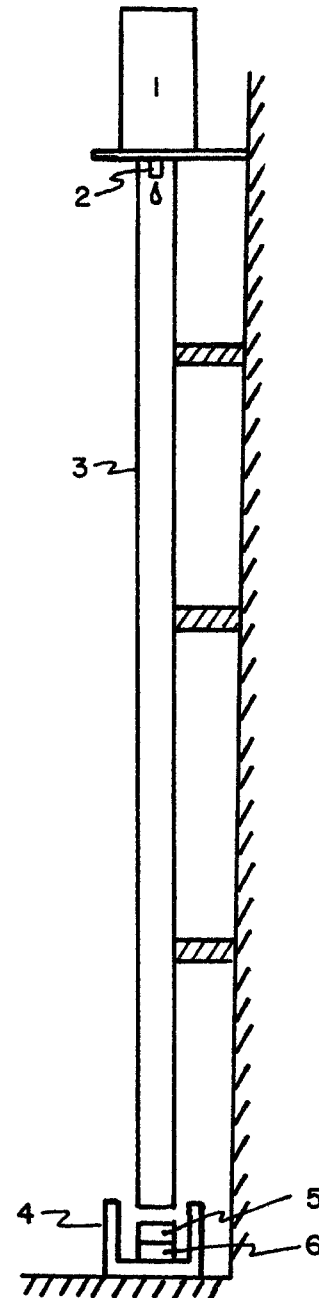


**Figure A.1: Apparatus for Raindrop Test  
(not to scale)**

TABLE A.1 MAKEUP OF GRADED TUBES

Tube Designation*	Gage Tubing	Inside Diameter (cm)
21 to 8 (Drop diameter=5.0mm)	21	0.0495
	18	0.0838
	15	0.1371
	12	0.2159
	10	0.2692
	8	0.3430
21 to 18 (Drop diameter=3.7mm)	21	0.0495
	18	0.0838

\*Tube Designation refers to gage size of the tubing.

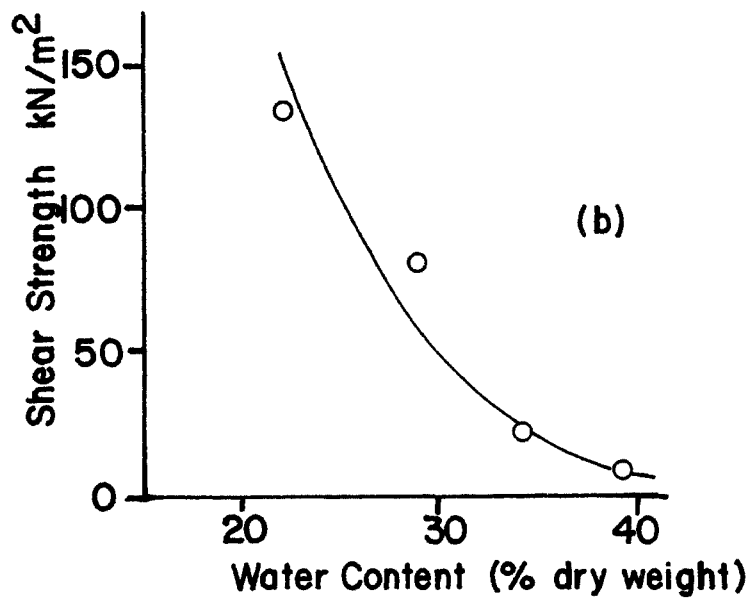
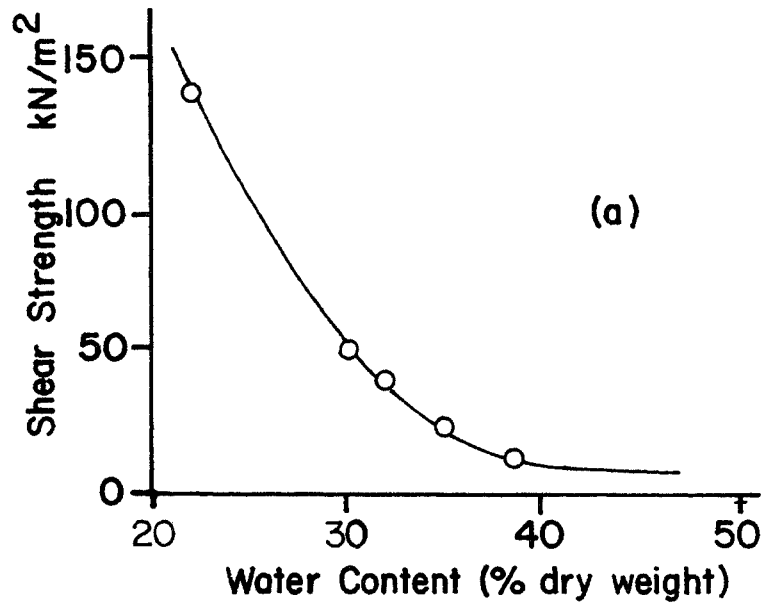


Figure A.2: Relation between Shear Strength and Water Content, (a) Kaolinite, (b) Grundite



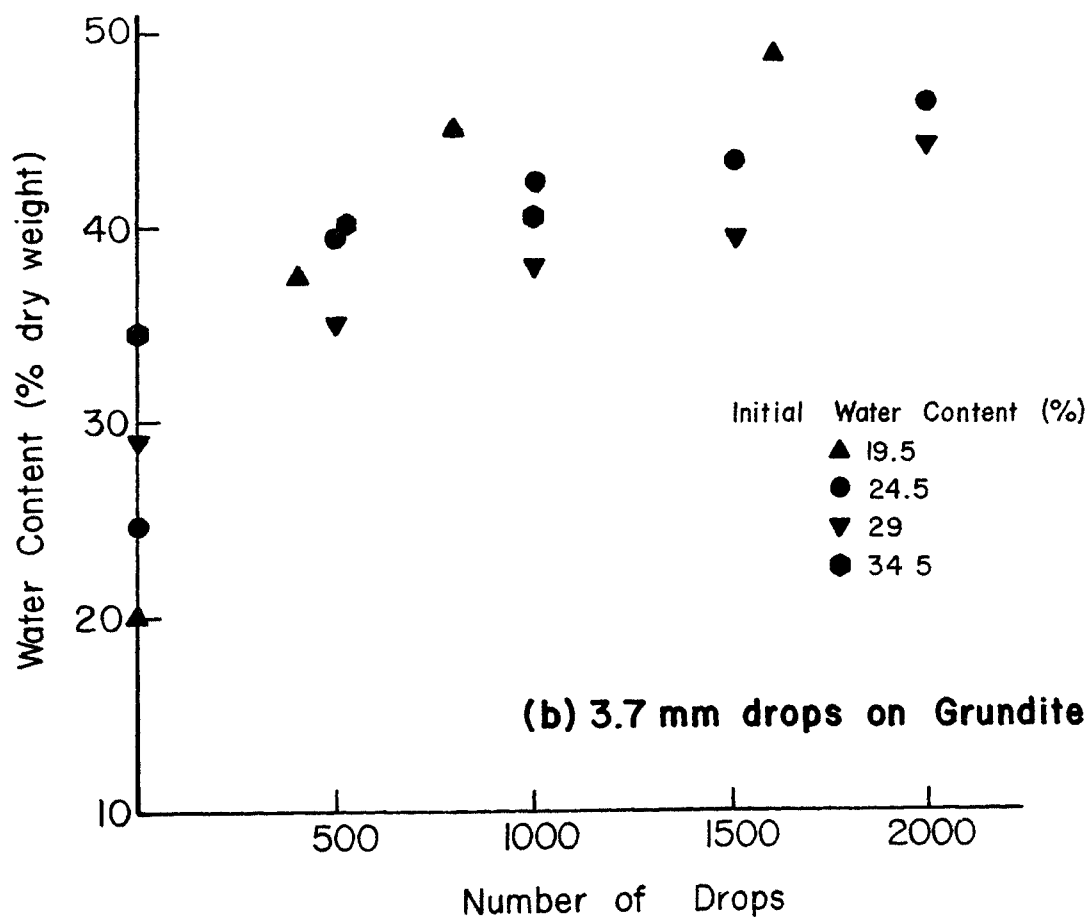
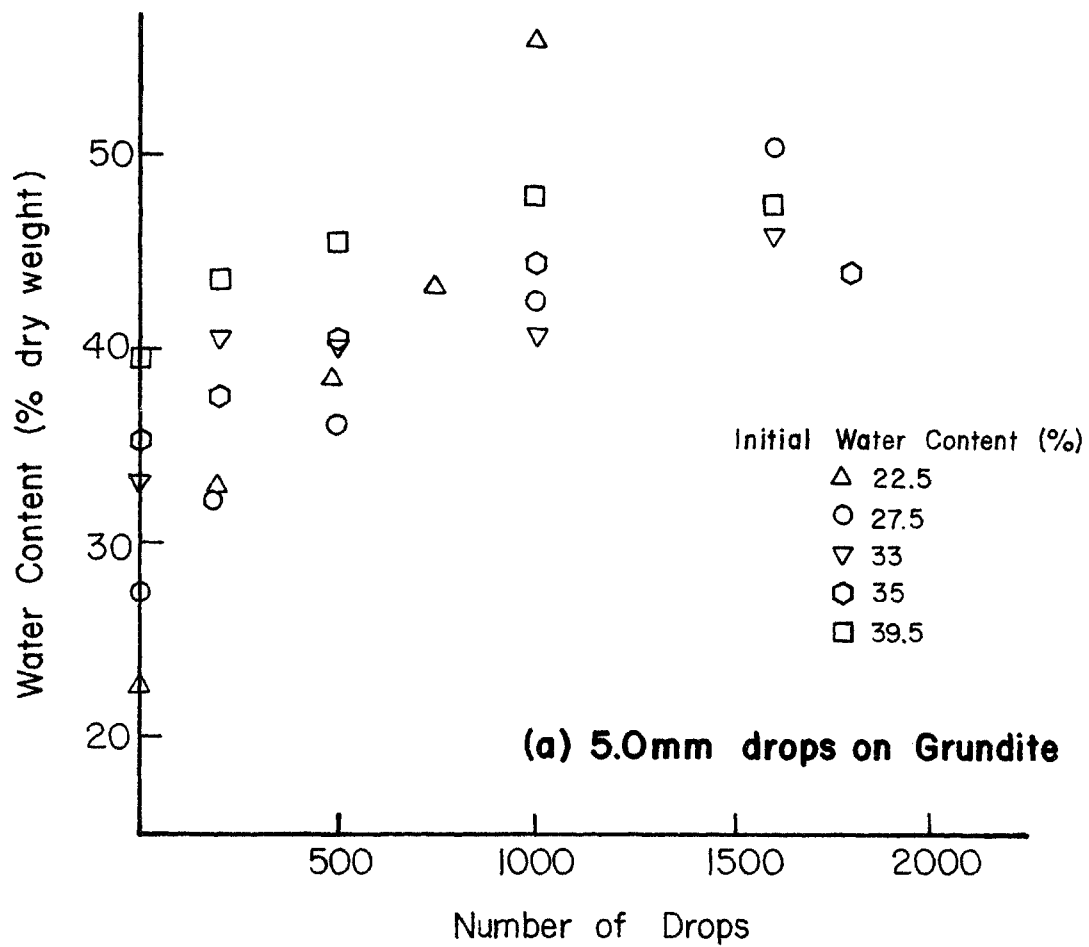
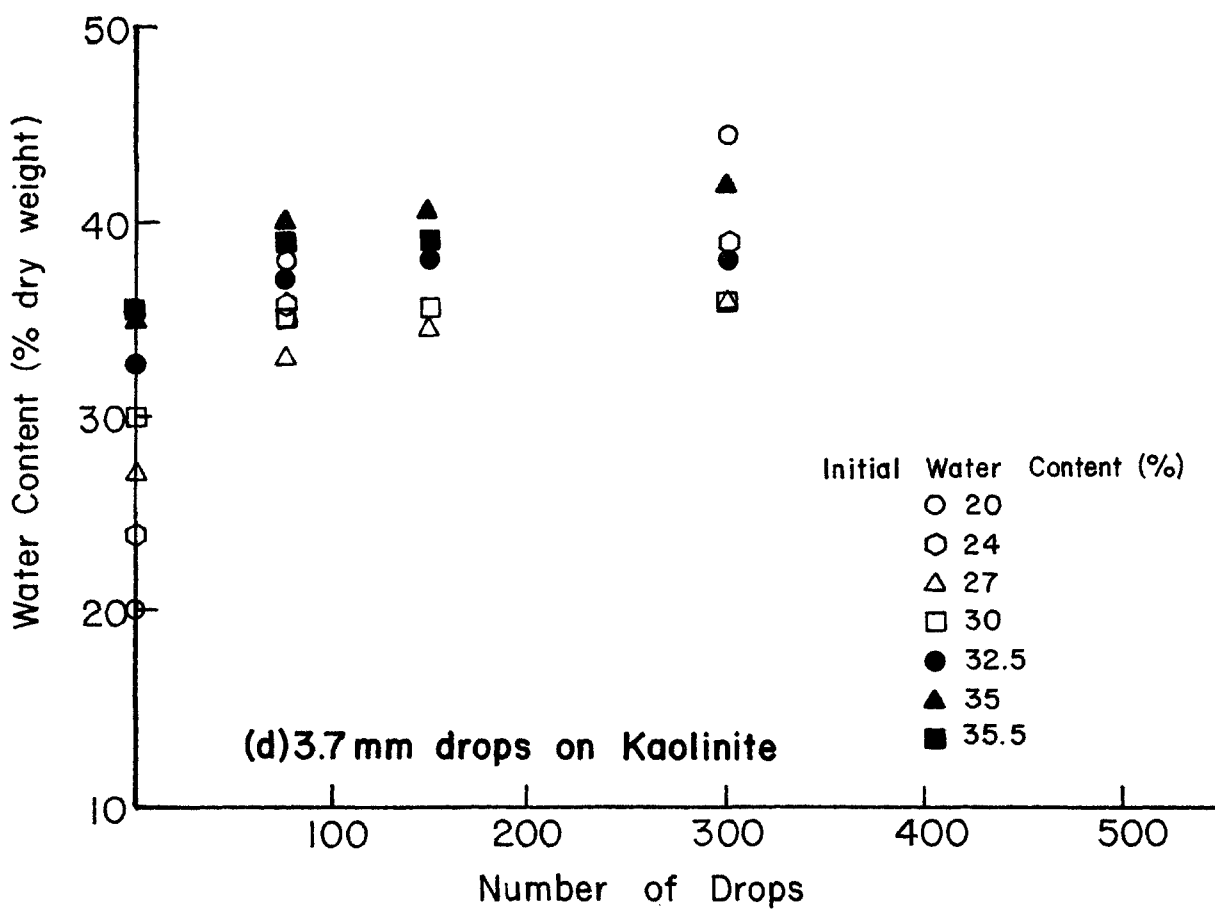
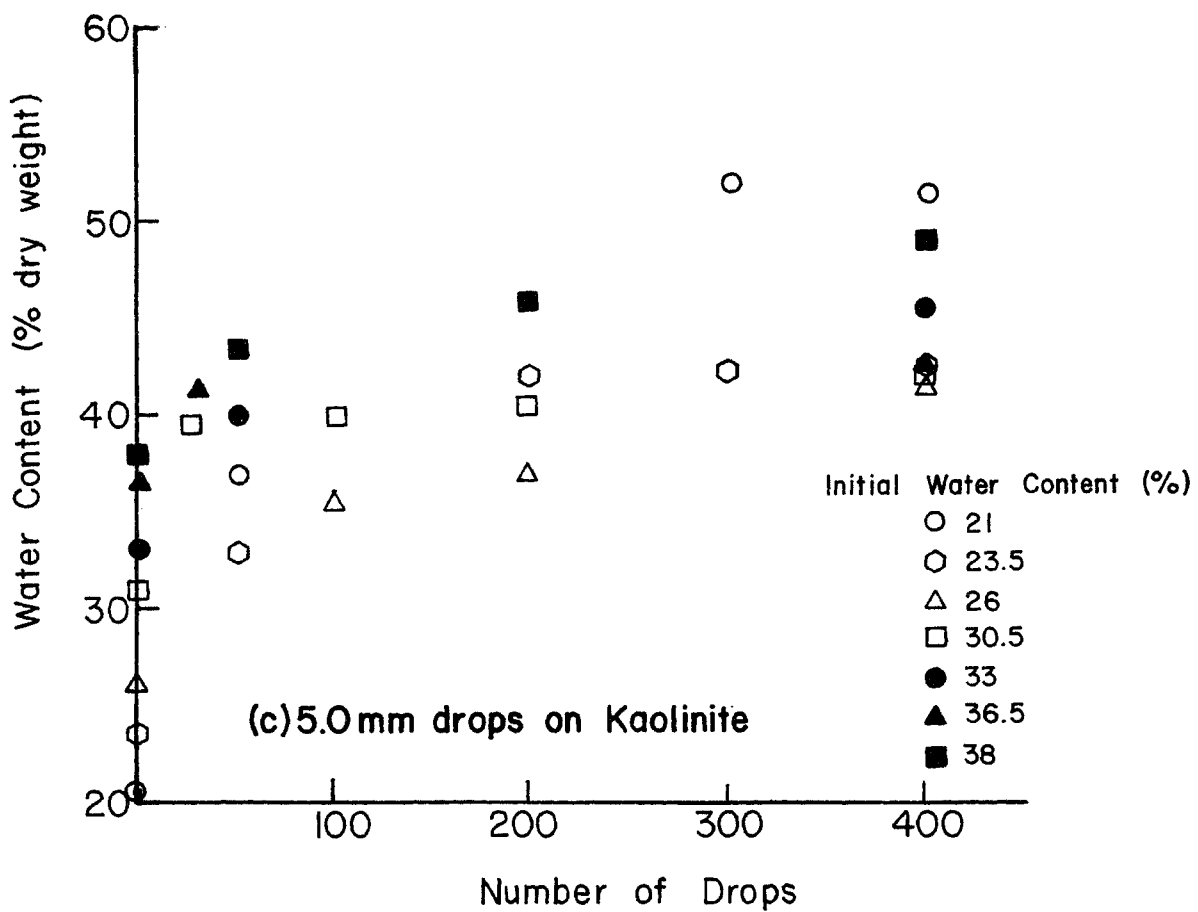


Figure A.3a,b: Change in Water Content with Raindrops



**Figure A.3c,d: Change in Water Content with Raindrops**

5.0 and 3.7mm in diameter. The flow rate through the formers are .078 and .030 N/min respectively. The lucite tube serves as a shield against air currents that may deflect the raindrops. The soil sample sits on a pedestal that is centered beneath the drop former, and the detached soil particles are retained in the container.

The soil samples were prepared from commercially made Kaolinite and Grundite whose index properties are summarized in Table A.2. The soil was compacted by the Harvard miniature compactor into a mold(39) with inside diameter of 3.33cm and a height of 7.15cm. The compaction was done in 5 layers with 25 tamps per layer and a force of 89 N. The water content was varied within a broad range and the undrained shear strength of the compacted soil was measured by the unconfined compression test. The relation between the shear strength, taken as equal to one-half the unconfined compression strength, and water content is shown in Fig. A.2 for the two materials.

The first series of raindrop tests measured the change in water content of the soil sample as it was subjected to increasing number of raindrops. In these tests the water content of the top layer, about 3mm. thick, of a soil sample was measured after a given number of raindrops had hit the top surface. The results are shown in Fig. A.3. The curves show the increase in water content with the number of raindrops for the two drop sizes and the two soils. In most cases, the water content increased rapidly at first and then approached a constant value. Some exceptions are noted; the samples with the low water contents in both groups show significant increases in water content throughout the test.

The second series of raindrop tests measured the amount of soil detached from the samples after it was subjected to a given number of raindrops. In these tests a sample was placed under the raindrop former and subjected to impact from raindrops. Soil particles that were detached

TABLE A.2  
INDEX PROPERTIES OF KAOLINITE  
AND GRUNDITE

Soils	Liquid Limit %	Plastic Limit %	Initial Water Content %	Clay Fraction ( $<0.002$ mm) %	Specific Gravity of Solid
Kaolinite	59	32	40	53	2.64
Grundite	54.4	26.1	45	53	2.78

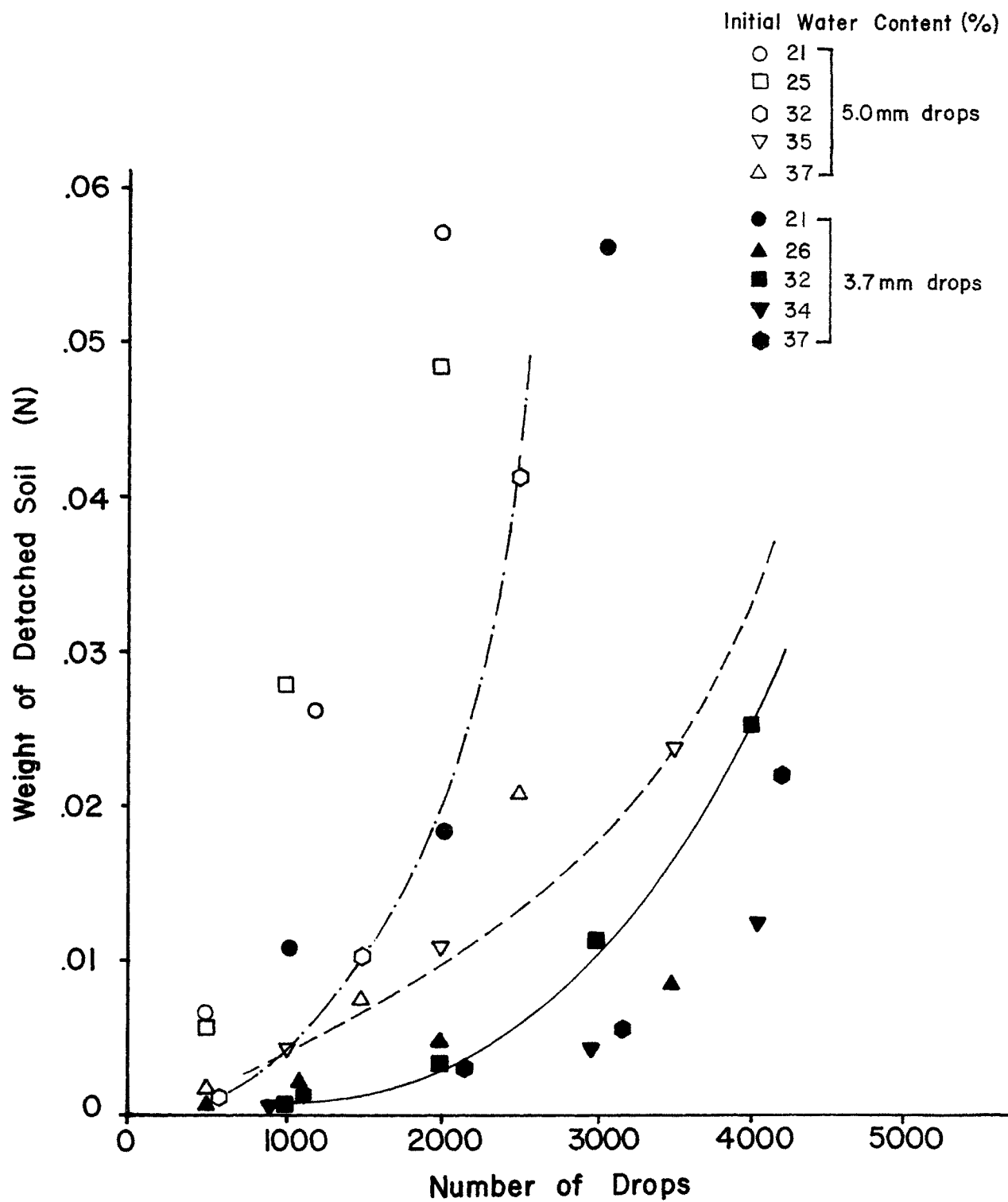


Figure A.4 (a): Weight of Soil Detached and Number of Raindrops, Grundite

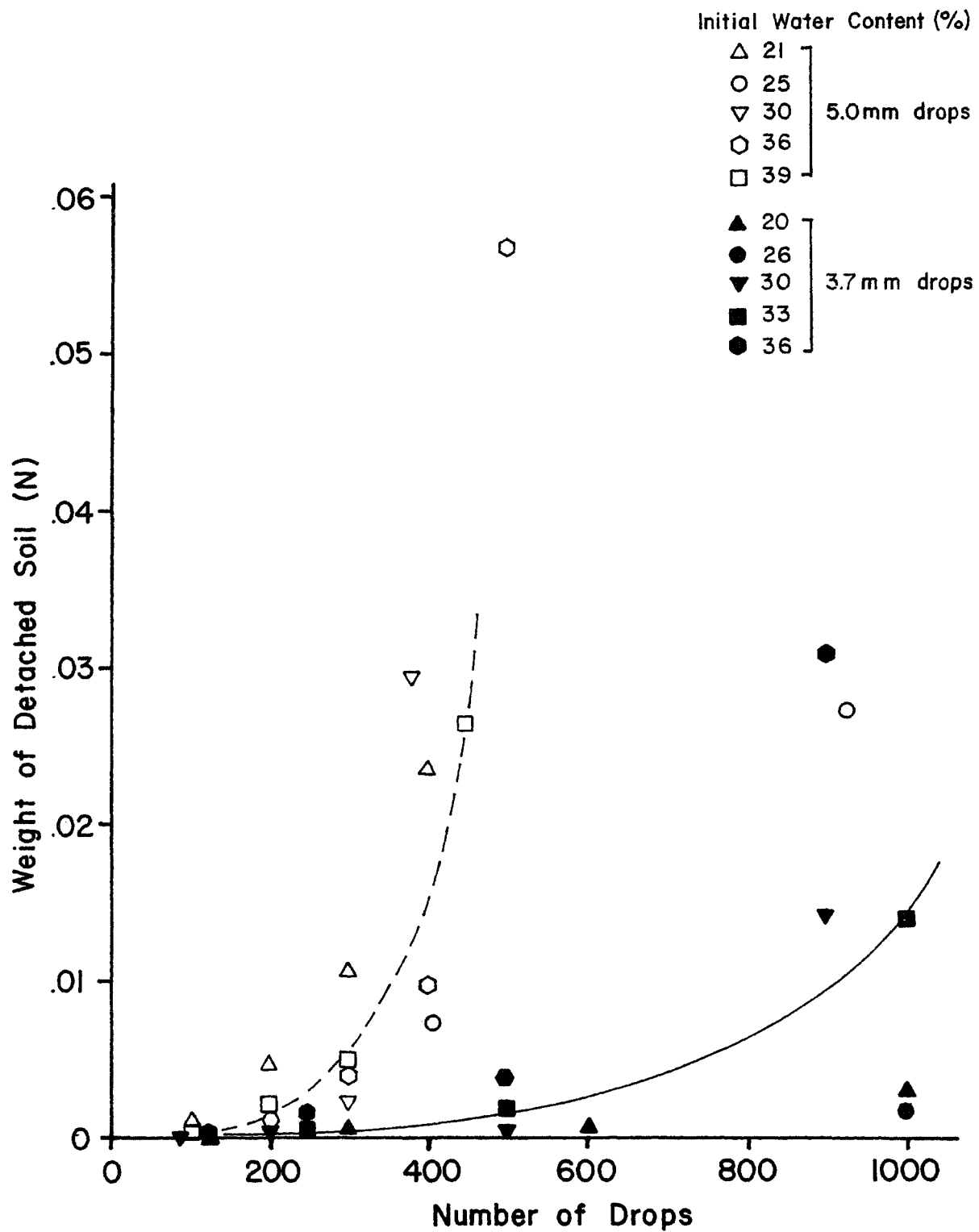


Figure A.4 (b): Weight of Soil Detached and Number of Raindrops, Kaolinite

were collected in the container that enclosed the sample. After a certain number of drops had fallen on the sample, the detached soil in the container was collected and their dry weights were measured. The weight of soil detached as a function of the number of raindrops are plotted in Fig. A.4.

### A.3 ANALYSIS OF RESULTS

The main objective of these experiments is to explore possible ways to model detachment of cohesive soil by raindrops. The data in Fig. A.4 indicate that the rate of soil detachment is at first slow and then increases rapidly. Lines are drawn through data points of selected tests to show the trend. The threshold number of raindrops  $N_0$ , beyond which detachment becomes very large depends on the soil, the water content, and the raindrop size. It should be noted that after about .05N of soil had been detached, the top 1cm of the soil samples was in a state of disintegration. At this point, the sample had absorbed enough water as indicated by the data in Fig. A.3, that its strength was very low and could offer little resistance to the raindrops.

Based on the above observations, a model that may be used as a first approximation of the detachment of cohesive soils is that, up to the threshold number of drops  $N_0$ , no soils is detached and the erosion is zero. After the number of drops exceeds  $N_0$ , the soil clod disintegrates and behaves as a cohesionless material. The laws of sediment transport for cohesionless soils may then be applied. For convenience, the number of drops  $N_0$  should be expressed in terms of rainfall quantities. This can be done by computing the volume of water and dividing it by the area of the soil sample. For the 5mm diameter drop, 1000 drops corresponds to 6.54 cm. of rainfall.

## APPENDIX B

### COMPARISON OF COMPUTED AND MEASURED RILL EROSION

Meyer et al. (24) measured will erosion under simulated rainfall on artificial rills, prepared in a Russell silt loam field. The rills were 4.6 m long and had bed slope of 6% and side slopes of 25%. The present comparison is made for the case of 64 mm/hr rainfall intensity. The test was conducted for several values of base flow, as shown in Table A.1.

To use Equation (3.18), which is derived for rill erosion, several constants and parameters in the equation must be estimated. The silt loam was assumed to aggregate and form larger particles of diameter 0.2 mm. Since the test was performed on rill erosion, the value of the constant  $a_s$  was taken as 300. The exponent  $p$  was kept equal to 2.0. For a Manning coefficient of 0.025 and a runoff factor of 0.5, the computed erosion for different base flows is given in Table B.1.



TABLE B.1 COMPARISON BETWEEN MEASURED AND COMPUTED VALUES OF RILL EROSION

Base Flow $Q_1$ , N/hr	End Flow $Q_2$ , N/hr	Soil Loss* N	MEASURED	COMPUTED FROM EQUATION (3.18)	
			Erosion Rate N/hr/m	$m^3 E_R$ /sec/m	Erosion Rate N/hr/m
0	1140	15.1	03.2	$0.031 \times 10^{-6}$	01.5
7000	7300	49.8	10.8	$0.53 \times 10^{-6}$	25
7000	7100	48.9	10.7	$0.53 \times 10^{-6}$	25
14000	14360	184.5	40.1	$0.53 \times 10^{-6}$	45
14000	12000	93.5	20.3	$0.53 \times 10^{-6}$	45
20000	20500	357.2	77.6	$1.31 \times 10^{-6}$	61
20000	20070	132.0	28.7	$1.31 \times 10^{-6}$	61
28000	29600	374.0	81.3	$1.75 \times 10^{-6}$	81
28000	28850	418.5	91.0	$1.75 \times 10^{-6}$	81

\* Values indicated are the net soil loss from rill erosion only. It is computed by deducting the interrill erosion, as estimated by Meyer et al. (22), from the total measured soil loss.

## APPENDIX C

## REFERENCES

1. Barnett, A.P., Diseker, E.G., and Richardson, E.C. (1967) "Evaluation of Mulching Methods for Erosion Control on Newly Prepared and Seeded Highway Backslopes", *Agronomy Journal*, Vol. 59. pp 83-85.
2. B  th Markus (1974) *Spectral Analysis in Geophysics*. Elsevier Scientific Publishing Company, New York, N.Y.
3. Bubenzer, G.D. and Jones, B. A. (1971) Drop Size and Impact Velocity Effects on the Detachment of Soils under Simulated Rainfall, *Trans. Amer. Soc. Agr. Eng.*, Vol. 14 (4), pp 625-628.
4. Chow, V.T. (1959) *Open-Channel Hydraulics*, McGraw-Hill Book Co., New York.
5. Cruse, R. M. and Larson W.E. (1977) Effect of Soil Shear Strength on Soil Detachment due to Raindrop Impact, *Soil Science Soc. of America J.*, Vol. 41, pp 777-781.
6. Foster, G. R. and Meyer, L.D. (1972) "A Closed-Form Soil Erosion Equation for Upland Areas", In Shen H.W. (ed.), *Sedimentation: Symposium To Honor Professor H.A. Einstein*, pp. 12.1-12.19. H.W. Shen, Fort Collins, Colo.
7. Foster, G.R. and Meyer, L.D. (1972) "Transport of Soil Particles by Shallow flow", *Transactions of the American Society of Agricultural Engineers*, IS (1):99-102.
8. Free, G. R. (1960) Erosion Characteristics of Rainfall, *Agric. Engineering*, Vol. 41, pp 447-449, 455.
9. Freeze, R. A. (1980) "A Stochastic-Conceptual Analysis of Rainfall-Runoff Processes on a Hillslope", *Water Resources Research*, Vol. 16, No. 2, pp 391-408.
10. Graf, W. H. (1971) *Hydraulics of Sediment Transport*. Mc-Graw Hill Book Co., New York, N.Y.
11. Henderson, F. M. (1966) *Open Channel Flow*. Macmillan, New York, N.Y.
12. Horton, R. E. (1945) "Erosional development of streams and their drainage basins; hydrophysical approach to quantitative morphology", *Geol. Soc. America Bull.*, v. 56, pp 275-370.
13. International Mathematical and Statistical Library
14. Kamil Eren (1979) Personal communication

15. Komura, S. (1976) "Hydraulics of Slope Erosion by Overland Flow", American Society of Civil Engineers, HY10, pp 1573-1586.
16. Laws, J. O., (1941) Measurements of the Fall Velocity of Waterdrops and Raindrops, Transactions, Amer. Geophysical Union, Vol. 22, pp 709-721.
17. Leopold, L. B., and Langbein, W. B. (1962) "The Concept of Entropy in Landscape Evolution", 20 pp., U.S. Geol. Surv. Profess. Paper 500-A.
18. Lij, R. M., Shen, H.W., and Simons, D.B. (1973) "Mechanics of Soil Erosion by Overland Flow", Proceedings of the 15th Congress, International Association for Hydraulics Research, Istanbul, Turkey, Vol. 1, Sept. 1973 pp 437-446.
19. Mahmood, K., and Ahmadi-Karvigh, H. (1976) Statistical Procedures for Bed Form Analysis. Engineering Research Center, Colorado State University Fort Collins, Colorado. CERTS-76 KM-HAK 41.
20. Merva, G.E., Brazee, R.D., Schwab, G.O., and Curry, R.B. (1970) "Theoretical Considerations of Watershed Surface Description", Transactions of Amer. Soc. of Agr. Eng.. Vol. 13 (4): 462-465.
21. Meyer, L.D. and Wischmeier, W.H. (1969) "Mathematical Simulation of the process of soil erosion by Water", Transactions of the Amer. Soc. of Agr. Eng. 12(6): 754-758, 762.
22. Meyer, L.D., Foster, G.R., and Nikolov, S. (1975)"Effect of Flow Rate and Canopy on Rill Erosion", Transactions of Amer. Soc. of Agr. Eng. 18(5): 905-911.
23. Meyer, L.D., Foster, G.R., and Romkens, M.J.M. (1975) "Origin of eroded soil from upland slopes", In present prospective Technology for Predicting Sediment Yields and sources. Proc. of the 1972 Sediment-Yield Work-shop, USDA Sedimentation Lab., Oxford, MS, U.S. Agr. Res. Ser (Rep) ARS-S-40: ;; 177-189.
24. Meyer, L.D., De Coursey, D.C., and Romkens, M.J.M. (1976) "Soil Erosion Concepts and Misconceptions", Proceedings of the third Federal Inter-Agency Sedimentation Conference. Water Resource Council, March 22-23, Denver, Colorado.
25. Mutchler, C.K., (1971) "Splash Production by Waterdrop Impact, Water Resources Research, Vol. 7, pp. 1024-1030.
26. Mutchler, C.K. and R.A. Young, (1975), Soil Detachment by Raindrops, Agricultural Research Service, Report ARS-S-40, USDA, pp. 113-117.
27. Newland, D.E. (1975) An Introduction to Random Vibrations and Spectral Analysis. Longman, London and New York.

28. Palmer, R.S. (1965), Waterdrop Impact Forces, Transactions, Amer. Soc. Agric. Eng., Vol. 8 pp. 69-72.
29. Rayner, John (1971) An Introduction to Spectral Analysis. Academic Press, Inc.
30. Ree, W.O., Wimberley, F.L., and Crow, F.R. (1976) "Manning and The Overland Flow Equation", Transactions of the Amer. Soc. of Agr. Eng. August pp 89-95.
31. Rouse, H. (1949) Engineering Hydraulics. John Wiley and Sons, Inc., New York p 707.
32. Scheidegger, A.E. (1967) "A Stochastic model for drainage patterns into an intramantane trench", Bull. Int. Ass. of Sci. Hydrol. 12, 15-20, 1.
33. Schenk, H. (1963) "Simulation of the evolution of drainage basin networks with a digital computer", J. Geophys. Res., 68 (20), 5739-5745.
34. Seginer, I. (1969) "Random Walk and Random Roughness Models of Drainage Networks", Water Resources Research, Vol. 5. No. 3 pp 591-607.
35. Shinozuka, M. and Jan, C.M. (1972) "Digital Simulation of Random Processes and its Applications", Journal of Sound and Vibration, 25 (1), pp 111-128.
36. Smart, J.S., Surkan, A.J., and Considine, J.P. (1967) "Digital Simulation of Channel Networks", in Symposium on River Morphology, General Assembly of Bern, pp 87-98.
37. Smith, R.E. (1976) "Simulating Erosion Dynamics with a Deterministic Distributed Watershed Model", Proc. 3rd Federal Interagency Sediment Conference.
38. Van Doren (1978) Personal communication.
39. Wilson, S.D., "Suggested Method of Test for Moisture-Density Relations of Soils Using Harvard Compaction Apparatus, "Procedures for Testing Soils, ASTM Committee D-18, ASTM, Baltimore, MD, 1958, pp. 133-135.
40. Yalin, M.S. (1976) Mechanics of Sediment Transport. 2nd Edition. Pergamon Press.
41. Yoon, Y.N. and Wenzel, H.G. (1971) "Mechanics of Sheet Flow under Simulated Rainfall", Journal of the Hydraulics Division, Amer. Soc. of Civil Eng., Vol. 97-No. HY9, Proc. Paper 8373, pp. 1367-1386.
42. Young, R.A., and J.L. Wiersma, (1973) The Role of Rainfall Impact in Soil Detachment and Transportation, Water Resources Research, Vol. 9, pp. 1629-1636.

## APPENDIX D

### LISTING AND SAMPLE OUTPUT OF THE COMPUTER PROGRAM

C		A00010
C		A00020
C		A00030
C		A00040
C		A00050
C		A00060
C		A00070
C		A00080
C		A00090
C		A00100
C		A00110
C		A00120
C		A00130
C		A00140
C		A00150
C		A00160
C		A00170
C		A00180
C		A00190
C		A00200
C		A00210
C		A00220
C		A00230
C		A00240
C		A00250
C		A00260
C		A00270
C		A00280
C		A00290
C		A00300
C		A00310
C		A00320
C		A00330
C		A00340
C		A00350
C		A00360
C		A00370
C		A00380
C		A00390
C		A00400
C		A00410
C		A00420
C		A00430
C		A00440
C		A00450
C		A00460
C		A00470
C		A00480
C		A00490
C		A00500
C		A00510
C		A00520
C		A00530
C		A00540
C		A00550
C		A00560
C		A00570
C		A00580
C		A00590
C		A00600
C		A00610
C		A00620
C		A00630
C		A00640
C		A00650
C		A00660
C		A00670
C		A00680
C		A00690
C		A00700
C		A00710
C		A00720
C		A00730
C		A00740
C		A00750
C		A00760

```

*****
* A STOCHASTIC MODEL *
*       FOR          *
*   SOIL EROSION    *
*       BY           *
*   MOSTAFA MOSSAAD *
*   APRIL 1981      *
*****

*****
DEFINITION OF PRINCIPAL VARIABLES :
*****
NP= # OF POINTS ON EACH PROFILE
NPF= # OF PROFILES
CUT= CUTOFF LENGTH (IF USED AS A LOW-PASS FILTER).
TLEN= TOTAL LENGTH OF MICRORELIEF PROFILE.
DX= DISTANCE BETWEEN ROUGHNESS DATA MEASUREMENTS

DMLM= REPRESENTATIVE SOIL PARTICLE DIAMETER, MILLIMETER
UWT= UNIT WEIGHT OF SOIL ,N/CUBIC METER
RO= DENSITY OF WATER, KG/C. METER
G= GRAVITY ACCEL. N/SQ. SEC
SG= SPECIFIC GRAVITY OF SOIL

RN= MANNING'S COEFFICIENT
P= EXPONENT IN KALINSKE'S EQUATION
ASR= CONSTANT IN RILL EROSION EQUATION
ASH= CONSTANT IN INTERRILL EROSION EQUATION

NX= # OF MESH POINTS IN X-DIRECTION
NY= # OF MESH POINTS IN Y-DIRECTION
SLOPE= AVERAGE SLOPE OF SURFACE, DEGREES
RNL= RAIFALL INTENSITY, MLMTR/HR
RNF= RUNOFF COEFFICIENT
ANRATE= ANNUAL RATE OF RAIN
TI= DURATION OF TIME INTERVAL, MINUTES
NTI= # OF TIME INTERVALS
NRS= # OF RANDOM SURFACES (I.E. SAMPLE SIZE)

AMP= AMPLITUDE OF BASIC WAVE
WL= WAVELENGTH OF " " " " " " " " " " " " " " " "
SL= LENGTH OF SHORT SIDE OF BASIC RECTANGULAR MESH ELEMENT, METER
SH= HORIZONTAL PROJECTION OF SL

SDT(I)= TOTAL VOLUME OF SEDIMENT WHICH PASSED BY POINT I
DURING A TIME INTERVAL, CUBIC METERS
TRE(I)= VOLUME OF RILL EROSION PART OF SEDIMENT WHICH PASSED
BY POINT I DURING A TIME INTERVAL, C. METERS
TIRE(I)= VOLUME OF INTERRILL EROSION PART OF SEDIMENT WHICH
PASSED BY POINT I DURING A TIME INTERVAL, C. METERS
TBTM= WEIGHT OF TOTAL SEDIMENT ACCUMULATED AT THE BOTTOM DURING
A TIME INTERVAL ,NEWTONS
TBTM= WT. OF INTER-RILL EROSION " " " " " " " " " " " "
TRBTM= WT. OF RILL-EROSION " " " " " " " " " " " "
RATIO= RILL/INTERRILL EROSION DURING A TIME INTERVAL
RATE= EROSION RATE IN N/SQ. M/HR " " " " " " " " " "
FTSDT(NS)= TOTAL SDMT. FROM RANDOM SURFACE NO. NS ,NEWTONS
FRSDT(NS)= RILL EROSION " " " " " " " " " " " "
FHSDT(NS)= INTER RILL EROSION " " " " " " " " " "
FRATIO(NS)= TOTAL RILL/INTERRILL EROSION RATIO " " " "
FRATE(NS)= TOTAL EROSION RATE " " " " " " " " " "
*****
*****
DATA CARDS ARE PUT IN THE FOLLOWING ORDER :
1) NP,NPF,CUT,TLEN,DX (SEE FORMAT STATMENT # 1)
2) ROUGHNESS DATA CARDS (SEE FORMAT STATMENT # 2)
3) DMLM,UWT,RO,G,SG (SEE FORMAT STATMENT # 3)
4) RN,P,ASR,ASH (SEE FORMAT STATMENT # 4)
5) NX,NY,SLOPE,RNL,RNF,ANRATE (SEE FORMAT STATMENT # 5)

```

C	6) TI,NTI,NRS	(SEE FORMAT STATMENT # 6)	A00770
C	7) SLIMIT,SSTART	(SEE FORMAT STATMENT # 7)	A00780
C	8) NRUN (15), SEE NOTE # 2		A00790
C	9) NRUN VALUES OF PARAMETER BEING STUDIED, SEE NOTE # 2		A00800
C	*****		A00810
C	NOTE # 1		A00820
C	*****		A00830
C	THIS PROGRAM USES TWO SUBROUTINES CALLED FFTR AND FFTP FROM		A00840
C	THE "IMSL" LIBRARY:		A00850
C	FFTR : COMPUTES FOURIER TRANSFORM, AND		A00860
C	FFTP : COMPUTES INVERSE FOURIER TRANSFORM.		A00870
C	MAKE SURE THEY STILL EXIST IN THE COMPUTER LIBRARY UNDER		A00880
C	THE SAME NAME		A00890
C	*****		A00900
C			A00910
C			A00920
C	DIMENSION VARPLT(10)		A00930
C	DIMENSION XP(200),YP(200),RSD(200)		A00940
C	DIMENSION YYP(1000)		A00950
C	DIMENSION TBTM(100),RBTM(100),HBTM(100)		A00960
C	DIMENSION FTSDT(100),FRSDT(100),FHSDDT(100),FRATIO(100),FRATE(100)		A00970
C	COMMON/MESH/NX,NY,NMAX,SL,SH,WL,QQ		A00980
C	COMMON/NODES/X(2000),Y(2000),CODE(2000),ELV(2000)		A00990
C	COMMON/QFLOW/QT(2000),QL(2000),QR(2000)		A01000
C	COMMON/SDMNT/SDT(2000),TRE(2000),TIRE(2000)		A01010
C	COMMON/PONDG/KPND(2000),NAJ(2000),DH(2000)		A01020
C	COMMON/HMPP/HMP(500),XHMP(500),YHMP(500)		A01030
C	COMMON/SLOPES/HMP1(500),HMP2(500),HMP3(500),HMP4(500),HMP5(500),		A01040
C	* HMP6(500)		A01050
C	COMMON /SAME/TLEN,CUT		A01060
C	COMMON /PROP/GAMA,RO,G,SG,RN		A01070
C	COMMON NT		A01080
C	*****		A01090
C	READ SURFACE ROUGHNESS DATA		A01100
C	*****		A01110
C	READ(5,1) NP,NPF,CUT,TLEN,DX		A01120
C	NTOTAL=NP*NPF		A01130
C	READ(5,2)(YYP(I),I=1,NTOTAL)		A01140
C	*****		A01150
C	READ PHYSICAL PARAMETERS		A01160
C	*****		A01170
C	READ(5,3) DMLM,UWT,RO,G,SG		A01180
C	READ(5,4) RN,P,ASR,ASH		A01190
C	*****		A01200
C	READ STORM AND SLOPE DATA		A01210
C	*****		A01220
C	READ(5,5) NX,NY,SLOPE,RNL,RNF,ANRATE		A01230
C	READ(5,6) TI,NTI,NRS		A01240
C	READ(5,7) SLIMIT,SSTART		A01250
C	D=DMLM/1000.		A01260
C	TTIME=TI*NTI/60.		A01270
C	*****		A01280
C	THE FOLLOWING FOUR CARDS ARE TO BE USED ONLY WHEN		A01290
C	COMPUTING RESULTS FOR (NRUN) VALUES OF ANY PARAMETER. FOR		A01300
C	EXAMPLE, RN, IN THE CASE BELOW		A01310
C	READ(5,2000) KRUN		A01320
C	READ(5,3000)(VARPLT(I),I=1,KRUN)		A01330
C	DO 1000 NRUN=1,KRUN		A01340
C	RN=VARPLT(NRUN)		A01350
C	WRITE(25) NRUN,VARPLT(NRUN)		A01360
C	2000 FORMAT(I5)		A01370
C	3000 FORMAT(10F8.3)		A01380
C			A01390
C	SLPR=TAN(SLOPE*22./7./180.)*100		A01400
C	RAINYR=RNL*TTIME/ANRATE/10.		A01410
C	WRITE(6,50)		A01420
C	WRITE(6,209)		A01430
C	WRITE(6,203)		A01440
C	WRITE(6,230)		A01450
C	WRITE(6,203)		A01460
			A01470
			A01480
			A01490
			A01500
			A01510
			A01520

WRITE(6,209)	A01530
WRITE(6,310)	A01540
WRITE(6,315)	A01550
WRITE(6,320) NPF,NP,DX	A01560
WRITE(6,330)	A01570
WRITE(6,315)	A01580
WRITE(6,340) DMLM,UWT,SG	A01590
WRITE(6,350) P,ASR,ASH,RN	A01600
WRITE(6,360)	A01610
WRITE(6,315)	A01620
WRITE(6,370) NX,NY,SLOPE,SLPR,RNL,RNF	A01630
WRITE(6,375) ANRATE,RAINYP	A01640
WRITE(6,380) TI,TTIME,NRS	A01650
WRITE(6,390) SLIMIT,SSTART	A01660
WRITE(6,60)	A01670
XP(1)=0.0	A01680
DO 14 I=2,NP	A01690
XP(I)=XP(I-1)+DX	A01700
14 CONTINUE	A01710
IF(NRUN.GT.1) GO TO 4000	A01720
WRITE(6,50)	A01730
WRITE(6,209)	A01740
WRITE(6,203)	A01750
WRITE(6,400)	A01760
WRITE(6,203)	A01770
WRITE(6,209)	A01780
C	A01790
C *****	A01800
C ... DETERMINE THE CHARACTERISTICS OF THE BASIC WAVE	A01810
C *****	A01820
C	A01830
CALL CWAVER(XP,YP,YP,NP,NPF,CUT,TLEN,AMP,WL,RSD,	A01840
* RMEAN,STDEV)	A01850
WRITE(6,300) AMP,WL	A01860
C	A01870
WRITE(6,305) RMEAN,STDEV	A01880
C ... CONVERT TO METERS	A01890
C	A01900
AMP=AMP/1000.	A01910
WL=WL/100.	A01920
STDEV=STDEV/1000.	A01930
RMEAN=RMEAN/1000.	A01940
C	A01950
C *****	A01960
C ... CONSTRUCT THE HEXAGONAL MESH	A01970
C *****	A01980
C	A01990
SL=WL/(2.*(3.**0.5))	A02000
SLP=SLOPE*22./7./180.	A02010
SH=SL*COS(SLP)	A02020
4000 CONTINUE	A02030
DO 3007 I=1,NMAX	A02040
X(I)=0.	A02050
Y(I)=0.	A02060
CODE(I)=0	A02070
NAJ(I)=0	A02080
KPND(I)=0	A02090
3007 CONTINUE	A02100
CALL HXNMESH	A02110
TAREA=Y(NY)*X(NMAX)	A02120
FSHAPE=X(NMAX)/Y(NY)	A02130
PL=Y(NY)	A02140
PW=X(NMAX)	A02150
WRITE(6,40) PL,PW	A02160
WRITE(6,30) TAREA,FSHAPE	A02170
WRITE(6,60)	A02180
GAMA=R0*C/9.81	A02190
C	A02200
C *****	A02210
C ... COMPUTE PARAMETERS OF EROSION EQUATIONS	A02220
C *****	A02230
C	A02240
CALL PARAM(D,P,ASR,ASH,RCH,HCH,EX)	A02250
C	A02260
C ... START DO LOOP 200 FOR DIFFERENT RANDOM SURFACES	A02270



```

C      DO 200 NS=1,NRS
      DO 201 I=1,NMAX
      ELV(I)=0.0
      DH(I)=0.0
201    HHMP(I)=0.0
      DO 202 I=1,NRS
      FTSDT(I)=0.0
      FRSDT(I)=0.0
      FHSDT(I)=0.0
      FRATIO(I)=0.0
202    FRATE(I)=0.0
C
C      ... ASSIGN ORIGINAL ELEVATIONS TO ALL MESH POINTS
C      CALL          ELEVTN(SLOPE,AMP,RMEAN,STDEV,NS)
C
C      ... ASSIGN CALL NUMBERS,COORDINATES ,AND ELEVATIONS TO ALL HUMPS
C      CALL          HUMP(RMEAN,STDEV,SLOPE,AMP,NHUMP)
      WRITE(6,204)
      WRITE(6,203)
      WRITE(6,205)  NS
      WRITE(6,203)
      WRITE(6,209)
      WRITE(6,206)
      WRITE(6,207)
      WRITE(6,208)
C
C      ... START DO LOOP 100 FOR THE SEQUENCE OF TIME INTERVALS FOR THE
C      RANDOM SURFACE UNDER CONSIDERATION
C
      DO 100 NT=1,NTI
      DO 101 I=1,NMAX
      SDT(I)=0.0
      TRE(I)=0.0
      TIRE(I)=0.0
      QL(I)=0.0
      QR(I)=0.0
      QT(I)=0.0
      IF(Y(I).EQ.0.0.AND.KPND(I+1).EQ.0) DH(I)=DH(I+1)
      ELV(I)=ELV(I)-DH(I)
      DH(I)=0.0
101    CONTINUE
      CALL          SFILR(SLIMIT,SSTART)
      CALL          POND
      CALL          ACJNT
888    FORMAT(3(I5,F15.5,I5))
C
C      ... STORE INITIAL ELEVATIONS OF ALL POINTS ON FILE # 35
C      IF(NT.GT.1) GO TO 635
      REWIND 35
      CALL          STORE(NNOD,NHUMP)
635    CONTINUE
C
C      *****
C      ... COMPUTE STEADY STATE FLOW AT MESH POINTS DURING A TIME INTERVAL
C      *****
C
      CALL          FLOW(RNL,RNF)
      NVOID=0
      DO 70 LL=1,NY
      KK=NY+(1-LL)
      DO 70 I=KK,NMAX,NY
      IF(Y(I).EQ.0.0) GO TO 75
      IF(CODE(I)-1) 75,80,85
C
C      *****
C      ... COMPUTE EROSION FOR RILL SEGMENTS WITH UPSTREAM POINT HAVING
C      CODE=1.
C      *****
C
80    CALL          ERSN1(I,QT(I-1),HCH,RCH,EX,TI)
      GO TO 70
C

```

C	*****	A03040
C	... COMPUTE EROSION FOR RILL SEGMENTS WITH UPSTREAM POINT HAVING	A03050
C	CODE=2.	A03060
C	*****	A03070
C		A03080
85	CALL ERSN2(I,QL(I),QR(I),HCH,RCH,EX,TI)	A03090
75	IF(CODE(I).EQ.0.0) NVOID=NVOID+1	A03100
70	CONTINUE	A03110
777	FORMAT(3(15,2F15.5))	A03120
	DO 105 I=1,NHUMP	A03130
999	FORMAT(15,7F15.5)	A03140
105	HHMP(I)=(HMP1(I)+HMP2(I)+HMP3(I)+HMP4(I)+HMP5(I)+HMP6(I))/6.	A03150
	TTBTM=0.0	A03160
	TRBTM=0.0	A03170
	THBTM=0.0	A03180
	DO 110 K=1,NX	A03190
	J=1+(K-1)* NY	A03200
	TBTM(K)=SDT(J)*UWT	A03210
	TTBTM=TTBTM+TBTM(K)	A03220
	RBTM(K)=TRE(J)*UWT	A03230
	TRBTM=TRBTM+RBTM(K)	A03240
	HBTM(K)=TIRE(J)*UWT	A03250
	THBTM=THBTM+HBTM(K)	A03260
110	CONTINUE	A03270
	RATIO=TRBTM/THBTM	A03280
	RATE=TTBTM*60/TAREA/TI	A03290
C		A03300
C	... STORE EROSION RATE RESULTS ON FILE # 25	A03310
C		A03320
	XPLT=TI*NT	A03330
	YPLT=RATE	A03340
	ZPLT=RATIO	A03350
	WRITE(25) XPLT,YPLT,ZPLT	A03360
	FTSDT(NS)=FTSDT(NS)+TTBTM	A03370
	FRSDT(NS)=FRSDT(NS)+TRBTM	A03380
	FHSDT(NS)=FHSDT(NS)+THBTM	A03390
	FRATIO(NS)= FTSDT(NS)/FHSDT(NS)	A03400
	FRATE(NS)=FTSDT(NS)*60.0/TAREA/TI/NT	A03410
	WRITE(6,210) NT,TTBTM,RATIO,RATE,FTSDT(NS),FRATIO(NS),FRATE(NS)	A03420
260	FORMAT(130('*'),/,130('*'))	A03430
100	CONTINUE	A03440
	NNOD=NMAX-NVOID	A03450
C		A03460
C	... STORE FINAL ELEVATIONS OF ALL POINTS ON FILE # 35	A03470
C		A03480
	CALL STORE(NNOD,NHUMP)	A03490
	END FILE 35	A03500
C		A03510
C	... CHECK DATA STORED ON FILE # 35	A03520
C	REWIND 35	A03530
C625	READ(35,END=600)NY,NNOD,NHUMP	A03540
C	WRITE(6,630) NY,NNOD,NHUMP	A03550
C630	FORMAT(3110)	A03560
C	READ(35)XMAX,YMAX	A03570
C	WRITE(6,612)XMAX,YMAX	A03580
C612	FORMAT(2F20.5)	A03590
C605	READ(35,END=600) XXX,YYY,ZZZ	A03600
C	WRITE(6,610) XXX,YYY,ZZZ	A03610
C	IF(XXX.GT.88887.) GO TO 625	A03620
C	GO TO 605	A03630
C600	CONTINUE	A03640
C610	FORMAT(3F20.5)	A03650
C		A03660
200	CONTINUE	A03670
	WRITE(6,220)	A03680
	WRITE(6,211)	A03690
	WRITE(6,212)	A03700
	WRITE(6,215)(I,FTSDT(I),FRSDT(I),FHSDT(I),FRATIO(I),FRATE(I),I=1,	A03710
	* NRS)	A03720
	XPLT=99999.	A03730
	WRITE(25) XPLT,YPLT,ZPLT	A03740
1000	CONTINUE	A03750
	END FILE 25	A03760
C		A03770
C	... CHECK DATA STORED ON FILE # 25	A03780
C	REWIND 25	A03790
C	READ(25) NRUN,VARPLT(NRUN)	A03800

C	WRITE(6,611) NRUN,VARPLT(NRUN)	A03810
C611	FORMAT(110,F10.5)	A03820
C333	READ(25,END=334)XX,YY	A03830
C	WRITE(6,335) XX,YY	A03840
C335	FORMAT(2F20.5)	A03850
C	GO TO 333	A03860
C 334	CONTINUE	A03870
C		A03880
1	FORMAT(214,3F8.2)	A03890
2	FORMAT(10F6.2)	A03900
3	FORMAT(5F10.4)	A03910
4	FORMAT(4F10.4)	A03920
5	FORMAT(215,4F10.3)	A03930
6	FORMAT(F10.3,215)	A03940
7	FORMAT(2F10.4)	A03950
30	FORMAT(///,10X,'TEST AREA =',F10.3,' SQ. METERS',///,10X, * 'SHAPE FACTOR =',F10.3)	A03960
40	FORMAT(///,10X,'PLOT LENGTH=',F10.3,' METERS',///,10X, * 'PLOT WIDTH =',F10.3,' METERS')	A03970
50	FORMAT(1H1,5X,110('*'),///)	A03980
60	FORMAT(///,5X,110('*'))	A03990
203	FORMAT(T23,'*',T54,'*',/,T23,'*',T54,'*')	A04000
204	FORMAT(1H1,///,23X,30('*'))	A04010
205	FORMAT(T23,'*',T29,'RANDOM SURFACE NO. ',13,T54,'*')	A04020
206	FORMAT(///,T11,'RESULTS OF EACH INTERVAL',T51,'CUMULATIVE RESULTS' * ',T11,24('-'),T51,18('-'))	A04030
207	FORMAT(/,3X,'INTRVL #',T13,'TTL SDMT',T23,'R/I RATIO',T34, * 'ERSN RATE',T47,'TTL SDMT',T57,'R/I RATIO',T69,'ERSN RATE')	A04040
208	FORMAT(T15,'( N)',T33,'( N/SM/HR)',T49,'( N)',T68,'( N/SM/HR)')	A04050
209	FORMAT(23X,30('*'))	A04060
210	FORMAT(/,2X,15,2X,3F10.2,' *,3F10.2)	A04070
211	FORMAT(///,T4,'NRS',T9,'TTL SDMT',T22,'R. ERSN.',T30, * 'I. ERSN.',T40,'R/I RATIO',T50,'ERSN. RATE')	A04080
212	FORMAT(T9,'( N)',T23,'( N)',T33,'( N)',T50,'( N/SM/HR)',///)	A04090
215	FORMAT(15,5F10.3,/) )	A04100
220	FORMAT(1H1,///,15X,'FINAL RESULTS FOR ALL RANDOM SURFACES',/, * 15X,36('*'))	A04110
305	FORMAT(/,10X,'MEAN OF NORMAL DIST. =',F8.3,' MLMTR',///, * 10X,'STAND. DEVIATION OF NORMAL DIST. =',F8.3,' MLMTR')	A04120
300	FORMAT(///,10X,'AMPLITUDE OF REPRESENTATIVE WAVE=',F8.3,2X,'MLMR', * ///,10X,'LENGTH OF REPRESENTATIVE WAVE =',F8.3,2X,'CM')	A04130
230	FORMAT(T23,'*',T29,' I N P U T D A T A ',T54,'*')	A04140
310	FORMAT(///,10X,'GROUP # 1 :',10X,'SURFACE ROUGHNESS DATA')	A04150
315	FORMAT(10X,11('*'),10X,22('*'),/,10X,11('*'))	A04160
320	FORMAT(///,15X,'NO. OF ELEVATION TRACES =',15,///,15X, * 'NO. OF POINTS PER TRACE =',15, * ///,15X,'SPACING =',F5.2,3X,'CM')	A04170
330	FORMAT(///,10X,'GROUP # 2 :',10X,' PROBLEM PARAMETERS ')	A04180
340	FORMAT(///,15X,'SOIL PARTICLE DIAMETER =',F5.3,3X,'MLMTR', * ///,15X,'SOIL UNIT WEIGHT =',F6.0,3X,' N/C. METER', * ///,15X,'SOIL SPECIFIC WEIGHT =',F5.2)	A04190
350	FORMAT(///,15X,'EXPONENT OF KALINSKE EQN. =',F5.2, * ///,15X,'EQN. CONSTANT FOR RILLS =',F5.1, * ///,15X,'EQN. CONSTANT FOR HUMPS =',F5.1, * ///,15X,'MANNING CONSTANT =',F5.3)	A04200
360	FORMAT(///,10X,'GROUP # 3 :',10X,' STORM AND SLOPE DATA ')	A04210
370	FORMAT(///,15X,'NO. OF MESH POINTS IN CROSS-DIRECTION =',15, * ///,15X,'NO. OF MESH POINTS IN LONGT-DIRECTION =',15, * ///,15X,'AVERAGE SLOPE =',F5.1, * 3X,'DEGREES',/,T54,'=' ,F7.2,3X,'PERCENT', * ///,15X,'RAINFALL INTENSITY =',F5.1, * 3X,'MLMTR/HR',///,15X,'RUNOFF COEFFICIENT =', * F5.2)	A04220
375	FORMAT(///,T16,'ANNUAL RAINFALL RATE',T54,'=' ,F5.1,T64,'CNTMTR', * ///,T16,'EQUIVALENT YEARS OF RAIN',T54,'=' ,F5.2,T64,'YEARS')	A04230
380	FORMAT(///,15X,'TIME INTERVAL =',F5.1,3X, * 'MINUTES',///,15X,'TOTAL RAIN PERIOD =',F5.2, * 3X,'HOURS',///,15X,'NO. OF RANDOM SURFACES =', * 15,///)	A04240
390	FORMAT(15X,'FAILURE LIMIT FOR SIDE SLOPE', 9X,'=' ,F5.2, * ///,15X,'STARTING LIMIT FOR SIDE SLOPE', 9X,'=' ,F5.2,///)	A04250
400	FORMAT(T23,'*',T26,' SPECTRAL ANALYSIS RESULTS ',T54,'*')	A04260
250	STOP	A04270
	END	A04280
		A04290
		A04300
		A04310
		A04320
		A04330
		A04340
		A04350
		A04360
		A04370
		A04380
		A04390
		A04400
		A04410
		A04420
		A04430
		A04440
		A04450
		A04460
		A04470
		A04480
		A04490
		A04500
		A04510
		A04520
		A04530
		A04540

```

SUBROUTINE STORE(NNOD,NHUMP)
COMMON/MESH/NX,NY,NMAX,SL,SH,WL,QQ
COMMON/NODES/X(2000),Y(2000),CODE(2000),ELV(2000)
COMMON/HMPP/HMPP(500),XHMP(500),YHMP(500)
WRITE(35) NY,NNOD,NHUMP
WRITE(35) X(NMAX),Y(NY),SL
DO 505 I=1,NMAX
IF(CODE(I).LE.0.0) GO TO 505
WRITE(35) X(I),Y(I),ELV(I)
505 CONTINUE
DO 620 I=1,NHUMP
WRITE(35) XHMP(I),YHMP(I),HMPP(I)
620 CONTINUE
XEND=88888.
WRITE(35) XEND,YEND,ZEND
RETURN
END

SUBROUTINE CWAVE(XP,YP,YYP,NP,NPF,CUT,TLEN,AMP,WL,RSD
*,RMEAN,STDEV)
*****
C THE FUNCTION OF THIS SUBPROGRAM IS:
C 1) PROCESS SURFACE ROUGHNESS DATA FOR SPECTRAL ANALYSIS, AND
C 2) IDENTIFY THE BASIC WAVE
C
C COMPUTATIONS ARE BASED ON THE METHOD OF AVERAGE COEFFICIENTS.
C *****
REAL*8 FMEAN
REAL*4 XP(1),YP(1),YYP(1)
REAL*8 AN(1000),BN(1000),DPOW(1000),R(1000),C(1000),WLAM(1000)
REAL*8 AAN(1000),BBN(1000),RR(1000),CC(1000),DDPOW(1000)
REAL*4 RSD(1000),YW(1000)
DIMENSION NDEG(1000)
NH1=NP/2+1
DO 401 I=1,NH1
AAN(I)=0.0
BBN(I)=0.0
DDPOW(I)=0.0
RR(I)=0.0
CC(I)=0.0
401 CONTINUE
DO 405 K=1,NPF
DO 404 I=1,NP
M=(K-1)*NP
YP(I)=YYP(M+I)
404 CONTINUE
CALL FILTER(XP,YP,NP,NDEG,AN,BN,DPOW,R,C,WLAM,FMEAN)
C ... COMPUTE AVERAGE VALUES OF AN,BN,...,ETC FOR ALL PROFILES:
C
DO 410 J=1,NH1
AAN(J)=AAN(J)+AN(J)/(1.*NPF)
BBN(J)=BBN(J)+BN(J)/(1.*NPF)
DDPOW(J)=DDPOW(J)+DPOW(J)/(1.*NPF)
RR(J)=RR(J)+R(J)/(1.*NPF)
CC(J)=CC(J)+C(J)/(1.*NPF)
410 CONTINUE
405 CONTINUE
WRITE(6,419)
WRITE(6,421)
WRITE(6,423)
WRITE(6,426) (NDEG(J),AAN(J),BBN(J),DDPOW(J),RR(J),CC(J),
* WLAM(J),J=1,NH1)
C
C ... DETERMINE THE BASIC WAVE : PICK-UP THE WAVE WITH MAX. POWER IN
C THE "MICRO ROUGHNESS" RANGE.THE MICR. ROUGH. RANGE INCLUDES
C ALL WAVES LENGTH LESS THAN OR EQUAL TO 30.0 CENTIMETERS.
C
PWMAX=0.0
K=0
DO 430 I=1,NH1
IF(WLAM(I).GT.30.) GO TO 430

```

	IF(DDPOW(I).LE.PWMAX) GO TO 430	C00540
	PWMAX=DDPOW(I)	C00550
	K=I	C00560
430	CONTINUE	C00570
	AMP=(AAN(K)*AAN(K)+BBN(K)*BBN(K))*0.5	C00580
	WL=WLAM(K)	C00590
	PSI=2*NDEG(K)*22.0/7.0/TLEN	C00600
	DO 460 KK=1,NPF	C00610
	DO 450 I=1,NP	C00620
	M=(KK-1)*NP	C00630
	YP(I)=YYP(M+1)	C00640
	XPSI=XP(I)*PSI	C00650
	FAZ1=COS(XPSI)	C00660
	FAZ2=SIN(XPSI)	C00670
	YW(I)=AAN(K)*FAZ1+BBN(K)*FAZ2+FMEAN	C00680
	RSD(I)=YP(I)-YW(I)	C00690
450	CONTINUE	C00700
	CALL RESDL(RSD,NP,RMUE,SIGMA)	C00710
	RMEAN=RMEAN+RMUE/(1.*NPF)	C00720
	STDEV=STDEV+SIGMA/(1.*NPF)	C00730
C	WRITE(6,455) (RSD(I),I=1,NP)	C00740
460	CONTINUE	C00750
419	FORMAT(//,10X,'AVERAGE VALUES FOR ALL PROFILES',/)	C00760
421	FORMAT(10X,31(' '))	C00770
423	FORMAT(///,T6,'DEGREE',T16,'AN',T24,'BN',T32,'POWER',T40,'CONTR.',	C00780
	* T48,'TOTAL',T56,'L (CM) ',/)	C00790
425	FORMAT(2(I10,2F8.2,F11.3,2F8.4,F8.1,2X))	C00800
426	FORMAT(110,2F8.2,F11.3,2F8.4,F8.2)	C00810
455	FORMAT(10(2X,F6.2))	C00820
	RETURN	C00830
	END	C00840
	SUBROUTINE FILTER(X,Y,N,NDEG,AN,BN,DPOW,R,C,WLAM,FMEAN)	D00010
C	*****	D00020
C	THIS SUBPROGRAM PROCESSES THE DATA BEFORE AND AFTER SPECTRAL ANAL.	D00030
C	IF MEASUREMENTS ARE NOT EQUALLY SPACED, THE PROGRAM GENERATES	D00040
C	AN INTERPOLATED PROFILE WITH INTERVAL=DX, USING THE FUNCTION TERP1.	D00050
C	*****	D00060
C		D00070
	IMPLICIT REAL*8(A-H,O-Z)	D00080
	REAL*4 TLEN,CUT	D00090
	REAL*4 X(1),Y(1)	D00100
	REAL*4 YNS(1000),YORG(1000)	D00110
	REAL*4 XX(1000),YTEMP(1000)	D00120
	REAL*8 AN(1),BN(1),R(1),C(1)	D00130
	DIMENSION NDEG(1)	D00140
	DIMENSION F(1000),DPOW(1000),WLAM(1000)	D00150
	DIMENSION IL(2000),ILL(2000),ILLL(2000)	D00160
	COMPLEX*16 FN(1000)	D00170
	EQUIVALENCE (IL(1),ILL(1),ILLL(1))	D00180
	COMMON /SAME/TLEN,CUT	D00190
C ...	INTERPOLATE TO HAVE EQUALLY SPACED DATA	D00200
C	WRITE(6,720)	D00210
C	WRITE(6,705) (X(I),Y(I),I=1,N)	D00220
C	WRITE(6,700)	D00230
	DO 9 I=1,N	D00240
	YORG(I)=Y(I)	D00250
9	CONTINUE	D00260
	FINT=0.5	D00270
	XX(I)=X(I)	D00280
	F(I)=Y(I)	D00290
	DELTA=TLEN/(N-1)	D00300
	ABSIS=X(1)	D00310
	DO 11 I=2,N	D00320
	ABSIS=ABSIS+DELTA	D00330
	XX(I)=ABSIS	D00340
11	F(I)=TERP1(ABSIS,X,Y,N,FINT)	D00350
C	WRITE(9,705) (XX(I),F(I),I=1,N)	D00360
C ...	REMOVE THE MEAN	D00370
	SUM=0.	D00380
	DO 10 I=1,N	D00390
10	SUM=SUM+F(I)	D00400
	FMEAN=SUM/N	D00410
C	WRITE(6,715) FMEAN	D00420
	DO 15 I=1,N	D00430
15	F(I)=F(I)-FMEAN	D00440
C	WRITE(6,721)	D00450

C	WRITE(6,705)(XX(I),F(I),I=1,N)	D00460
C	WRITE(6,700)	D00470
C ...	COMPUTE COMPLEX FOURIER COEFFICIENTS	D00480
	CALL POWER(F,FN,NDEG,AN,BN,DPOW,R,C,WLAM,N)	D00490
C ...	COMPUTE DATA VECTOR IN TIME DOMAIN	D00500
	NH=N/2	D00510
	NH1=NH+1	D00520
	NH2=NH+2	D00530
C ...	FILTER OUT HIGH FREQUENCIES	D00540
C...	SPLIT -FN(1)- AND -FN(NH1)- INTO HALF TO USE FOLLOWING LOGIC	D00550
	FN(1)=FN(1)/2.	D00560
	FN(NH1)=FN(NH1)/2.	D00570
	DO 16 I=2,NH1	D00580
	IF(DABS(WLAM(I)).LT.CUT)GO TO 100	D00590
16	CONTINUE	D00600
100	CONTINUE	D00610
	NHIGH=1	D00620
	IF(I.EQ.NH1)NHIGH=I+1	D00630
	DO 20 I=NHIGH,N	D00640
20	FN(I)=(0.,0.)	D00650
C ...	COMPUTE INVERSE FOURIER TRANSFORM	D00660
	CALL FFTP(FN,N,IL,ILL,ILLL)	D00670
	DO 25 I=1,N	D00680
25	FN(I)=FN(I)+DCONJG(FN(I))	D00690
	DO 26 I=1,N	D00700
26	F(I)=FN(I)+FMEAN	D00710
	DO 30 I=1,N	D00720
30	YTEMP(I)=F(I)	D00730
	DO 35 I=1,N	D00740
	ABSIS=X(I)	D00750
35	Y(I)=TERP1(ABSIS,XX,YTEMP,N,FINT)	D00760
C	WRITE(6,700)	D00770
C	WRITE(6,722)	D00780
C	WRITE(6,705)(XX(I),Y(I),I=1,N)	D00790
C...	COMPUTE FILTERED-OUT DATA"YNS"	D00800
	DO 36 I=1,N	D00810
	YNS(I)=YORG(I)-F(I)	D00820
36	CONTINUE	D00830
C	WRITE(6,700)	D00840
C	WRITE(6,705)(XX(I),YNS(I),I=1,N)	D00850
C	WRITE(6,723)	D00860
700	FORMAT(////////)	D00870
705	FORMAT(5(2F10.2,5X))	D00880
715	FORMAT(///,' MEAN VALUE =',F10.3,' MLMTR',///)	D00890
720	FORMAT(///,55X,'ORIGINAL DATA',///)	D00900
721	FORMAT( 55X,'REMOVED-MEAN DATA',///)	D00910
722	FORMAT( 55X,'FILTERED DATA',///)	D00920
723	FORMAT( 55X,'FILTERED-OUT DATA',///)	D00930
	RETURN	D00940
	END	D00950
	SUBROUTINE POWER(F,FN,NDEG,AN,BN,DPOW,R,C,WLAM,N)	E00010
C	*****	E00020
C	THIS SUBPROGRAM PERFORMS SPECTRAL ANALYSIS ON SURFACE ROUGHNESS	E00030
C	MEASUREMENTS	E00040
C	*****	E00060
C		E00070
	IMPLICIT REAL*8(A-H,O-Z)	E00080
	REAL*4 CUT,TLEN	E00090
	DIMENSION F(1),DPOW(1),WLAM(1)	E00100
	DIMENSION AN(1000),BN(1000),NDEG(1000),S(1000),C(1000),R(1000)	E00110
	DIMENSION IWK(2000)	E00120
	COMPLEX*16 GAMN,FN(1)	E00130
	COMMON /SAME/TLEN,CUT	E00140
C .....		E00150
	NH=N/2	E00160
	NH1=NH+1	E00170
C ...	COMPUTE THE VARIANCE OF THE SIGNAL	E00180
	VARI=0.	E00190
	DO 10 I=1,N	E00200
10	VARI=VARI+F(I)**2	E00210
	VARI=VARI/N	E00220
C ...	COMPUTE COMPLEX FOURIER COEFFICIENTS OF -F- BY FFT	E00230
	CALL FFTR(F,GAMN,N,IWK)	E00240
C ...	TAKE CONJUGATE OF OUTPUT AND DIVIDE BY N TO GET INV. FFT	E00250
	FN(1)=DCMLPX(F(1),-F(2))/N	E00260
	DO 15 I=2,NH	E00270

	11=2*1	E00280
	FN(1)=DCMPLX(F(11-1),-F(11))/N	E00290
15	FN(N+2-1)=DCONJG(FN(1))	E00300
	FN(NH1)=DCONJG(GAMN)/N	E00310
C ...	COMPUTE -AN- AND -BN- COEFFICIENTS	E00320
	AN(1)=FN(1)	E00330
	WLAM(1)=0	E00340
	DO 16 I=2,NH	E00350
	AN(I)=2.*FN(I)	E00360
	BN(I)=2.*DIMAG(FN(I))	E00370
	WLAM(I)=TLEN/(I-1)	E00380
16	CONTINUE	E00390
	AN(NH1)=FN(NH1)	E00400
	WLAM(NH1)=TLEN/NH	E00410
C ...	COMPUTE DEGREE POWER, CONTRIBUTION ETC....	E00420
	VAR2=0.	E00430
	BN(1)=0.	E00440
	BN(NH1)=0.	E00450
	DO 17 I=1,NH1	E00460
	NDEG(I)=I-1	E00470
	DPOW(I)=(AN(I)**2+BN(I)**2)/2.D0	E00480
	IF(I.EQ.1.OR.1.EQ.NH1)DPOW(I)=2.*DPOW(I)	E00490
	VAR2=VAR2+DPOW(I)	E00500
	S(I)=VAR2	E00510
17	CONTINUE	E00520
	SUM=VAR2	E00530
	R(1)=0.	E00540
	C(1)=0.	E00550
	DO 20 I=2,NH1	E00560
	R(I)=DPOW(I)/VAR2	E00570
	C(I)=S(I)/VAR2	E00580
20	CONTINUE	E00590
C	WRITE(6,700)	E00600
C	WRITE(6,705)(NDEG(I),AN(I),BN(I),DPOW(I),R(I),C(I),WLAM(I),I=1,NH1	E00610
C	*)	E00620
	DPOW(I)=FN(I)*DCONJG(FN(I))	E00630
C	WRITE(6,710)VAR1,VAR2	E00640
C	FIND THE POWER FROM COMPLEX FOURIER COEFF. TO CHECK THE RESULT	E00650
	DO 25 I=2,NH1	E00660
	DPOW(I)=2.*(FN(I)*DCONJG(FN(I)))	E00670
	DPOW(NH1)=FN(NH1)*DCONJG(FN(NH1))	E00680
25	CONTINUE	E00690
C	WRITE(9,700)	E00700
C	WRITE(9,705)(NDEG(I),AN(I),BN(I),DPOW(I),R(I),C(I),WLAM(I),I=1,NH1	E00710
C	*)	E00720
700	FORMAT(///,T6,'DEGREE',T16,'AN',T24,'BN',T32,'POWER',T40,'CONTR.',	E00730
	*T48,'TOTAL',T56,'L (CMD',T69,'DEGREE',T79,'AN',T87,'BN',T95,'POWER	E00740
	*',T103,'CONTR.',T111,'TOTAL',T119,'L (CMD',/)	E00750
705	FORMAT(2(110,2F8.2,F11.3,2F8.4,F8.1,2X))	E00760
710	FORMAT(/30X,'TOTAL POWER IN TIME DOMAIN=',F17.5,' MLMTR**2',/,30X,	E00770
	*'TOTAL POWER IN FREQ.DOMAIN=',F17.5,' MLMTR**2',/)	E00780
	RETURN	E00790
	END	E00800
	FUNCTION TERP1(X,XI,YI,N,F)	F00010
C	*****	F00020
C	THIS SUBPROGRAM PRODUCES AN EQUALLY SPACED PROFILE (IF	F00030
C	MEASUREMENTS WERE NOT SO)	F00040
C	*****	F00050
C	*****	F00060
	IMPLICIT REAL*8(A-H,O-Z)	F00070
	REAL*4 XI(1),YI(1)	F00080
C	X IS THE INDEPENDENT VARIABLE	F00090
C	XI IS AN ARRAY OF VALUES OF THE INDEPENDENT VARIABLE	F00100
C	YI IS AN ARRAY OF CORRESPONDING VALUES OF DEPENDENT VARIABLE	F00110
C	N IS THE SIZE OF THE ARRAYS	F00120
C	F IS A FACTOR FOR THE END SEGMENTS; BALANCE OF FIRST OND SECOND	F00130
C	ORDER INTERPOLATION	F00140
C	ALL VALUES OUTSIDE THE LIMITS OF THE ARRAY ARE COMPUTED BY	F00150
C	FIRST ORDER EXTRAPOLATION	F00160
C	FUNCTION RETURNS INTERPOLATED VALUE OF DEPENDENT VARIABLE	F00170
	DIMENSION P(2),E(2),IS(4,2)	F00180
	LOGICAL OUT	F00190
	DATA IS /-1,0,-2,-1,0,1,-1,0/	F00200
	OUT = .FALSE.	F00210
	J=1	F00220

1	IF (N-2) 1,12,3	F00230
1	TERP1=YI(J)	F00240
	RETURN	F00250
3	KPL=1	F00260
	KPU=2	F00270
	DO 4 J=1,N	F00280
7	IF (XI(J) - X) 4,1,6	F00290
4	CONTINUE	F00300
	J = N	F00310
	GO TO 2	F00320
6	IF (J-2) 12,8,9	F00330
8	KPL =2	F00340
	GO TO 10	F00350
9	IF (J - N) 10,11,2	F00360
12	J=2	F00370
2	OUT=.TRUE.	F00380
11	KPU=1	F00390
10	AL = (X-XI(J-1)) / (XI(J)-XI(J-1))	F00400
	TERP1=AL*YI(J)+(1.0-AL)*YI(J-1)	F00410
	IF (OUT) RETURN	F00420
	DO 16 KP=KPL,KPU	F00430
	P(KP)=0.0	F00440
	DO 15 K=1,3	F00450
	J0=J+KP + K - 4	F00460
	X0=XI(J0)	F00470
	Y0=YI(J0)	F00480
	J1=J+IS(K,KP)	F00490
	J2=J+IS(K+1,KP)	F00500
15	P(KP)=P(KP)+Y0*(X-XI(J1))/(X0-XI(J1))	F00510
*	*(X-XI(J2))/(X0-XI(J2))	F00520
	IF (KPL .NE. KPU) GO TO 16	F00530
	J1=3-KPL	F00540
	P(J1)=TERP1+F*(P(KP)-TERP1)	F00550
C ...		F00560
C ...	BE CAREFUL FOR FOLLOWING CARDS IF ..ABS..OR ..DABS...	F00570
	E(J1)=DABS(P(J1)-TERP1)	F00580
16	E(KP)=DABS(P(KP)-TERP1)	F00590
	IF (E(1)+E(2) .EQ. 0.0) RETURN	F00600
	TERP1=((E(1)*AL)*P(2)+(E(2)*(1.0-AL))*P(1)) /	F00610
*	((E(1)*AL) + (E(2)*(1.0-AL)))	F00620
	RETURN	F00630
	END	F00640
	SUBROUTINE RESDL(RSD,NP,RMEAN,STDEV)	G00010
C	*****	G00020
C	THIS SUBPROGRAM COMPUTES THE MEAN AND THE STANDARD DEVIATION OF	G00030
C	THE NORMALLY DISTRIBUTED RESIDUAL DATA.	G00040
C	*****	G00050
C		G00060
	DIMENSION RSD(200)	G00070
C ...	COMPUTE MEAN	G00080
	SUM=0.0	G00090
	DO 101 I=1,NP	G00100
	SUM=SUM+RSD(I)	G00110
101	CONTINUE	G00120
	RMEAN=SUM/NP	G00130
C ...	COMPUTE THE VARIANCE	G00140
	SUMV=0.0	G00150
	DO 102 I=1,NP	G00160
	SUMV=SUMV+(RSD(I)-RMEAN)*(RSD(I)-RMEAN)	G00170
102	CONTINUE	G00180
	VARV=SUMV/NP	G00190
	SD=VARV**0.5	G00200
	STDEV=ABS(SD)	G00210
	RETURN	G00220
	END	G00230



C	SUBROUTINE PARAM(D,P,ASR,ASH,RCH,HCH,EX)	H00010
C	*****	H00020
C	THIS SUBPROGRAM USES THE PROBLEM PARAMETERS TO COMPUTE THE MAIN	H00030
C	COEFFICIENTS IN EROSION EQUATIONS.	H00040
C	GAMA = UNIT WEIGHT OF SOIL	H00050
C	SG = SPECIFIC WEIGHT OF SOIL	H00060
C	RO = WATER DENSITY	H00070
C	G = GRAVITY ACCELERATION	H00080
C	RN = MANNING'S COEFFICIENT OF FRICTION	H00090
C	*****	H00100
	COMMON /PROP/GAMA,RO,G,SG,RN	H00110
	Z=(( (SG-1.)*G)**P)*(D**(P-1))	H00120
	RBETA=ASR/Z	H00130
	HBETA=ASH/Z	H00140
	X=(1.+2.*P)/2.	H00150
	RCH=RBETA*(1.+2.*P)/2./RO**X	H00160
	HCH=HBETA*(1.+2.*P)/2./RO**X	H00170
	EX=(2.*P-1.)/2.	H00180
	RETURN	H00190
	END	H00200
		H00210
	SUBROUTINE RANDU(IX,IY,R)	I00010
C	*****	I00020
C	THIS SUBPROGRAM GENERATES A RANDOM NUMBER WITH VALUE 0.0 TO 1.0	I00030
C	FROM A UNIFORM DISTRIBUTION	I00040
C	*****	I00050
	IY=IX*65539	I00060
	IF(IY)5,6,6	I00070
5	IY=IY+2147483647+1	I00080
6	R=IY	I00090
	R=R*0.465613E-9	I00100
	RETURN	I00110
	END	I00120
		I00130
	SUBROUTINE RANORM(NMAX,RMEAN,STDEV,RY,NS)	J00010
C	*****	J00020
C	IT GENERATES NORMALLY DISTRIBUTED RANDOM NUMBERS FOR THE GIVEN	J00030
C	MEAN AND STANDARD DEVIATION	J00040
C	*****	J00050
	DIMENSION RY(2000)	J00060
	IF(NS.GT.1) GO TO 800	J00070
	IX=123456789	J00080
800	DO 810 I=1,NMAX	J00090
	SUM=0.0	J00100
	DO 820 K=1,12	J00110
	CALL RANDU(IX,IY,R)	J00120
	IX=IY	J00130
	SUM=SUM+R	J00140
820	CONTINUE	J00150
	X=(SUM-6.0)*STDEV+RMEAN	J00160
	RY(I)=X	J00170
810	CONTINUE	J00180
C	WRITE(6,12)(I,RY(I),I=1,NMAX)	J00190
12	FORMAT(15,5X,F10.6)	J00200
	RETURN	J00210
	END	J00220
		J00230
	SUBROUTINE HXMESH	K00010
C	*****	K00020
C	THIS SUBPROGRAM CALCULATES THE COORDINATES AND ASSIGNS CODES	K00030
C	FOR NODAL POINTS OF THE HEXAGONAL MESH	K00040
C	FOR BIFURCATION POINTS, CODE=2,	K00050
C	FOR NON-BIFURCATION POINTS, CODE=1, AND	K00060
C	FOR OTHER POINTS CODE=0	K00070
C	THE X-Y PLANE COINCIDES WITH THE SLOPE SURFACE.	K00080
C	MESH DIMENSIONS ARE BASED ON CHARACTERISTICS OF BASIC WAVE	K00090
C	*****	K00100
	DIMENSION XX(2000)	K00110
	COMMON/MESH/NX,NY,NMAX,SL,SH,WL,QQ	K00120
	COMMON/NODES/X(2000),Y(2000),CODE(2000),ELV(2000)	K00130
C ...	COMPUTE X AND Y COORDINATES OF NODAL POINTS	K00140
	NMAX=NX*NY	K00150
	J=1	K00160
	XX(J)=0	K00170
		K00180

	NS=1	K00190
	NE=NY	K00200
11	DO 10 I=NS,NE,2	K00210
	K=I+1	K00220
	IF(I.EQ.1) GO TO 15	K00230
	IF(I.EQ.NS) GO TO 16	K00240
	IF(K.GT.NE) GO TO 17	K00250
	Y(I)=Y(I-1)+ SL	K00260
	Y(K)=Y(I)+2*SL	K00270
	X(K)=XX(J)	K00280
	X(I)=XX(J)	K00290
	GO TO 10	K00300
15	Y(I)=0	K00310
	Y(2)=Y(1)+2*SL	K00320
	X(1)=XX(J)	K00330
	X(2)=XX(J)	K00340
	GO TO 10	K00350
16	Y(NS)=0	K00360
	Y(NS+1)=Y(NS)+2*SL	K00370
	X(NS)=XX(J)	K00380
	X(NS+1)=XX(J)	K00390
	GO TO 10	K00400
17	Y(I)=Y(I-1)+ SL	K00410
	X(I)=X(I-1)	K00420
10	CONTINUE	K00430
	J=J+1	K00440
	IF(J.GT.NX) GO TO 1000	K00450
	XX(J)=XX(J-1)+WL/2.	K00460
	NE=NE+NY	K00470
	NS=NS+NY	K00480
	IF(NE.GT.NMAX) GO TO 1000	K00490
	GO TO 11	K00500
1000	M=NY	K00510
C ...	ASSIGN CODES TO NODAL POINTS	K00520
	MAX=2*NY	K00530
	K=1	K00540
	DO 30 J=K,M,4	K00550
	DO 30 I=J,NMAX,MAX	K00560
	CODE(I)=2	K00570
30	CONTINUE	K00580
	M=2*NY	K00590
	K=NY+3	K00600
	DO 40 J=K,M,4	K00610
	DO 40 I=J,NMAX,MAX	K00620
	CODE(I)=2	K00630
40	CONTINUE	K00640
	M=NY	K00650
	K=2	K00660
	DO 50 J=K,M,4	K00670
	DO 50 I=J,NMAX,MAX	K00680
	CODE(I)=1	K00690
50	CONTINUE	K00700
	M=2*NY	K00710
	K=NY+4	K00720
	DO 60 J=K,M,4	K00730
	DO 60 I=J,NMAX,MAX	K00740
	CODE(I)=1	K00750
60	CONTINUE	K00760
	RETURN	K00770
	END	K00780
C	SUBROUTINE ELEVTV(SLOPE,AMP,RMEAN,STDEV,NS)	L00010
C	*****	L00020
C	THIS SUBPROGRAM CALCULATES THE ORIGINAL (PRE-EROSION) ELEVATIONS	L00030
C	OF NODAL POINTS	L00040
C	ELEVATION OF EACH NODAL POINT IS COMPUTED AS THE SUM OF THE	L00050
C	FOLLOWING COMPONENTS	L00060
C	1) FROM THE AVERAGE SLOPE	L00070
C	2) FROM THE BASIC WAVE, WY	L00080
C	3) RESIDUAL COMPONENT GENERATED RANDOMLY ,RY	L00090
C	*****	L00100
C		L00110
C		L00120
C	DIMENSION RY(2000)	L00130
	COMMON/MESH/NX,NY,NMAX,SL,SH,WL,QQ	L00140
	COMMON/NODES/X(2000),Y(2000),CODE(2000),ELV(2000)	L00150
	PI=22.0/7.0	L00160
	THETA=SLOPE*PI/180	L00170

	L=1	L00180
	PHI=PI*(1./6.)	L00190
	WY=AMP*SIN(PHI)*COS(THETA)	L00200
	DO 700 I=1,NMAX	L00210
700	RY(I)=0.0	L00220
	CALL RANORM(NMAX,RMEAN,STDEV,RY,NS)	L00230
C	CALL RANORM(NMAX,RMEAN,STDEV,RY,NS)	L00240
	DO 710 M=NY,NMAX,NY	L00250
	DO 720 I=L,M,4	L00260
	ELV(I)=Y(I)*SIN(THETA)-WY+RY(I)	L00270
	IF(Y(I).EQ.Y(NY)) GO TO 730	L00280
	ELV(I+1)=Y(I+1)*SIN(THETA)-WY+RY(I+1)	L00290
	IF(Y(I+1).EQ.Y(NY)) GO TO 730	L00300
	ELV(I+2)=Y(I+2)*SIN(THETA)+WY+RY(I+2)	L00310
	IF(Y(I+3).EQ.Y(NY)) ELV(I+3)=Y(I+3)*SIN(THETA)+WY+RY(I+3)	L00320
730	IF(Y(I).EQ.0) GO TO 720	L00330
	ELV(I-1)=Y(I-1)*SIN(THETA)+WY+RY(I-1)	L00340
720	CONTINUE	L00350
	L=L+NY	L00360
	WY=-WY	L00370
710	CONTINUE	L00380
C	WRITE(6,790)(I,X(I),Y(I),RY(I),ELV(I),I=1,NMAX)	L00390
790	FORMAT(10X,15,4F10.6)	L00400
	RETURN	L00410
	END	L00420
	SUBROUTINE HUMP(RMEAN,STDEV,SLOPE,AMP,NHUMP)	M00010
C	*****	M00020
C	THIS SUBPROGRAM COMPUTES COORDINATES AND ELEVATIONS OF CIRCULAR	M00030
C	HUMPS' CENTERS.	M00040
C	*****	M00050
C		M00060
	DIMENSION RHY(500)	M00070
	COMMON/MESH/NX,NY,NMAX,SL,SH,WL,QQ	M00080
	COMMON/NODES/X(2000),Y(2000),CODE(2000),ELV(2000)	M00090
	COMMON/HMPP/HMPP(500),XHMP(500),YHMP(500)	M00100
	COMMON/SLOPES/HMP1(500),HMP2(500),HMP3(500),HMP4(500),HMP5(500),	M00110
	* HMP6(500)	M00120
C		M00130
C ...	DETERMINE THE TOTAL NUMBER OF HUMPS ,NHUMP	M00140
	NZ=NY+1	M00150
	M1=NZ/4	M00160
	RM1=1.*NZ/4	M00170
	DM1=RM1-M1	M00180
	IF(DM1.GT.0.AND.DM1.LE.0.5) GO TO 1210	M00190
	GO TO 1220	M00200
1210	NHUMP=M1*NX	M00210
	GO TO 1225	M00220
1220	N1=NX/2	M00230
	RN1=1.*NX/2.0	M00240
	DN1=RN1-N1	M00250
	IF(DM1.EQ.0) GO TO 1230	M00260
	IF(DN1.EQ.0) GO TO 1231	M00270
	NHUMP=2*M1*N1+N1+M1	M00280
	GO TO 1225	M00290
1231	NHUMP=N1*(2*M1+1)	M00300
	GO TO 1225	M00310
1230	IF(DN1.EQ.0) GO TO 1235	M00320
	NHUMP=2*N1*M1-N1+M1-1	M00330
	GO TO 1225	M00340
1235	NHUMP=N1*(2*M1-1)	M00350
	GO TO 1225	M00360
1225	CONTINUE	M00370
C		M00380
C ...	COMPUTE X AND Y COORDINATES	M00390
	K=1	M00400
	DO 1250 I=1,NMAX	M00410
	IF(CODE(I)-1) 1260,1270,1270	M00420
1270	GO TO 1250	M00430
1260	IF(CODE(I-1).NE.0) GO TO 1250	M00440
	IF(Y(I-1).EQ.Y(NY)) GO TO 1250	M00450
	XHMP(K)=X(I)	M00460
	YHMP(K)=(Y(I)+Y(I-1))/2.0	M00470
	K=K+1	M00480
1250	CONTINUE	M00490
C		M00500
C ...	COMPUTE ELEVATIONS	M00510
	CALL RANORM(NHUMP,RMEAN,STDEV,RHY)	M00520
C	CALL RANORM(NHUMP,RMEAN,STDEV,RHY)	M00530

	A=AMP*COS(SLOPE*22./7./180.)	M00540
	DO 1280 I=1,NHUMP	M00550
	HHMP(I)=(YHMP(I)+2.*SL)*SIN(SLOPE*22./7./180.)+A +RHY(I)	M00560
1280	CONTINUE	M00570
C	WRITE(6,1290)(I,XHMP(I),YHMP(I),HHMP(I), I=1,NHUMP)	M00580
1290	FORMAT(15,3F20.6)	M00590
C		M00600
C ...	COMPUTE "FICTICIOUS" ELEVATIONS OF THE HUMP CENTER FOR EACH OF	M00610
C	THE SIX SIDES OF THE "PYRAMID"	M00620
	DO 1295 I=1,NHUMP	M00630
	HMP1(I)=HHMP(I)	M00640
	HMP2(I)=HHMP(I)	M00650
	HMP3(I)=HHMP(I)	M00660
	HMP4(I)=HHMP(I)	M00670
	HMP5(I)=HHMP(I)	M00680
	HMP6(I)=HHMP(I)	M00690
1295	CONTINUE	M00700
	RETURN	M00710
	END	M00720
	SUBROUTINE IDHMP(NY,I,IDL,IDR,IDC)	N00010
C	*****	N00020
C	THIS SUBPROGRAM IDENTIFIES THE HUMPS ASSOCIATED WITH DIFFERENT	N00030
C	RILL SEGMENTS	N00040
C	IDL=CALL# OF HUMP LEFT OF I	N00050
C	IDR=CALL# OF HUMP RIGHT OF I	N00060
C	IDC=CALL# OF HUMP BELOW I (IF CODE(I)=2)	N00070
C	NC= # COMPLETE MESH COLUMNS BEFORE I	N00080
C	NHB= # OF HUMPS BELOW I	N00090
C	*****	N00100
C		N00110
	COMMON NT	N00120
	NZ=NY+1	N00130
	M=NZ/4	N00140
	RM=1.*NZ/4.	N00150
	DM=RM-M	N00160
	KD=DM*4+1	N00170
	NC=I/NY	N00180
	RNC=(1.*I)/(1.*NY)	N00190
	IF(RNC.GT.NC) GO TO 1501	N00200
	NC=NC-1	N00210
1501	NHB=((I+NC+1)-(NC*NZ))/4	N00220
	IF(I.LT.NY) GO TO 1505	N00230
	INC=NC/2	N00240
	RRNC=1.*NC/2.	N00250
	IF(RRNC.EQ.INC) GO TO 1505	N00260
	GO TO (1510,1515,1515,1520),KD	N00270
1510	IDL=(NC-1)/2*M+(NC-1)/2*(M-1)+NHB	N00280
	GO TO 1530	N00290
1515	IDL=(NC-1)*M+NHB	N00300
	GO TO 1535	N00310
1520	IDL=(NC-1)/2*(M+1)+(NC-1)/2*M+NHB	N00320
	GO TO 1540	N00330
1530	IDR=(NC+1)/2*M+(NC+1)/2*(M-1)+NHB	N00340
	GO TO 1550	N00350
1535	IDR=(NC+1)*M+NHB	N00360
	GO TO 1555	N00370
1540	IDR=(NC+1)/2*(M+1)+(NC+1)/2*M+NHB	N00380
	GO TO 1560	N00390
1550	IDC=(NC/2+1)*(M-1)+(NC/2)*M+NHB	N00400
	GO TO 1595	N00410
1555	IDC=NC*M+NHB	N00420
	GO TO 1595	N00430
1560	IDC=(NC/2+1)*M+NC/2*(M+1)+NHB	N00440
	GO TO 1595	N00450
1505	GO TO (1570,1575,1575,1580),KD	N00460
1570	IDL=((NC-1)/2+1)*(M-1)+(NC-1)/2*M+NHB+1	N00470
	GO TO 1573	N00480
1575	IDL=(NC-1)*M+NHB+1	N00490
	GO TO 1578	N00500
1580	IDL=((NC-1)/2+1)*M+(NC-1)/2*(M+1)+NHB+1	N00510
	GO TO 1585	N00520
1573	IDR=((NC+1)/2+1)*(M-1)+(NC+1)/2*M+NHB+1	N00530

	GO TO 1574	N00540
1578	IDR=(NC+1)*M+NHB+1	N00550
	GO TO 1579	N00560
1585	IDR=((NC+1)/2+1)*M+(NC+1)/2*(M+1)+NHB+1	N00570
	GO TO 1590	N00580
1574	IDC=(NC/2)*M+(NC/2)*(M-1)+NHB	N00590
	GO TO 1595	N00600
1579	IDC=NC*M+NHB	N00610
	GO TO 1595	N00620
1590	IDC=(NC/2)*(M+1)+(NC/2)*M+NHB	N00630
1595	CONTINUE	N00640
	RETURN	N00650
	END	N00660
	SUBROUTINE FLOW(RNL,RNF)	000010
C	*****	000020
C	FLOW RATE IN A RILL SEGMENT IS THE SUM OF :	000030
C	1) DIRECT RAINFALL ON SURFACES OF RILL AND INTERRILL AREAS ,AND	000040
C	2) FLOW ARRIVING FROM AREA UPSLOPE	000050
C		000060
C	AT A BIFURCATION POINT THE FLOW IS DEVIDED BETWEEN THE LEFT AND	000070
C	THE RIGHT BRANCH ACCORDING TO THE RELATIVE MAGNITUDES OF BED	000080
C	SLOPES RAISED TO THE POWER OF 0.5 .	000090
C		000100
C	QT(I) IS THE AMOUNT OF WATER ACCUMULATED AT POINT I	000110
C	QR(I) IS THE AMOUNT OF WATER BRANCHING OUT FROM POINT I	000120
C	QL(I) IS THE AMOUNT OF WATER BRANCHING OUT FROM POINT I	000130
C	FLOW QUANTITY IS IN CUBIC METERS/SEC.	000140
C		000150
C	IF A "LOW" HUMP OCCURS, THE FLOW IS REDISTRIBUTED IN (RDISTB).	000160
C	*****	000170
C		000180
	COMMON/MESH/NX,NY,NMAX,SL,SH,WL,QQ	000190
	COMMON/NODES/X(2000),Y(2000),CODE(2000),ELV(2000)	000200
	COMMON/PONDG/KPND(2000),NAJ(2000),DH(2000)	000210
	COMMON/HMPP/HHMP(500),XHMP(500),YHMP(500)	000220
	COMMON/QFLOW/QT(2000),QL(2000),QR(2000)	000230
	COMMON NT	000240
C		000250
C	COMPUTE RAINFALL FLOW RATE / UNIT TIME / UNIT AREA :	000260
C		000270
	QQ=(RNF*RNL)/(3.6*10**6)	000280
C	DQ IS THE AMOUNT OF WATER DRAINED TO A RILL SEGMENT FROM BOTH SIDES	000290
C	PER UNIT TIME.	000300
	DQ=2.*QQ*SL*SL*(3.**0.5)	000310
C		000320
C	COMPUTE TOTAL FLOW RATE AT EACH NODAL POINT :	000330
C		000340
	DO 901 L=1,NY	000350
	K=NY+(1-L)	000360
	DO 901 I=K,NMAX,NY	000370
	IF(CODE(I)-1) 902,903,904	000380
C		000390
C	POINTS WITH CODE=0 :	000400
C		000410
	902 QR(I)=0	000420
	QL(I)=0	000430
	QT(I)=0	000440
	GO TO 901	000450
C		000460
C	POINTS WITH CODE=1 :	000470
C		000480
	903 IF(Y(I).LT.Y(NY)) GO TO 905	000490
	GO TO 902	000500
	905 IF(X(I).EQ.0) GO TO 915	000510
	SLL=(ELV(I-NY+1)-ELV(I))/2.0/SH	000520
	IF(X(I).EQ.X(NMAX)) GO TO 907	000530
	915 SLR=(ELV(I+NY+1)-ELV(I))/2.0/SH	000540
	IF(X(I).EQ.0) GO TO 906	000550
	IF(X(I).GE.X(NMAX)) GO TO 907	000560
	IF(SLL.LE.0.AND.SLR.LE.0) GO TO 908	000570
	IF(SLL.LE.0.AND.SLR.GT.0) GO TO 909	000580
	IF(SLL.GT.0.AND.SLR.LE.0) GO TO 910	000590
	QT(I)=QT(I)+QR(I-NY+1)+QL(I+NY+1)+2*DQ	000600
	CALL RDISTB(I,CODE(I))	000610
	GO TO 901	000620
	908 QT(I)=0	000630

	GO TO 901	000640
909	QT(I)=QT(I)+QR(I-NY+1)+DQ	000650
	CALL RDISTB(I, CODE(I))	000660
	GO TO 901	000670
910	QT(I)=QT(I)+QL(I+NY+1)+DQ	000680
	CALL RDISTB(I, CODE(I))	000690
	GO TO 901	000700
906	IF(SLR.LE.0.0) GO TO 911	000710
	QT(I)=QT(I)+QL(I+NY+1)+DQ	000720
	CALL RDISTB(I, CODE(I))	000730
	GO TO 901	000740
911	QT(I)=0.0	000750
	GO TO 901	000760
907	IF(SLL.LE.0.0) GO TO 911	000770
	QT(I)=QT(I)+QR(I-NY+1)+DQ	000780
	CALL RDISTB(I, CODE(I))	000790
	GO TO 901	000800
C		000810
C	POINTS OF CODE=2 (BIFURCATION POINTS)	000820
C		000830
904	IF(Y(I).EQ.Y(NY)) GO TO 902	000840
	SLM=(ELV(I+1)-ELV(I))/2.0/SH	000850
	IF(SLM.GT.0) GO TO 916	000860
	QT(I)=0	000870
	GO TO 902	000880
916	IF(X(I).EQ.0) GO TO 930	000890
	IF(X(I).EQ.X(NMAX)) GO TO 940	000900
	QT(I)=QT(I)+QT(I+1)+DQ	000910
	SLL=(ELV(I)-ELV(I-NY-1))/2.0/SH	000920
	SLR=(ELV(I)-ELV(I+NY-1))/2.0/SH	000930
	IF(SLL.LE.0.AND.SLR.LE.0) GO TO 920	000940
	IF(SLL.LE.0.AND.SLR.GT.0) GO TO 921	000950
	IF(SLL.GT.0.AND.SLR.LT.0) GO TO 922	000960
	SLL1=(ELV(I-NY-1)-ELV(I-NY-2))/2.0/SH	000970
	SLR2=(ELV(I+NY-1)-ELV(I+NY-2))/2.0/SH	000980
	SLAV=(SLL+SLL1)/2.	000990
	IF(SLAV.LT.0.0) SLAV=0.0	001000
	SRAV=(SLR+SLR1)/2.	001010
	IF(SRAV.LT.0.0) SRAV=0.0	001020
	SQR=SLAV**0.5+ SRAV**0.5	001030
	QL(I)=QL(I)+QT(I)*((SLAV**0.5)/SQR)	001040
	QR(I)=QR(I)+QT(I)*((SRAV**0.5)/SQR)	001050
	CALL RDISTB(I, CODE(I))	001060
	GO TO 901	001070
920	QL(I)=0	001080
	QR(I)=0	001090
	GO TO 901	001100
921	QL(I)=0	001110
	QR(I)=QR(I)+QT(I)	001120
	CALL RDISTB(I, CODE(I))	001130
	GO TO 901	001140
922	QR(I)=0	001150
	QL(I)=QL(I)+QT(I)	001160
	CALL RDISTB(I, CODE(I))	001170
	GO TO 901	001180
930	QT(I)=QT(I)+QT(I+1)+DQ	001190
	SLR=(ELV(I)-ELV(I+NY-1))/2.0/SH	001200
	SLL=0.0	001210
	QL(I)=0.0	001220
	IF(SLR.GT.0) GO TO 932	001230
	QR(I)=0.0	001240
	GO TO 901	001250
932	QR(I)=QR(I)+QT(I)	001260
	CALL RDISTB(I, CODE(I))	001270
	GO TO 901	001280
940	QT(I)=QT(I)+QT(I+1)+DQ	001290
	SLL=(ELV(I)-ELV(I-NY-1))/2.0/SH	001300
	SLR=0.0	001310
	QR(I)=0.0	001320
	IF(SLL.GT.0) GO TO 942	001330
	QL(I)=0.0	001340
	GO TO 901	001350
942	QL(I)=QL(I)+QT(I)	001360
	CALL RDISTB(I, CODE(I))	001370
901	CONTINUE	001380
	IF(NT.NE.1) RETURN	001390
C	WRITE(6,990)(I,X(I),Y(I),CODE(I),QR(I),QL(I),QT(I), I=1,NMAX)	001400
990	FORMAT(2X, I5, 6F20.8)	001410
	RETURN	001420
	END	001430

	SUBROUTINE RDISTB(I,CKODE)	P00010
	*****	P00020
C	THIS SUBPROGRAM CHECKS THE EXISTANCE OF NEGATIVE SIDE SLOPES	P00030
C	RESULT FROM HUMPS DEPRESSED BY FAILURE MECHANISM. THE PROGRAM	P00040
C	THEN REDISTRIBUTES THE QUANTITY OF WATER AMONG NODAL POINTS. THIS	P00050
C	PROCESS IS REPEATED BEFORE EVERY TIME INTERVAL.	P00060
C	*****	P00070
	COMMON/MESH/NX,NY,NMAX,SL,SH,WL,QQ	P00080
	COMMON/NODES/X(2000),Y(2000),CODE(2000),ELV(2000)	P00090
	COMMON/HMPP/HMPP(500),XHMP(500),YHMP(500)	P00100
	COMMON/PONDG/KPND(2000),NAJ(2000),DH(2000)	P00110
	COMMON/QFLOW/QT(2000),QL(2000),QR(2000)	P00120
	COMMON/SLOPES/HMP1(500),HMP2(500),HMP3(500),HMP4(500),HMP5(500),	P00130
	* HMP6(500)	P00140
	COMMON NT	P00150
	IF(Y(I).EQ.0.0) GO TO 100	P00160
	IF(CKODE-1.0) 100,200,300	P00170
200	AELV=(ELV(I)+ELV(I-1))/2.	P00180
	SO=(ELV(I)-ELV(I-1))/2./SH	P00190
	CALL IDHMP(NY,I,IDL,IDR,IDC)	P00200
	IF(X(I).EQ.0.0) GO TO 210	P00210
	IF(X(I).EQ.X(NMAX)) GO TO 220	P00220
	S1=(HMP4(IDL)-AELV)/SH/3.**0.5	P00230
	S2=(HMP1(IDR)-AELV)/SH/3.**0.5	P00240
20	FORMAT(/,' SLOPES : ',I5,3F20.6)	P00250
	AS1=ABS(S1)	P00260
	AS2=ABS(S2)	P00270
	IF(S1.GT.0.0.AND.S2.GT.0.0) GO TO 100	P00280
	IF(S1.LE.0.0.AND.S2.GT.0.0) GO TO 215	P00290
	IF(S1.GT.0.0.AND.S2.LE.0.0) GO TO 225	P00300
1	CONTINUE	P00310
	NK=I-2*NY	P00320
	NV=I	P00330
	F=0.5	P00340
	KK=1	P00350
	HHH=(ELV(NK)+ELV(NK-1))/2.	P00360
	IF(HHH.GT.HMP1(IDL)) QT(NV)=0.0	P00370
	GO TO 2000	P00380
211	NK=I+2*NY	P00390
	NV=I	P00400
	F=0.5	P00410
	KK=2	P00420
	GO TO 2000	P00430
215	IF(SO.GE.AS1) GO TO 290	P00440
	NK=I-2*NY	P00450
	NV=I	P00460
	F=1.0	P00470
	KK=2	P00480
	HHH=(ELV(NK)+ELV(NK-1))/2.	P00490
	IF(HHH.GT.HMP1(IDL)) QT(NV)=0.0	P00500
	GO TO 2000	P00510
225	IF(SO.GE.AS2) GO TO 290	P00520
	NK=I+2*NY	P00530
	NV=I	P00540
	F=1.0	P00550
	KK=2	P00560
	GO TO 2000	P00570
210	S2=(HMP1(IDR)-AELV)/SH/3.**0.5	P00580
	AS2=ABS(S2)	P00590
	IF(S2.LE.0.0) GO TO 225	P00600
	GO TO 100	P00610
220	S1=(HMP4(IDL)-AELV)/SH/3.**0.5	P00620
	AS1=ABS(S1)	P00630
	IF(S1.LE.0.0) GO TO 215	P00640
	GO TO 100	P00650
2000	QT(NK)=QT(NK)+F*QT(NV)	P00660
	IF(KK.EQ.1) GO TO 211	P00670
	QT(NV)=0.0	P00680
290	IF(SO.LE.0.0) GO TO 100	P00690
	NAJ(I)=NAJ(I)-1	P00700
	NAJ(I-1)=NAJ(I-1)-1	P00710
	GO TO 100	P00720
300	CALL IDHMP(NY,I,IDL,IDR,IDC)	P00730
10	FORMAT(/,I5,3F20.8,/)	P00740
	IF(X(I).EQ.0.0) GO TO 400	P00750
	AELV=(ELV(I)+ELV(I-NY-1))/2.	P00760
		P00770

	SOL=(ELV(I)-ELV(I-NY-1))/2./SH	P00780
	S2=(HMP2(IDC)-AELV)/SH/3.**0.5	P00790
	IF(Y(I).EQ.Y(NY)) HMP5(IDL)=HMP2(IDC)	P00800
	S1=(HMP5(IDL)-AELV)/SH/3.**0.5	P00810
	AS1=ABS(S1)	P00820
	AS2=ABS(S2)	P00830
	IF(S1.GT.0.0.AND.S2.GT.0.0) GO TO 400	P00840
	IF(S1.LE.0.0.AND.S2.GT.0.0) GO TO 315	P00850
	IF(S1.GT.0.0.AND.S2.LE.0.0) GO TO 325	P00860
	NK=I-NY+2	P00870
	NV=I	P00880
	IF(Y(NV).GE.Y(NY-1)) NK=NMAX+5	P00890
	IF(X(NV).EQ.X(NY+1)) NK=NMAX+5	P00900
	F=0.5	P00910
	KK=1	P00920
	HHH=(ELV(NK)+ELV(NK-NY-1))/2.	P00930
	IF(HHH.GT.HMP2(IDL)) QL(NV)=0.0	P00940
	GO TO 3000	P00950
311	NK=I+NY-2	P00960
	NV=I	P00970
	F=0.5	P00980
	KK=2	P00990
	GO TO 3000	P01000
315	IF(SOL.GE.AS1) GO TO 390	P01010
	NK=I-NY+2	P01020
	NV=I	P01030
	IF(Y(NV).GE.Y(NY-1)) NK=NMAX+5	P01040
	IF(X(NV).EQ.X(NY+1)) NK=NMAX+5	P01050
	F=1.0	P01060
	KK=2	P01070
	HHH=(ELV(NK)+ELV(NK-NY-1))/2.	P01080
	IF(HHH.GT.HMP2(IDL)) QL(NV)=0.0	P01090
	GO TO 3000	P01100
325	IF(SOL.GE.AS2) GO TO 390	P01110
	NK=I+NY-2	P01120
	NV=I	P01130
	F=1.0	P01140
	KK=2	P01150
3000	QL(NK)=QL(NK)+F*QL(NV)	P01160
	QL(NV)=0.0	P01170
	IF(KK.EQ.1) GO TO 311	P01180
390	IF(SOL.LE.0.0) GO TO 400	P01190
	NAJ(I)=NAJ(I)-1	P01200
	NAJ(I-NY-1)=NAJ(I-NY-1)-1	P01210
400	IF(X(I).EQ.X(NMAX)) GO TO 100	P01220
	IF(Y(I).EQ.Y(NY)) HMP6(IDR)=HMP3(IDC)	P01230
	AELV=(ELV(I)+ELV(I+NY-1))/2.	P01240
	SOR=(ELV(I)-ELV(I+NY-1))/2./SH	P01250
	S1=(HMP3(IDC)-AELV)/SH/3.**0.5	P01260
	S2=(HMP6(IDR)-AELV)/SH/3.**0.5	P01270
	AS1=ABS(S1)	P01280
	AS2=ABS(S2)	P01290
	IF(S1.GT.0.0.AND.S2.GT.0.0) GO TO 100	P01300
	IF(S1.LE.0.0.AND.S2.GT.0.0) GO TO 415	P01310
	IF(S1.GT.0.0.AND.S2.LE.0.0) GO TO 425	P01320
	NK=I-NY-2	P01330
	NV=I	P01340
	IF(Y(NV).GE.Y(NY-1)) NK=NMAX+5	P01350
	IF(X(NV).EQ.X(NY+1)) NK=NMAX+5	P01360
	F=0.5	P01370
	KK=1	P01380
	GO TO 4000	P01390
411	NK=I+NY+2	P01400
	NV=I	P01410
	IF(Y(NV).GE.Y(NY-1)) NK=NMAX+5	P01420
	IF(X(NV).EQ.X(NY+1)) NK=NMAX+5	P01430
	F=0.5	P01440
	KK=2	P01450
	HHH=(ELV(NK)+ELV(NK+NY-1))/2.	P01460
	IF(HHH.GT.HMP3(IDR)) QR(NV)=0.0	P01470
	GO TO 4000	P01480
415	IF(SOR.GE.AS1) GO TO 490	P01490
	NK=I-NY-2	P01500
	NV=I	P01510
	F=1.0	P01520
	KK=2	P01530
	GO TO 4000	P01540



425	IF(SOR.GE.AS2) GO TO 490	P01550
	NK=I+NY+2	P01560
	NV=I	P01570
	IF(Y(NV).GE.Y(NY-1)) NK=NMAX+5	P01580
	IF(X(NV).EQ.X(NY+1)) NK=NMAX+5	P01590
	F=1.0	P01600
	KK=2	P01610
	HHH=(ELV(NK)+ELV(NK+NY-1))/2.	P01620
	IF(HHH.GT.HMP3(IDR)) QR(NV)=0.0	P01630
4000	QR(NK)=QR(NK)+F*QR(NV)	P01640
	QR(NV)=0.0	P01650
	IF(KK.EQ.1) GO TO 411	P01660
490	IF(SOR.LE.0.0) GO TO 100	P01670
	NAJ(I)=NAJ(I)-1	P01680
	NAJ(I+NY-1)=NAJ(I+NY-1)-1	P01690
100	CONTINUE	P01700
500	FORMAT(/,120(' '),/)	P01710
990	FORMAT(2X,15,6F20.8)	P01720
	RETURN	P01730
	END	P01740
	SUBROUTINE SFAILR(SLIMIT,SSTART)	Q00010
C	*****	Q00020
C	THIS SUBPROGRAM CHECKS THE STABILITY OF SIDESLOPES OF ALL RILL	Q00030
C	SEGMENTS BEFORE EVERY TIME INTERVAL.	Q00040
C	SLIMIT= THE UPPER LIMIT A SIDESLOPE CAN REACH BEFORE FAILURE	Q00050
C	SSTART= THE STARTING VALUE OF THE SIDESLOPE AFTER FAILURE	Q00060
C	DSDT= THE VOLUME OF THE SOIL CHUNK SEPARATED DUE TO FAILURE	Q00070
C	NOTE: AT THE PRESENT STAGE DSDT IS NOT ADDED TO THE AMOUNT OF	Q00080
C	SOIL ERODED . I. E. DSDT=0.	Q00090
C	*****	Q00100
C		Q00110
	COMMON/MESH/NX,NY,NMAX,SL,SH,WL,QQ	Q00120
	COMMON/NODES/X(2000),Y(2000),CODE(2000),ELV(2000)	Q00130
	COMMON/HMPP/HMP(500),XHMP(500),YHMP(500)	Q00140
	COMMON/SLOPES/HMP1(500),HMP2(500),HMP3(500),HMP4(500),HMP5(500),	Q00150
	* HMP6(500)	Q00160
	COMMON/SDMNT/SDT(2000),TRE(2000),TIRE(2000)	Q00170
	COMMON NT	Q00180
16	FORMAT(15,2F20.6,/)	Q00190
10	FORMAT(15,3F10.5)	Q00200
15	FORMAT(15,F10.5)	Q00210
1000	FORMAT(3110,2F10.5,//)	Q00220
	BETA=ATAN(SSTART)	Q00230
	PHI=ATAN(SLIMIT)-BETA	Q00240
	DY=SH*(SLIMIT-SSTART)*3.**0.5*COS(BETA)	Q00250
	DSDT=SH*SH*SH*(SLIMIT-SSTART)	Q00260
	DSDT=0.0	Q00270
	DO 100 J=1,NY	Q00280
	K=NY+(1-J)	Q00290
	DO 100 I=K,NMAX,NY	Q00300
	IF(Y(I).EQ.0.0) GO TO 100	Q00310
	IF(CODE(I)-1) 100,200,300	Q00320
200	AELV=(ELV(I)+ELV(I-1))/2.	Q00330
	CALL IDHMP(NY,I,IDL,IDR,IDC)	Q00340
	IF(X(I).EQ.0.0) GO TO 210	Q00350
	IF(X(I).EQ.X(NMAX)) GO TO 220	Q00360
	S1=(HMP4(IDL)-AELV)/SH/(3.**0.5)	Q00370
	S2=(HMP1(IDR)-AELV)/SH/(3.**0.5)	Q00380
230	IF(S1.LT.SLIMIT) GO TO 205	Q00390
	HMP4(IDL)=HMP4(IDL)-(S1-SSTART)*SH*3.**0.5	Q00400
	SDT(I)=SDT(I)+DSDT	Q00410
	TIRE(I)=TIRE(I)+DSDT	Q00420
205	IF(S2.LT.SLIMIT) GO TO 100	Q00430
	HMP1(IDR)=HMP1(IDR)-(S2-SSTART)*SH*3.**0.5	Q00440
	SDT(I)=SDT(I)+DSDT	Q00450
	TIRE(I)=TIRE(I)+DSDT	Q00460
	GO TO 100	Q00470
210	S2=(HMP1(IDR)-AELV)/SH/3.**0.5	Q00480
	S1=S2	Q00490
	GO TO 230	Q00500
220	S1=(HMP4(IDL)-AELV)/SH/3.**0.5	Q00510
	S2=S1	Q00520
	GO TO 230	Q00530

300	CALL IDHMP(NY, I, IDL, IDR, IDC)	Q00540
3000	FORMAT(4I8, 2F12.8, //)	Q00550
	IF(X(I).EQ.0.0) GO TO 330	Q00560
	AELV=(ELV(I)+ELV(I-NY-1))/2.	Q00570
	S2=(HMP2(IDC)-AELV)/SH/3.**0.5	Q00580
	HP5=HMP5(IDL)	Q00590
	IF(Y(I).EQ.Y(NY)) HP5=HMP2(IDC)	Q00600
	S1=(HP5-AELV)/SH/3.**0.5	Q00610
	IF(S1.LT.SLIMIT) GO TO 310	Q00620
	IF(Y(I).EQ.Y(NY)) GO TO 305	Q00630
	HMP5(IDL)=HMP5(IDL)-(S1-SSTART)*SH*3.**0.5	Q00640
305	CONTINUE	Q00650
	SDT(I-NY-1)=SDT(I-NY-1)+DSDT	Q00660
	TIRE(I-NY-1)=TIRE(I-NY-1)+DSDT	Q00670
310	IF(S2.LT.SLIMIT) GO TO 330	Q00680
	HMP2(IDC)=HMP2(IDC)-(S2-SSTART)*SH*3.**0.5	Q00690
	SDT(I-NY-1)=SDT(I-NY-1)+DSDT	Q00700
	TIRE(I-NY-1)=TIRE(I-NY-1)+DSDT	Q00710
330	IF(X(I).EQ.X(NMAX)) GO TO 100	Q00720
	HP6=HMP6(IDR)	Q00730
	IF(Y(I).EQ.Y(NY)) HP6=HMP3(IDC)	Q00740
	AELV=(ELV(I)+ELV(I+NY-1))/2.	Q00750
	S1=(HMP3(IDC)-AELV)/SH/3.**0.5	Q00760
	S2=(HP6-AELV)/SH/3.**0.5	Q00770
	IF(S1.LT.SLIMIT) GO TO 340	Q00780
	HMP3(IDC)=HMP3(IDC)-(S1-SSTART)*SH*3.**0.5	Q00790
	SDT(I+NY-1)=SDT(I+NY-1)+DSDT	Q00800
	TIRE(I+NY-1)=TIRE(I+NY-1)+DSDT	Q00810
340	IF(S2.LT.SLIMIT) GO TO 100	Q00820
	IF(Y(I).EQ.Y(NY)) GO TO 350	Q00830
	HMP6(IDR)=HMP6(IDR)-(S2-SSTART)*SH*3.**0.5	Q00840
350	CONTINUE	Q00850
	SDT(I+NY-1)=SDT(I+NY-1)+DSDT	Q00860
	TIRE(I+NY-1)=TIRE(I+NY-1)+DSDT	Q00870
100	CONTINUE	Q00880
	RETURN	Q00890
	END	Q00900
	SUBROUTINE POND	R00010
C	*****	R00020
C	THIS SUBPROGRAM IDENTIFIES NODAL POINTS WHICH ARE THE UPSTREAM	R00030
C	POINTS OF RILL SEGMENTS OF NEGATIVE SLOPE, (UPWARD), AND AT WHICH	R00040
C	PONDING OCCURS	R00050
C	*****	R00060
C		R00070
	COMMON/MESH/NX, NY, NMAX, SL, SH, WL, QQ	R00080
	COMMON/NODES/X(2000), Y(2000), CODE(2000), ELV(2000)	R00090
	COMMON/PONDG/KPND(2000), NAJ(2000), DH(2000)	R00100
	COMMON NT	R00110
	DO 10 I=1, NMAX	R00120
	KPND(I)=0	R00130
	IF(Y(I).EQ.0.0) GO TO 10	R00140
	IF(CODE(I)-1.0) 10, 20, 30	R00150
C		R00160
C	FOR NODAL POINTS WITH CODE=1	R00170
C		R00180
C	KPND(I)=0 IMPLIES NO PONDING	R00190
C	KPND(I)=11 IMPLIES PONDING	R00200
20	DZ=ELV(I)-ELV(I-1)	R00210
	IF(DZ.GT.0.0) GO TO 10	R00220
	KPND(I)=11	R00230
	GO TO 10	R00240
C		R00250
C	FOR NODAL POINTS WITH CODE=2	R00260
C		R00270
C	KPND(I)=0 IMPLIES NO PONDING	R00280
C	KPND(I)=11 IMPLIES TOTAL PONDING	R00290
C	KPND(I)=1 IMPLIES PARTIAL PONDING, (LEFT BRANCH ONLY).	R00300
C	KPND(I)=2 IMPLIES PARTIAL PONDING, (RIGHT BRANCH ONLY).	R00310
30	IF(X(I).EQ.0.0) GO TO 35	R00320
	DZL=ELV(I)-ELV(I-NY-1)	R00330
	IF(X(I).EQ.X(NMAX)) GO TO 40	R00340
	DZR=ELV(I)-ELV(I+NY-1)	R00350
	IF(DZL.LE.0.0.AND.DZR.LE.0.0) GO TO 45	R00360
	IF(DZL.GT.0.0.AND.DZR.GT.0.0) GO TO 10	R00370
	IF(DZL.GT.0.0.AND.DZR.LE.0.0) GO TO 50	R00380
	KPND(I)=1	R00390
	GO TO 10	R00400

50	KPND(I)=2	R00410
	GO TO 10	R00420
45	KPND(I)=11	R00430
	GO TO 10	R00440
35	DZR=ELV(I )-ELV(I+NY-1 )	R00450
	IF(DZR.GT.0.0) GO TO 10	R00460
	GO TO 45	R00470
40	DZL=ELV(I )-ELV(I-NY-1 )	R00480
	IF(DZL.GT.0.0) GO TO 10	R00490
	GO TO 45	R00500
10	CONTINUE	R00510
	RETURN	R00520
	END	R00530
	SUBROUTINE ACJNT	S00010
C	*****	S00020
C	THIS SUBPROGRAM COMPUTES THE NUMBER OF RILL SEGMENTS AT EACH	S00030
C	NODAL POINT	S00040
C	*****	S00050
	COMMON/MESH/NX,NY,NMAX,SL,SH,WL,QQ	S00060
	COMMON/NODES/X(2000),Y(2000),CODE(2000),ELV(2000)	S00070
	COMMON/PONDG/KPND(2000),NAJ(2000),DH(2000)	S00080
	COMMON NT	S00090
	DO 10 I=1,NMAX	S00100
	IF(CODE(I)-1) 10,20,30	S00110
20	IF(Y(I).EQ.Y(NY)) GO TO 15	S00120
	IF(X(I).EQ.0.0.OR.X(I).EQ.X(NMAX)) GO TO 25	S00130
	NAJ(I)=3	S00140
	GO TO 10	S00150
15	NAJ(I)=1	S00160
	GO TO 10	S00170
25	NAJ(I)=2	S00180
	GO TO 10	S00190
30	IF(Y(I).EQ.0.0) GO TO 15	S00200
	IF(Y(I).EQ.Y(NY)) GO TO 35	S00210
	IF(X(I).EQ.X(NMAX).OR.X(I).EQ.0.0) GO TO 25	S00220
	NAJ(I)=3	S00230
	GO TO 10	S00240
35	IF(X(I).NE.0.0.AND.X(I).NE.X(NMAX)) GO TO 25	S00250
	GO TO 15	S00260
10	CONTINUE	S00270
C	WRITE(6,5)(I,X(I),Y(I),	S00280
5	FORMAT(15,3F20.5,2I5)	S00290
	CODE(I),KPND(I),NAJ(I),I=1,NMAX)	S00300
	RETURN	S00310
	END	S00320
	SUBROUTINE CSEC(SL,Q,S1,S2,S0,H,B,C1)	T00010
C	*****	T00020
C	THIS SUBPROGRAM COMPUTES DEPTH AND BREADTH OF THE FLOW AT ANY	T00030
C	NODAL POINT. COMPUTATIONS ARE BASED ON M A N N I N G 'S FORMULA.	T00040
C	FLOW MEAN VELOCITY AND VELOCITY HEAD ARE ALSO COMPUTED HERE.	T00050
C	*****	T00060
	COMMON /PROP/GAMA,RO,G,SG,RN	T00070
	COMMON NT	T00080
	THETA1=ATAN(S1)	T00090
	THETA2=ATAN(S2)	T00100
	C1=1/S1+1/S2	T00110
	C2=1/SIN(THETA1)+1/SIN(THETA2)	T00120
	C3=C1/C2	T00130
	CC=2.**(5./3.)*RN/C1/C3**(2./3.)	T00140
	H=(CC/S0**0.5)**0.375*Q**0.375	T00150
C		T00160
C	CHECK FOR OVERFLOW	T00170
	HM1=S1*SL*(3.**0.5)	T00180
	HM2=S2*SL*(3.**0.5)	T00190
	IF(HM1.LT.HM2) GO TO 1710	T00200
	HMAX=HM2	T00210
	GO TO 1720	T00220
1710	HMAX=HM1	T00230
1720	IF(H.GT.HMAX) H=HMAX	T00240
	B=H*C1	T00250
	RH=0.5*H*C3	T00260
	V=1./RN *(RH**(2./3.)) * S0**0.5	T00270
	EG=V*V/2./G	T00280
C	WRITE(6,10) V,EG	T00290
10	FORMAT(/,10X,'VELOCITY=',F12.8,10X,'ENERGY=',F12.8,/) )	T00300
	RETURN	T00310
	END	T00320
		T00330

C	SUBROUTINE RERSN(SO,SL,SH,RCH,C1,H1,H2,EX,B1,B2,T1,TE,DE)	U00010
C	*****	U00020
C	THIS SUBPROGRAM COMPUTES THE AMOUNT OF MATERIAL ERODED FROM	U00030
C	A RILL SEGMENT (RILL EROSION).	U00040
C	COMPUTATIONS ARE BASED ON THE ASSUMPTION OF UNIFORM RILL FLOW.	U00050
C	K A L I N S K E 'S BED LOAD FORMULA IS USED AS THE SEDIMENT	U00060
C	PICK-UP CRITERION.	U00070
C	DE = THE REDUCTION IN BED ELEVATION DUE TO EROSION.	U00080
C	*****	U00090
	REAL*4 TE,DE	U00100
	COMMON /PROP/GAMA,RO,G,SG,RN	U00110
	COMMON NT	U00120
	TAU1=GAMA*C1*S0*H1*H1/2.	U00130
	TAU2=GAMA*C1*S0*H2*H2/2.	U00140
	XL=2.*SL	U00150
	E= RCH*(TAU2-TAU1)/XL*((TAU2+TAU1)/2.)*EX*60	U00160
C ...	E= EROSION RATE IN CUBIC METERS/METER LENGTH/MINUTE	U00170
	TE=E*XL*T1	U00180
C ...	TE IS DEDUCTED UNIFORMLY ALONG THE RILL LENGTH	U00190
	KF=2	U00200
	WD=2.*SL*3.**0.5	U00210
30	BB=(B1+B2)/2.*KF	U00220
	IF(BB.GT.0.0) GO TO 40	U00230
	DE=0.0	U00240
	RETURN	U00250
40	IF(BB.GT.WD) GO TO 35	U00260
	DE=2.*TE/SH/BB	U00270
	GO TO 50	U00280
35	KF=KF-1	U00290
	IF(KF.LT.1) KF=1	U00300
	GO TO 30	U00310
50	RETURN	U00320
	END	U00330
	SUBROUTINE HERSN(QQ,SL,EM,EH,HCH,B1,B2,H1,H2,EX,T1,TEH)	U00340
C	*****	V00010
C	THIS SUBPROGRAM COMPUTES THE AMOUNT OF MATERIAL ERODED FROM SIDE	V00020
C	HUMPS OF ANY RILL SEGMENT (INTERRILL AREAS).	V00030
C	COMPUTATIONS ARE BASED ON THE ASSUMPTION OF UNIFORM SHEET FLOW	V00040
C	OVER AN EQUIVALENT RECTANGULAR AREA.	V00050
C	K A L I N S K E 'S BED LOAD FORMULA IS USED AS THE SEDIMENT	V00060
C	PICK-UP CRITERION.	V00070
C	*****	V00080
C		V00090
	REAL*4 EM,EH,TEH	V00100
	COMMON /PROP/GAMA,RO,G,SG,RN	V00110
	COMMON NT	V00120
	ZRO=1/(10.**20.)	V00130
	IF(B1.GE.1000..AND.B2.GE.1000.) GO TO 30	V00140
	XH=SL*(3.**0.5)	V00150
	HH=EH-EM	V00160
	SO=(EH-EM)/XH	V00170
	THETA=ATAN(SO)	V00180
	ZL=HH/SIN(THETA)	V00190
	HAV=(H1+H2)/2.	V00200
	RL=ZL-HAV/SIN(THETA)	V00210
C	IF WATER OVERFLOWS ON THIS SIDE ,THEN N EROSION WILL TAKE	V00220
C	PLACE ON IT.	V00230
	IF(RL.LE.0.0) GO TO 100	V00240
	YL=2.*RL*SL/ZL	V00250
	XL=RL/2.	V00260
50	Q=QQ*XL	V00270
	Y=(RN*Q/SO**0.5)**0.6	V00280
	TAU=GAMA*Y*SO	V00290
	E=HCH*TAU/XL*((TAU/2.)*EX*60.	V00300
	TEH=E*XL*YL*T1	V00310
10	FORMAT(7F15.8)	V00320
	RETURN	V00330
100	TEH=0.0	V00340
	RETURN	V00350
30	SO=ABS(H1)	V00360
	IF(SO.LE.ZRO) RETURN	V00370
	XL=0.5*SL	V00380
	YL=2.*SL	V00390
	GO TO 50	V00400
	END	V00410
		V00420

```

C      SUBROUTINE ERSN1(I, QTT, HCH, RCH, EX, TI)
C      *****
C      THIS SUBPROGRAM PERFORMS EROSION COMPUTATIONS ON RILL SEGMENTS
C      WITH UP-STREAM POINT HAVING CODE=1 .
C      S1 = SLOPE OF THE LEFT SIDE OF THE RILL SIDE WALLS
C      S2 = SLOPE OF THE RIGHT SIDE OF THE RILL SIDE WALLS
C      Q1 = FLOW RATE AT UPSTREAM END OF THE RILL SEGMENT
C      Q2 = FLOW RATE AT DOWNSTREAM END OF THE RILL SEGMENT
C      SDT(I), TRE(I), TIRE(I) ARE DEFINED IN MAIN PGM
C      DH(I) = CHANGE IN ELEVATION OF I AT THE END OF A TIME INTERVAL
C      *****
C
C      COMMON/MESH/NX, NY, NMAX, SL, SH, WL, QQ
C      COMMON/NODES/X(2000), Y(2000), CODE(2000), ELV(2000)
C      COMMON/HMPP/HMPP(500), XHMP(500), YHMP(500)
C      COMMON/PONDG/KPND(2000), NAJ(2000), DH(2000)
C      COMMON/SDMNT/SDT(2000), TRE(2000), TIRE(2000)
C      COMMON/SLOPES/HMP1(500), HMP2(500), HMP3(500), HMP4(500), HMP5(500),
C      * HMP6(500)
C      COMMON /PROP/CAMA, RO, G, SG, RN
C      COMMON NT
C      ZRO=1.0/(10.0**20.)
C      KODE=1
C      DE=0.0
C      TE=0.0
C      E1=ELV(I)
1015 E2=ELV(I-1)
      AELV=(E1+E2)/2.
C
C ... IDENTIFY HUMPS ON LEFT AND ON RIGHT
C      CALL IDHMP(NY, I, IDL, IDR, NDUMY)
C      IF(X(I).EQ.0) GO TO 1020
C      IF(X(I).EQ.X(NMAX)) GO TO 1030
C
C ... COMPUTATIONS FOR RILL SEGMENTS NOT ON THE BOUNDARIES
C      *****
C      S1=(HMP4(IDL)-AELV)/SH/3.**0.5
C      S2=(HMP1(IDR)-AELV)/SH/3.**0.5
C      S0=(E1-E2)/2./SH
C      IF(S0.LE.ZRO) GO TO 1065
10 CONTINUE
      DQ=2.*QQ*SL*SL*(3.**0.5)
      Q2=QTT
      Q1=Q2-DQ
      IF(Q1.LT.0.0) Q1=0.0
      IF(Q2.LT.0.0) Q2=0.0
C
C ... CHECK FOR NEGATIVE SIDE SLOPES
C      IF(S1.LE.ZRO.OR.S2.LE.ZRO) GO TO 1025
11 CONTINUE
C
C ... COMPUTE DEPTH AND WIDTH OF THE FLOW AT THE TWO END POINTS
C      CALL CSEC(SL, Q1, S1, S2, S0, H1, B1, C1)
C      CALL CSEC(SL, Q2, S1, S2, S0, H2, B2, C1)
C
C ... COMPUTE EROSION FROM NEIGHBORING HUMPS
C      CALL HERSN(QQ, SL, AELV, HMP4(IDL), HCH, B1, B2, H1, H2, EX, TI, TEHL)
C      CALL HERSN(QQ, SL, AELV, HMP1(IDR), HCH, B1, B2, H1, H2, EX, TI, TEHR)
C
C ... CHECK FOR PONDING . IF IT OCCURS, DEPOSIT SEDIMENT LOAD AT
C      DESIGNATED POINTS(SEE NEXT COMMENT STATEMENT).
C      IF(KPND(I-1).NE.11) GO TO 1017
C      TDP=SDT(I)+TEHL+TEHR
C
C ... SEDIMENT LOAD AT I IS DEPOSITED ON RILL SEGMENTS OF SIX MESH
C      "BACK STEPS" (BETWEEN I-1 AND I+3) .
C      DD1, ..., DD5 ARE DEPTHS OF MATERIAL DEPOSITED AT DIFFERENT
C      BACK STEPS.
29 CONTINUE
      KF=2
      WD=WL
30 BB=(B1+B2)/2.*KF
      IF(BB.GT.WD) GO TO 35
      DD1=2.5/29.*2.*TDP/SH/BB
      GO TO 40
35 KF=KF-1
      IF(KF.LT.1) KF=1

```

	GO TO 30	W00780
40	DD2=0.8*DD1	W00790
	DD3=0.6 *DD1	W00800
	DD4=0.4* DD1	W00810
	DD5=0.2* DD1	W00820
	DH(I-1)=DH(I-1)-1.*DD1	W00830
	DH(I)=DH(I)-1.*DD2	W00840
	IF(Y(I+NY+1).LT.Y(I)) GO TO 200	W00850
	IF((I+NY+1).GT.NMAX) GO TO 20	W00860
	DH(I+NY+1)=DH(I+NY+1)-1.*DD3	W00870
20	IF((I-NY+1).LE.0) GO TO 21	W00880
	DH(I-NY+1)=DH(I-NY+1)-1.*DD3	W00890
21	IF(Y(I+NY+2).LT.Y(I+NY+1)) GO TO 200	W00900
	IF((I+NY+2).GT.NMAX) GO TO 22	W00910
	DH(I+NY+2)=DH(I+NY+2)-1.*DD4	W00920
22	IF((I-NY+2).LE.0) GO TO 23	W00930
	DH(I-NY+2)=DH(I-NY+2)-1.*DD4	W00940
23	IF(Y(I+3).LT.Y(I)) GO TO 200	W00950
	DH(I+3)=DH(I+3)-1.*DD5	W00960
	IF((I+2*NY+3).GT.NMAX) GO TO 24	W00970
	DH(I+2*NY+3)=DH(I+2*NY+3)-1.*DD5	W00980
24	IF((I-2*NY+3).LE.0) GO TO 200	W00990
	DH(I-2*NY+3)=DH(I-2*NY+3)-1.*DD5	W01000
200	CONTINUE	W01010
	SDT(I-1)=0.0	W01020
	TRE(I-1)=0.0	W01030
	TIRE(I-1)=0.0	W01040
1021	RETURN	W01050
1017	CONTINUE	W01060
C		W01070
C	... COMPUTE RILL EROSION	W01080
	CALL RERSN(S0,SL,SH,RCH,C1,H1,H2,EX,B1,B2,TI,TE,DE)	W01090
C		W01100
C	... COMPUTE CHANGE IN ELEVATION OF TWO END POINTS	W01110
	DH(I)=DH(I)+DE/(NAJ(I)*1.)	W01120
	DH(I-1)=DH(I-1)+DE/(NAJ(I-1)*1.)	W01130
C		W01140
C	... COMPUTE SEDIMENT DISCHARGE AT NODAL POINTS	W01150
	SDT(I-1)=SDT(I-1)+SDT(I)+TE+TEHL+TEHR	W01160
	TRE(I-1)=TRE(I-1)+TRE(I)+TE	W01170
	TIRE(I-1)=TIRE(I-1)+TIRE(I)+TEHR+TEHL	W01180
	RETURN	W01190
C		W01200
C	... COMPUTATIONS FOR RILL SEGMENTS WITH NEGATIVE SIDE SLOPE(S).	W01210
C	NO RILL EROSION IN THIS CASE.	W01220
1025	B1=1000.	W01230
	B2=1000.	W01240
C	... LARGE VALUES OF B1 AND B2(1000) IS FOR IDENTIFICATION ONLY	W01250
	CALL HERSN(QQ,SL,AELV,HMP4(IDL),HCH,B1,B2,S1,H2,EX,TI,TE1)	W01260
	CALL HERSN(QQ,SL,AELV,HMP1(IDR),HCH,B1,B2,S2,H2,EX,TI,TE2)	W01270
C		W01280
C	... REDISTRIBUTE THE SEDIMENT LOAD WHEN EITHER SIDE SLOPES IS -VE.	W01290
	CALL SNEGTV(I,S1,S2,TE1,TE2,KODE,T,R,H,NBRCH)	W01300
	RETURN	W01310
C		W01320
C	... COMPUTATIONS FOR RILL SEGMENTS ON THE BOUNDARIES	W01330
C	*****	W01340
C	... RILL SEGMENTSON THE BOUNDARY ARE ASSUMED TO HAVE SYMMETRICAL	W01350
C	SIDE SLOPES	W01360
C	THE SAME SEQUENCE OF COMPUTATION IS FOLLOWED	W01370
1020	S=(HMP1(IDR)-AELV)/SH/3.**0.5	W01380
	EH=HMP1(IDR)	W01390
	GO TO 1040	W01400
1030	S=(HMP4(IDL)-AELV)/SH/3.**0.5	W01410
	S1=S	W01420
	S2=S	W01430
	EH=HMP4(IDL)	W01440
1040	S0=(ELV(I)-ELV(I-1))/2./SH	W01450
	IF(S0.LE.ZRO) GO TO 1065	W01460
12	CONTINUE	W01470
	AELV=(ELV(I)+ELV(I-1))/2.	W01480
	DQ=2.*QQ*SL*SL*(3.**0.5)	W01490
	Q2=QTT	W01500
	G1=Q2-DQ	W01510
	IF(Q1.LT.0.0) Q1=0.0	W01520
	IF(Q2.LT.0.0) Q2=0.0	W01530
	IF(S.LE.ZRO) GO TO 1035	W01540

13	CONTINUE	
	CALL CSEC(SL,Q1,S,S,SO,H1,B1,C1)	W01550
	CALL CSEC(SL,Q2,S,S,SO,H2,B2,C1)	W01560
	CALL HERSN(QQ,SL,AELV,EH,HCH,B1,B2,H1,H2,EX,TI,TEH)	W01570
	IF(KPND(I-1).NE.11) GO TO 1016	W01580
	TDP=SDT(I)+TEH	W01590
	GO TO 29	W01600
1016	CONTINUE	W01610
	CALL RERSN(SO,SL,SH,RCH,C1,H1,H2,EX,B1,B2,TI,TE,DE)	W01620
	DH(I)=DH(I)+DE/(NAJ(I)*1.)	W01630
	DH(I-1)=DH(I-1)+DE/(NAJ(I-1)*1.)	W01640
	SDT(I-1)=SDT(I-1)+SDT(I)+TE+TEH	W01650
	TRE(I-1)=TRE(I-1)+TRE(I)+TE	W01660
	TIRE(I-1)=TIRE(I-1)+TIRE(I)+TEH	W01670
	RETURN	W01680
1035	B1=1000.	W01690
	B2=1000.	W01700
	CALL HERSN(QQ,SL,AELV,EH,HCH,B1,B2,S,H2,EX,TI,TE)	W01710
	CALL SNEGTV(I,S,S,TE,TE,KODE,T,R,H,NBRNCH)	W01720
	RETURN	W01730
1065	CONTINUE	W01740
C	WRITE(6,1070) I,SO	W01750
1070	FORMAT(/,10X,'PONDING OCCURED AT PT. ',I5,5X,'SO=',F12.8)	W01760
	RETURN	W01770
	END	W01780
	SUBROUTINE ERSN2(I,QLL,GRR,HCH,RCH,EX,TI)	X00010
C	*****	X00020
C	THIS SUBPROGRAM PERFORMS EROSION COMPUTATIONS ON RILL SEGMENTS	X00030
C	WITH UP-STREAM POINT HAVING CODE=2 .	X00040
C		X00050
C	S1 = SLOPE OF THE LEFT SIDE OF THE RILL SIDE WALLS	X00060
C	S2 = SLOPE OF THE RIGHT SIDE OF THE RILL SIDE WALLS	X00070
C	Q1 = FLOW RATE AT UPSTREAM END OF THE RILL SEGMENT	X00080
C	Q2 = FLOW RATE AT DOWNSTREAM END OF THE RILL SEGMENT	X00090
C	SDT(I),TRE(I),TIRE(I) ARE DEFINED IN MAIN PGM	X00100
C	DH(I) = CHANGE IN ELEVATION OF I AT THE END OF A TIME INTERVAL	X00110
C	*****	X00120
C		X00130
	COMMON/MESH/NX,NY,NMAX,SL,SH,WL,QQ	X00140
	COMMON/PONDG/KPND(2000),NAJ(2000),DH(2000)	X00150
	COMMON/HMPP/HMPP(500),XHMP(500),YHMP(500)	X00160
	COMMON/NODES/X(2000),Y(2000),CODE(2000),ELV(2000)	X00170
	COMMON/SDMT/SDT(2000),TRE(2000),TIRE(2000)	X00180
	COMMON/SLOPES/HMP1(500),HMP2(500),HMP3(500),HMP4(500),HMP5(500),	X00190
	* HMP6(500)	X00200
	COMMON /PROP/GAMA,RO,G,SG,RN	X00210
	COMMON NT	X00220
	ZRO=1.0/(10.0**20.)	X00230
	KODE=2	X00240
	DE=0.0	X00250
	TE=0.0	X00260
	DQ=2.*QQ*SL*SL*(3.**0.5)	X00270
C		X00280
C	... IDENTIFY THE THREE NEIGHBORING HUMPS	X00290
	CALL IDHMP(NY,I,IDL,IDR,IDC)	X00300
	SOL=(ELV(I)-(ELV(I-NY-1)))/2./SH	X00310
	SOR=(ELV(I)-(ELV(I+NY-1)))/2./SH	X00320
	IF(X(I).EQ.0) GO TO 1110	X00330
	IF(X(I).EQ.X(NMAX)) GO TO 1120	X00340
	IF(SOL.LE.ZRO.AND.SOR.LE.ZRO) GO TO 1170	X00350
	IF(SOL.LE.ZRO.AND.SOR.GT.ZRO) GO TO 1110	X00360
	IF(SOL.GT.ZRO.AND.SOR.LT.ZRO) GO TO 1120	X00370
201	CONTINUE	X00380
C		X00390
C	... SEDIMENT LOAD IS DEVIDED BETWEEN THE TWO BRANCHES ACCORDING TO	X00400
C	THE RELATIVE MAGNITUDES OF BED SLOPES RAISED TO THE POWER OF 1.25	X00410
	SOL2=(ELV(I-NY-1)-ELV(I-NY-2))/2./SH	X00420
	SOR2=(ELV(I-NY-1)-ELV(I-NY-2))/2./SH	X00430
	SAVL=(SOL+SOL2)/2.	X00440
	IF(SAVL.LT.0.0) SAVL=0.0	X00450
	SAVR=(SOR+SOR2)/2.	X00460
	IF(SAVR.LT.0.0) SAVR=0.0	X00470
	SS=SAVL**1.25+SAVR**1.25	X00480
	IF(SS.LE.0.0) GO TO 210	X00490
	STL=SDT(I)*(SAVL**1.25)/SS	X00500
	RENL=TRE(I)*(SAVL**1.25)/SS	X00510
	HRENL=TIRE(I)*(SAVL**1.25)/SS	X00520
	GO TO 220	X00530

210	STL=0.5*SDT(I)	X00540
	RENL=0.5*TRE(I)	X00550
	HRENL=0.5*TIRE(I)	X00560
220	CONTINUE	X00570
C		X00580
C	... COMPUTATIONS FOR RILL SEGMENT ON THE LEFT	X00590
C	*****	X00600
C		X00610
	K=1	X00620
	GO TO 1140	X00630
1120	K=2	X00640
	IF(SOL.IE.0.0) GO TO 1170	X00650
	STL=SDT(I)	X00660
	RENL=TRE(I)	X00670
	HRENL=TIRE(I)	X00680
1140	S0=SOL	X00690
	AELV=(ELV(I )+ELV(I-NY-1 ))/2.	X00700
	S2=(HMP2(IDC)-AELV)/SH/3.**0.5	X00710
	HP5=HMP5(IDL)	X00720
C		X00730
C	... RILL SEGMENTSON THE BOUNDARY ARE ASSUMED TO HAVE SYMMETRICAL	X00740
C	SIDE SLOPES	X00750
	IF(Y(I).EQ.Y(NY)) HP5=HMP2(IDC)	X00760
	S1=(HP5-AELV)/SH/3.**0.5	X00770
	Q1=QLL	X00780
	IF(Q1.LT.0.0) Q1=0.0	X00790
	Q2=Q1+DQ	X00800
C		X00810
C	... CHECK FOR NEGATIVE SIDE SLOPES	X00820
	IF(S1.LE.ZR0.OR.S2.LE.ZR0) GO TO 1145	X00830
202	CONTINUE	X00840
C		X00850
C	... COMPUTE DEPTH AND WIDTH OF THE FLOW AT THE TWO END POINTS	X00860
	CALL CSEC(SL,Q1,S1,S2,S0,H1,B1,C1)	X00870
	CALL CSEC(SL,Q2,S1,S2,S0,H2,B2,C1)	X00880
C		X00890
C	... COMPUTE EROSION FROM NEIGHBORING HUMPS	X00900
	CALL HERSN(QQ,SL,AELV,HP5 ,HCH,B1,B2,H1,H2,EX,T1,TEHL)	X00910
	CALL HERSN(QQ,SL,AELV,HMP2(IDC),HCH,B1,B2,H1,H2,EX,T1,TEHLC)	X00920
C		X00930
C	... CHECK FOR PONDING . IF IT OCCURS, DEPOSIT SEDIMENT LOAD AT	X00940
C	DESIGNATED POINTS(SEE NEXT COMMENT STATEMENT).	X00950
	IF(KPND(I-NY-1).NE.11) GO TO 1115	X00960
C		X00970
C	... SEDIMENT LOAD AT I IS DEPOSITED ON RILL SEGMENTS OF SIX MESH	X00980
C	"BACK STEPS"	X00990
	TDP=STL+TEHL+TEHLC	X01000
	KF=2	X01010
	WD=WL	X01020
30	BB=(B1+B2)/2.*KF	X01030
	IF(BB.GT.WD) GO TO 35	X01040
C		X01050
C	DD1,....,DD5 ARE DEPTHS OF MATERIAL DEPOSITED AT DIFFERENT	X01060
C	BACK STEPS.	X01070
	DD1=2.5/35.*2.*TDP/SH/BB	X01080
	GO TO 40	X01090
35	KF=KF-1	X01100
	IF(KF.LT.1) KF=1	X01110
	GO TO 30	X01120
40	DD2=0.8*DD1	X01130
	DD3=0.6*DD1	X01140
	DD4=0.4*DD1	X01150
	DD5=0.2*DD1	X01160
	DH(I-NY-1)=DH(I-NY-1)-1.*DD1	X01170
	DH(I)=DH(I)-1.*DD2	X01180
	IF((I-2*NY).LE.0) GO TO 10	X01190
	DH(I-2*NY)=DH(I-2*NY)-1.*DD2	X01200
10	IF(Y(I+1).LT.Y(I)) GO TO 100	X01210
	DH(I+1)=DH(I+1)-1.*DD3	X01220
	IF((I-2*NY+1).LE.0) GO TO 11	X01230
	DH(I-2*NY+1)=DH(I-2*NY+1)-1.*DD3	X01240
11	IF(Y(I+NY+2).LT.Y(I)) GO TO 100	X01250
	IF((I+NY+2).GT.NMAX) GO TO 12	X01260
	DH(I+NY+2)=DH(I+NY+2)-1.*DD4	X01270
12	DH(I-NY+2)=DH(I-NY+2)-1.*DD4	X01280
	IF((I-3*NY+2).LE.0) GO TO 13	X01290
	DH(I-3*NY+2)=DH(I-3*NY+2)-1.*DD4	X01300



13	IF(Y(I+NY+3).LT.Y(I)) GO TO 100	X01310
	IF((I+NY+3).GT.NMAX) GO TO 14	X01320
	DH(I+NY+3)=DH(I+NY+3)-1.*DD5	X01330
14	IF((I-NY+3).LE.0) GO TO 15	X01340
	DH(I-NY+3)=DH(I-NY+3)-1.*DD5	X01350
15	IF((I-3*NY+3).LE.0) GO TO 100	X01360
	DH(I-3*NY+3)=DH(I-3*NY+3)-1.*DD5	X01370
100	CONTINUE	X01380
1021	RETURN	X01390
1115	CONTINUE	X01400
C		X01410
C	... COMPUTE RILL EROSION	X01420
	CALL RERSN(SO,SL,SH,RCH,C1,H1,H2,EX,B1,B2,TI,TE,DE)	X01430
C		X01440
C	... COMPUTE CHANGE IN ELEVATION OF TWO END POINTS	X01450
	DH(I)=DH(I)+DE/(1.*NAJ(I))	X01460
	DH(I-NY-1)=DH(I-NY-1)+DE/(1.*NAJ(I-NY-1))	X01470
C		X01480
C	... COMPUTE SEDIMENT DISCHARGE AT NODAL POINTS	X01490
	SDT(I-NY-1)=SDT(I-NY-1)+STL+TE+TEHL+TEHLC	X01500
	TRE(I-NY-1)=TRE(I-NY-1)+RENL+TE	X01510
	TIRE(I-NY-1)=TIRE(I-NY-1)+HRENL+TEHL+TEHLC	X01520
C		X01530
C	... CHECK FOR -VE. SIDE SLOPES	X01540
1145	IF(S1.GT.0.0.AND.S2.GT.0.0) GO TO 1150	X01550
	NBRNCH=1	X01560
	B1=1000.	X01570
	B2=1000.	X01580
C	NOTE: THE LARGE VALUES OF B1, AND B2 (1000.) ARE USED ONLY AS FLAGS	X01590
C		X01600
C	... COMPUTATIONS FOR RILL SEGMENTS WITH NEGATIVE SIDE SLOPE(S).	X01610
C	NO RILL EROSION IN THIS CASE.	X01620
	CALL RERSN(QQ,SL,DMY1,DMY2,HCH,B1,B2,S2,H2,EX,TI,TE2)	X01630
	CALL RERSN(QQ,SL,DMY1,DMY2,HCH,B1,B2,S1,H2,EX,TI,TE1)	X01640
	KODE=2	X01650
C		X01660
C	... REDISTRIBUTE THE SEDIMENT LOAD WHEN EITHER SIDE SLOPES IS -VE.	X01670
	CALL SNECTV(I,S1,S2,TE1,TE2,KODE,STL,RENL,HRENL,NBRNCH)	X01680
1150	IF(K.EQ.1) GO TO 1160	X01690
	RETURN	X01700
C		X01710
C	... COMPUTATIONS FOR RILL SEGMENT ON THE RIGHT	X01720
C	*****	X01730
C		X01740
C	THE SAME SEQUENCE OF COMPUTATIONS IS FOLLOWED	X01750
1110	IF(SOR.LE.0) GO TO 1170	X01760
	STL=0	X01770
	RENL=0.0	X01780
	HRENL=0.0	X01790
1160	STR=SDT(I)-STL	X01800
	RENR=TRE(I)-RENL	X01810
	HRENR=TIRE(I)-HRENL	X01820
	SO=SOR	X01830
	AELV=(ELV(I)+ELV(I+NY-1))/2.	X01840
	S1=(HMP3(IDC)-AELV)/SH/3.**0.5	X01850
	HP6=HMP6(IDR)	X01860
	IF(Y(I).EQ.Y(NY)) HP6=HMP3(IDC)	X01870
	S2=(HP6-AELV)/SH/3.**0.5	X01880
	Q1=QRR	X01890
	IF(Q1.LT.0.0) Q1=0.0	X01900
	Q2=Q1+DQ	X01910
	IF(S1.LE.ZRO.OR.S2.LE.ZRO) GO TO 1155	X01920
203	CONTINUE	X01930
	CALL CSEC(SL,Q1,S1,S2,SO,H1,B1,C1)	X01940
	CALL CSEC(SL,Q2,S1,S2,SO,H2,B2,C1)	X01950
	CALL RERSN(QQ,SL,AELV,HP6,HCH,B1,B2,H1,H2,EX,TI,TEHR)	X01960
	CALL RERSN(QQ,SL,AELV,HMP3(IDC),HCH,B1,B2,H1,H2,EX,TI,TEHRC)	X01970
	IF(KPND(I+NY-1).NE.11) GO TO 1116	X01980
	TDP=STL+TEHR+TEHRC	X01990
	KF=2	X02000
	WD=WL	X02010
60	BB=(B1+B2)/2.*KF	X02020
	IF(BB.GT.WD) GO TO 65	X02030
	DD1=2.5/35.*2.*TDP/SH/BB	X02040
	GO TO 70	X02050
65	KF=KF-1	X02060
	IF(KF.LT.1) KF=1	X02070

	GO TO 60	X02080
70	DD2=0.8*DD1	X02090
	DD3=0.6*DD1	X02100
	DD4=0.4*DD1	X02110
	DD5=0.2*DD1	X02120
	DH(I+NY-1)=DH(I+NY-1)-1.*DD1	X02130
	DH(I)=DH(I)-1.*DD2	X02140
	IF((I+2*NY).GT.NMAX) GO TO 20	X02150
	DH(I+2*NY)=DH(I+2*NY)-1.*DD2	X02160
20	IF(Y(I+1).LT.Y(I)) GO TO 200	X02170
	DH(I+1)=DH(I+1)-1.*DD3	X02180
	DH(I+2*NY+1)=DH(I+2*NY+1)-1.*DD3	X02190
	IF(Y(I+NY+2).LT.Y(I)) GO TO 200	X02200
	IF((I+NY+2).GT.NMAX) GO TO 21	X02210
	DH(I+NY+2)=DH(I+NY+2)-1.*DD4	X02220
21	IF((I+3*NY+2).GT.NMAX) GO TO 22	X02230
	DH(I+3*NY+2)=DH(I+3*NY+2)-1.*DD4	X02240
22	IF((I-NY+2).LT.0) GO TO 23	X02250
	DH(I-NY+2)=DH(I-NY+2)-1.*DD4	X02260
23	IF(Y(I+3*NY+3).LE.Y(I)) GO TO 200	X02270
	IF((I+3*NY+3).GT.NMAX) GO TO 24	X02280
	DH(I+3*NY+3)=DH(I+3*NY+3)-1.*DD5	X02290
24	IF((I+NY+3).GT.NMAX) GO TO 25	X02300
	DH(I+NY+3)=DH(I+NY+3)-1.*DD5	X02310
25	IF((I-NY+3).LE.0) GO TO 200	X02320
	DH(I-NY+3)=DH(I-NY+3)-1.*DD5	X02330
200	CONTINUE	X02340
	SDT(I+NY-1)=0.0	X02350
	TRE(I+NY-1)=0.0	X02360
	TIRE(I+NY-1)=0.0	X02370
1023	RETURN	X02380
1116	CONTINUE	X02390
	CALL RERSN(S0,SL,SH,RCH,C1,H1,H2,EX,B1,B2,TI,TE,DE)	X02400
	DH(I)=DH(I)+DE/(1.*NAJ(I))	X02410
	DH(I+NY-1)=DH(I+NY-1)+DE/(1.*NAJ(I+NY-1))	X02420
	SDT(I+NY-1)=SDT(I+NY-1)+STR+TE+TEHR+TEHRC	X02430
	TRE(I+NY-1)=TRE(I+NY-1)+RENH+TE	X02440
	TIRE(I+NY-1)=TIRE(I+NY-1)+HRENH+TEHR+TEHRC	X02450
	RETURN	X02460
1155	IF(S1.GT.ZRO.AND.S2.GT.ZRO) RETURN	X02470
204	CONTINUE	X02480
	NBRNCH=2	X02490
	B1=1000.	X02500
	B2=1000.	X02510
	CALL HERSN(QQ,SL,DMY1,DMY2,HCH,B1,B2,S1,H2,EX,TI,TE1)	X02520
	CALL HERSN(QQ,SL,DMY1,DMY2,HCH,B1,B2,S2,H2,EX,TI,TE2)	X02530
	KODE=2	X02540
	CALL SNECTV(I,S1,S2,TE1,TE2,KODE,STR,RENH,HRENH,NBRNCH)	X02550
	RETURN	X02560
1170	CONTINUE	X02570
C	WRITE(6,1175) I,SOL,SOR	X02580
1175	FORMAT(/,10X,'PONDING OCCURED AT PT. ',I5,5X,'SOL=',F12.8,	X02590
	# 5X,'SOR=',F12.8)	X02600
	RETURN	X02610
	END	X02620
	SUBROUTINE SNECTV(I,S1,S2,TE1,TE2,KODE,T,R,H,NBRNCH)	Y00010
C	*****	Y00020
C	THIS SUBPROGRAM MODEFIES THE EROSION COMPUTATIONS WHEN EITHER	Y00030
C	SIDESLOPES OF A RILL SEGMENT IS NEGATIVE.	Y00040
C		Y00050
C	NV= LOCATION OF SEDIMENT LOAD BEFORE MODEFICATION	Y00060
C	NK= LOCATION OF SEDIMENT LOAD AFTER MODEFICATION	Y00070
C	TE1= VOLUME OF SOIL ERODED FROM LEFT SIDESLOPE	Y00080
C	TE2= VOLUME OF SOIL ERODED FROM RIGHT SIDESLOPE	Y00090
C	*****	Y00100
C		Y00110
	COMMON/MESH/NX,NY,NMAX,SL,SH,WL,QQ	Y00120
	COMMON/HMPP/HMPP(500),XHMP(500),YHMP(500)	Y00130
	COMMON/SLOPES/HMP1(500),HMP2(500),HMP3(500),HMP4(500),HMP5(500),	Y00140
	HMP6(500)	Y00150
	COMMON/NODES/X(2000),Y(2000),CODE(2000),ELV(2000)	Y00160
	COMMON/SDMT/SDT(2000),TRE(2000),TIRE(2000)	Y00170
	COMMON NT	Y00180
	FORMAT(/,' POINT # ',I3,5F20.8,/) )	Y00190
	E1=TE1	Y00200
	E2=TE2	Y00210
	CALL IDHMP(NY,I,IDL,IDR,IDC)	Y00220

	GO TO (100,200),KODE	Y00230
100	S0=(ELV(I)-ELV(I-1))/2./SH	Y00240
	IF(X(I).EQ.0.0) GO TO 120	Y00250
	IF(X(I).EQ.X(NMAX)) GO TO 110	Y00260
	IF(S1.LE.0.0.AND.S2.GT.0.0) GO TO 110	Y00270
	IF(S1.GT.0.0.AND.S2.LE.0.0) GO TO 120	Y00280
	NK=I-2*NY-1	Y00290
	NV=I	Y00300
	IF(X(NV).LE.X(NY+1)) NK=NMAX+5	Y00310
	F=0.5	Y00320
	KK=1	Y00330
	E2=0.0	Y00340
	HHH=(ELV(NK)+ELV(NK+1))/2.	Y00350
	IF(HHH.GT.HMP1(IDL)) GO TO 105	Y00360
	GO TO 1000	Y00370
105	F=0.0	Y00380
	E1=0.0	Y00390
	E2=0.0	Y00400
	GO TO 1000	Y00410
111	NK=I+2*NY-1	Y00420
	NV=I	Y00430
	IF(X(NV).GE.X(NMAX-NY)) NK=NMAX+5	Y00440
	F=0.5	Y00450
	KK=2	Y00460
	E2=TE2	Y00470
	E1=0.0	Y00480
	HHH=(ELV(NK)+ELV(NK+1))/2.	Y00490
	IF(HHH.GT.HMP4(IDR)) GO TO 105	Y00500
	GO TO 1000	Y00510
110	NK=I-2*NY-1	Y00520
	NV=I	Y00530
	F=1.0	Y00540
	KK=2	Y00550
	IF(X(NV).LE.X(NY+1)) NK=NMAX+5	Y00560
	AS1=ABS(S1)	Y00570
	IF(S0.GE.AS1) GO TO 117	Y00580
	HHH=(ELV(NK)+ELV(NK+1))/2.	Y00590
	IF(HHH.GT.HMP1(IDL)) GO TO 115	Y00600
	GO TO 1000	Y00610
115	F=0.0	Y00620
	E1=0.0	Y00630
	E2=0.0	Y00640
	GO TO 1000	Y00650
117	F=0.0	Y00660
	E=E2	Y00670
	E2=0.0	Y00680
	KK=3	Y00690
	GO TO 1000	Y00700
120	NK=I+2*NY-1	Y00710
	NV=I	Y00720
	IF(X(NV).GE.X(NMAX-NY)) NK=NMAX+5	Y00730
	F=1.0	Y00740
	KK=2	Y00750
	HHH=(ELV(NK)+ELV(NK+1))/2.	Y00760
	IF(HHH.GT.HMP4(IDR)) GO TO 115	Y00770
	AS2=ABS(S2)	Y00780
	IF(S0.GE.AS2) GO TO 127	Y00790
	GO TO 1000	Y00800
127	F=0.0	Y00810
	E=E1	Y00820
	E1=0.0	Y00830
	KK=3	Y00840
	GO TO 1000	Y00850
1000	SDT(NK)=SDT(NK)+F*SDT(NV)+E1+E2	Y00860
	TRE(NK)=TRE(NK)+F*TRE(NV)	Y00870
	TIRE(NK)=TIRE(NK)+F*TIRE(NV)+E1+E2	Y00880
	IF(KK.EQ.1) GO TO 111	Y00890
	IF(KK.EQ.3) GO TO 1500	Y00900
	GO TO 1700	Y00910
1500	SDT(NV-1)=SDT(NV-1)+SDT(NV)+E	Y00920
	TRE(NV-1)=TRE(NV-1)+TRE(NV)	Y00930
	TIRE(NV-1)=TIRE(NV-1)+TIRE(NV)+E	Y00940
1700	CONTINUE	Y00950
	RETURN	Y00960
200	CALL IDHMP(NY,I,IDL,IDR,IDC)	Y00970
	IF(NBRNCH.EQ.2) GO TO 300	Y00980
	IF(X(I).EQ.0.0) GO TO 300	Y00990

	SOL=(ELV(I)-ELV(I-NY-1))/2./SH	Y01000
	AS1=ABS(S1)	Y01010
	AS2=ABS(S2)	Y01020
	IF(S1.LE.0.0.AND.S2.GT.0.0) GO TO 210	Y01030
	IF(S1.GT.0.0.AND.S2.LE.0.0) GO TO 220	Y01040
	NK=I-2*NY+1	Y01050
	IF(Y(I).GE.Y(NY-1)) NK=NMAX+5	Y01060
	IF(X(I).EQ.X(NY+1)) NK=NMAX+5	Y01070
	F=0.5	Y01080
	KK=1	Y01090
	E2=0.0	Y01100
	HHH=(ELV(NK)+ELV(NK+NY+1))/2.	Y01110
	IF(HHH.GT.HMP2(IDL)) GO TO 205	Y01120
	GO TO 2000	Y01130
205	F=0.0	Y01140
	E1=0.0	Y01150
	E2=0.0	Y01160
	GO TO 2000	Y01170
211	NK=I-3	Y01180
	IF(Y(I).EQ.Y(3)) NK=I+NY-2	Y01190
	F=0.5	Y01200
	KK=2	Y01210
	E2=TE2	Y01220
	E1=0.0	Y01230
	HHH=(ELV(NK)+ELV(NK+NY+1))/2.	Y01240
	IF(HHH.GT.HMP5(IDC)) GO TO 205	Y01250
	GO TO 2000	Y01260
210	NK=I-2*NY+1	Y01270
	IF(Y(I).GE.Y(NY-1)) NK=NMAX+5	Y01280
	IF(X(I).EQ.X(NY+1)) NK=NMAX+5	Y01290
	F=1.0	Y01300
	KK=2	Y01310
	IF(SOL.GT.AS1) GO TO 217	Y01320
	HHH=(ELV(NK)+ELV(NK+NY+1))/2.	Y01330
	IF(HHH.GT.HMP2(IDL)) GO TO 205	Y01340
	GO TO 2000	Y01350
217	F=0.0	Y01360
	E=E2	Y01370
	E2=0.0	Y01380
	KK=3	Y01390
	GO TO 2000	Y01400
220	NK=I-3	Y01410
	IF(Y(I).EQ.Y(3)) NK=I+NY-2	Y01420
	F=1.0	Y01430
	KK=2	Y01440
	IF(SOL.GT.AS2) GO TO 227	Y01450
	IF(X(I).EQ.X(NMAX)) GO TO 2000	Y01460
	HHH=(ELV(NK)+ELV(NK+NY+1))/2.	Y01470
	IF(HHH.GT.HMP5(IDC)) GO TO 205	Y01480
	GO TO 2000	Y01490
227	F=0.0	Y01500
	E=E1	Y01510
	E1=0.0	Y01520
	KK=3	Y01530
2000	SDT(NK)=SDT(NK)+F*T+E1+E2	Y01540
	TRE(NK)=TRE(NK)+F*R	Y01550
	TIRE(NK)=TIRE(NK)+F*H+E1+E2	Y01560
	IF(KK.EQ.1) GO TO 211	Y01570
	IF(KK.EQ.3) GO TO 2500	Y01580
	GO TO 2700	Y01590
2500	SDT(I-NY-1)=SDT(I-NY-1)+T+E	Y01600
	TRE(I-NY-1)=TRE(I-NY-1)+R	Y01610
	TIRE(I-NY-1)=TIRE(I-NY-1)+H+E	Y01620
2700	CONTINUE	Y01630
4	FORMAT(6F20.10,/)	Y01640
	RETURN	Y01650
300	IF(X(I).EQ.X(NMAX)) RETURN	Y01660
	SOR=(ELV(I)-ELV(I+NY-1))/2./SH	Y01670
	AS2=ABS(S2)	Y01680
	AS1=ABS(S1)	Y01690

	IF(S1.GT.0.0.AND.S2.LE.0.0) GO TO 310	Y01700
	IF(S1.LE.0.0.AND.S2.GT.0.0) GO TO 320	Y01710
	NK=I+2*NY+1	Y01720
	IF(Y(I).GE.Y(NY-1)) NK=NMAX+5	Y01730
	IF(X(I).EQ.X(NMAX-NY)) NK=NMAX+5	Y01740
	F=0.5	Y01750
	KK=1	Y01760
	E1=0.0	Y01770
	HHH=(ELV(NK)+ELV(NK-NY+1))/2.	Y01780
	IF(HHH.GT.HMP3(IDR)) GO TO 305	Y01790
305	GO TO 3000	Y01800
	F=0.0	Y01810
	E1=0.0	Y01820
	E2=0.0	Y01830
	GO TO 3000	Y01840
311	NK=I-3	Y01850
	IF(Y(I).EQ.Y(3)) NK=I-NY-2	Y01860
	F=0.5	Y01870
	KK=2	Y01880
	E1=TE1	Y01890
	E2=0.0	Y01900
	HHH=(ELV(NK)+ELV(NK-NY+1))/2.	Y01910
	IF(HHH.GT.HMP6(IDC)) GO TO 305	Y01920
	GO TO 3000	Y01930
310	NK=I+2*NY+1	Y01940
	IF(Y(I).GE.Y(NY-1)) NK=NMAX+5	Y01950
	IF(X(I).EQ.X(NMAX-NY)) NK=NMAX+5	Y01960
	F=1.0	Y01970
	KK=2	Y01980
	IF(SOR.GT.AS1) GO TO 317	Y01990
	HHH=(ELV(NK)+ELV(NK-NY+1))/2.	Y02000
	IF(HHH.GT.HMP6(IDC)) GO TO 305	Y02010
	GO TO 3000	Y02020
317	F=0.0	Y02030
	E=E1	Y02040
	E1=0.0	Y02050
	KK=3	Y02060
	GO TO 3000	Y02070
320	NK=I-3	Y02080
	IF(Y(I).EQ.Y(3)) NK=I-NY-2	Y02090
	F=1.0	Y02100
	KK=2	Y02110
	IF(SOR.GT.AS2) GO TO 327	Y02120
	IF(X(I).EQ.0.0) GO TO 3000	Y02130
	HHH=(ELV(NK)+ELV(NK-NY+1))/2.	Y02140
	IF(HHH.GT.HMP3(IDR)) GO TO 305	Y02150
	GO TO 3000	Y02160
327	F=0.0	Y02170
	E=E1	Y02180
	E1=0.0	Y02190
	KK=3	Y02200
3000	SDT(NK)=SDT(NK)+F*T +E1+E2	Y02210
	TRE(NK)=TRE(NK)+F*R	Y02220
	TIRE(NK)=TIRE(NK)+F*H +E1+E2	Y02230
	IF(KK.EQ.1) GO TO 311	Y02240
	IF(KK.EQ.3) GO TO 3500	Y02250
	GO TO 3700	Y02260
3500	SDT(I+NY-1)=SDT(I+NY-1)+T+E	Y02270
	TRE(I+NY-1)=TRE(I+NY-1)+R	Y02280
	TIRE(I+NY-1)=TIRE(I+NY-1)+H+E	Y02290
3700	CONTINUE	Y02300
	RETURN	Y02310
	END	Y02320

```

*****
*                                     *
*           I N P U T   D A T A       *
*                                     *
*****

```

```

GROUP # 1 :          SURFACE ROUGHNESS DATA
*****
*****

```

```

NO. OF ELEVATION TRACES =      7
NO. OF POINTS PER TRACE =   100
SPACING                  =  2.00   CM

```

```

GROUP # 2 :          PROBLEM PARAMETERS
*****
*****

```

```

SOIL PARTICLE DIAMETER   =0.010   MLMTR
SOIL UNIT WEIGHT         =16660.   N/C. METER
SOIL SPECIFIC WEIGHT     =  2.65

EXPONENT OF KALINSKE EQN. =  1.50
EQN. CONSTANT FOR RILLS  =400.0
EQN. CONSTANT FOR HUMPS  =  20.0
MANNING CONSTANT         =0.040

```

```

GROUP # 3 :          STORM AND SLOPE DATA
*****
*****

```

```

NO. OF MESH POINTS IN CROSS-DIRECTION =   65
NO. OF MESH POINTS IN LONGT-DIRECTION =   30
AVERAGE SLOPE                      =  20.0   DEGREES
                                   =  36.41   PERCENT
RAINFALL INTENSITY                  =  50.0   MLMTR/HR
RUNOFF COEFFICIENT                  =  0.50

ANNUAL RAINFALL RATE                 =100.0   CNTMTR
EQUIVALENT YEARS OF RAIN             =  0.25   YEARS

TIME INTERVAL                       =  10.0   MINUTES
TOTAL RAIN PERIOD                    =  5.00   HOURS
NO. OF RANDOM SURFACES               =    1

FAILURE  LIMIT FOR SIDE SLOPE        =  1.40
STARTING LIMIT FOR SIDE SLOPE        =  1.10

```

```

*****
*                                     *
*   SPECTRAL ANALYSIS RESULTS   *
*                                     *
*****

```

AVERAGE VALUES FOR ALL PROFILES

\*\*\*\*\*

DEGREE	AN	BN	POWER	CONTR.	TOTAL	L (CMD)
0	0.00	0.0	0.000	0.0	0.0	0.0
1	-3.73	5.08	26.373	0.1021	0.1021	198.00
2	5.14	3.01	28.660	0.1213	0.2234	99.00
3	-7.44	0.03	51.573	0.2030	0.4263	66.00
4	-1.39	2.23	6.368	0.0257	0.4520	49.50
5	0.08	1.61	4.803	0.0207	0.4727	39.60
6	-0.23	-0.25	5.473	0.0236	0.4963	33.00
7	-0.36	-0.94	3.866	0.0160	0.5123	28.29
8	0.36	1.16	3.864	0.0166	0.5290	24.75
9	-0.40	0.26	4.253	0.0187	0.5477	22.00
10	0.30	0.35	4.087	0.0156	0.5632	19.80
11	3.00	-2.23	10.397	0.0429	0.6061	18.00
12	-1.62	1.22	4.259	0.0171	0.6232	16.50
13	-0.30	0.51	4.770	0.0200	0.6432	15.23
14	1.00	0.25	3.735	0.0163	0.6595	14.14
15	0.55	1.08	3.243	0.0143	0.6737	13.20
16	0.72	-0.42	5.569	0.0217	0.6955	12.38
17	0.21	0.02	4.153	0.0173	0.7127	11.65
18	-1.22	-1.19	3.580	0.0147	0.7274	11.00
19	-0.55	-0.57	1.665	0.0066	0.7339	10.42
20	2.32	-0.62	3.820	0.0161	0.7501	9.90
21	0.24	-1.47	2.547	0.0102	0.7602	9.43
22	-0.46	0.80	2.371	0.0099	0.7702	9.00
23	1.96	-0.24	4.659	0.0179	0.7881	8.61
24	-1.05	-0.07	2.347	0.0094	0.7974	8.25
25	-0.73	0.83	5.703	0.0242	0.8217	7.92
26	0.18	0.37	1.808	0.0067	0.8283	7.62
27	0.07	0.11	2.606	0.0105	0.8388	7.33
28	0.98	-1.07	3.876	0.0160	0.8548	7.07
29	1.45	0.56	4.067	0.0167	0.8715	6.83
30	1.12	-0.42	1.495	0.0061	0.8776	6.60
31	0.36	0.02	0.577	0.0025	0.8801	6.39
32	1.12	-0.06	2.610	0.0105	0.8906	6.19
33	-0.22	0.12	1.397	0.0058	0.8964	6.00
34	0.50	-0.34	1.149	0.0044	0.9008	5.82
35	1.08	0.05	1.901	0.0074	0.9082	5.66
36	0.25	-0.47	1.384	0.0056	0.9137	5.50
37	0.59	-0.29	1.515	0.0061	0.9198	5.35
38	0.99	-0.94	2.421	0.0096	0.9294	5.21
39	1.17	0.19	2.047	0.0088	0.9382	5.08
40	0.52	0.51	3.057	0.0121	0.9504	4.95
41	0.23	0.33	1.819	0.0072	0.9576	4.83
42	0.75	0.78	1.401	0.0062	0.9638	4.71
43	0.00	0.25	1.030	0.0042	0.9680	4.60
44	0.48	-0.15	1.208	0.0047	0.9727	4.50
45	0.01	0.34	0.861	0.0037	0.9763	4.40
46	-0.16	0.76	1.333	0.0057	0.9820	4.30
47	0.57	0.07	1.139	0.0047	0.9867	4.21
48	0.01	-0.56	1.196	0.0048	0.9914	4.13
49	-0.22	-0.22	1.079	0.0043	0.9958	4.04
50	-0.17	0.0	0.993	0.0042	1.0000	3.96

AMPLITUDE OF REPRESENTATIVE WAVE= 3.740 MLMR  
LENGTH OF REPRESENTATIVE WAVE = 18.000 CM  
MEAN OF NORMAL DIST. = 4.719 MLMTR  
STAND. DEVIATION OF NORMAL DIST.= 15.906 MLMTR

PLOT LENGTH= 2.286 METERS  
PLOT WIDTH = 5.760 METERS

TEST AREA = 13.169 SQ. METERS  
SHAPE FACTOR = 2.519

\*\*\*\*\*



```
*****
**                                **
**  RANDOM SURFACE NO.    1    **
**                                **
*****
```

RESULTS OF EACH INTERVAL					CUMULATIVE RESULTS		
INTRVL #	TTL SDMT ( N )	R/I RATIO	ERSN RATE ( N/SM/HR)		TTL SDMT ( N )	R/I RATIO	ERSN RATE ( N/SM/HR)
1	13.27	0.22	6.04	*	13.27	0.22	6.04
2	24.78	0.23	11.29	*	38.04	0.23	8.67
3	30.12	0.24	13.73	*	68.17	0.23	10.35
4	37.34	0.24	17.01	*	105.51	0.23	12.02
5	36.49	0.24	16.63	*	142.00	0.23	12.94
6	37.52	0.23	17.09	*	179.52	0.23	13.63
7	42.37	0.23	19.31	*	221.89	0.23	14.44
8	39.04	0.21	17.79	*	260.94	0.23	14.86
9	40.28	0.21	18.35	*	301.22	0.23	15.25
10	43.46	0.20	19.80	*	344.68	0.22	15.70
11	43.06	0.20	19.62	*	387.75	0.22	16.06
12	44.32	0.20	20.19	*	432.07	0.22	16.40
13	42.74	0.18	19.47	*	474.81	0.22	16.64
14	54.38	0.19	24.78	*	529.19	0.21	17.22
15	49.46	0.18	22.54	*	578.65	0.21	17.58
16	45.40	0.16	20.69	*	624.06	0.21	17.77
17	45.21	0.17	20.60	*	669.26	0.20	17.94
18	52.54	0.17	23.94	*	721.80	0.20	18.27
19	47.14	0.16	21.48	*	768.94	0.20	18.44
20	51.98	0.16	23.68	*	820.92	0.20	18.70
21	56.11	0.17	25.56	*	877.03	0.19	19.03
22	57.40	0.16	26.15	*	934.43	0.19	19.35
23	58.24	0.16	26.54	*	992.68	0.19	19.66
24	55.59	0.16	25.33	*	1048.27	0.19	19.90
25	62.91	0.16	28.66	*	1111.17	0.19	20.25
26	56.27	0.15	25.64	*	1167.45	0.18	20.46
27	60.49	0.15	27.56	*	1227.94	0.18	20.72
28	54.82	0.15	24.98	*	1282.76	0.18	20.87
29	64.35	0.15	29.32	*	1347.11	0.18	21.16
30	56.14	0.15	25.58	*	1403.25	0.18	21.31